2
2000

This is to certify that the

thesis entitled

Synthesis and Characterization of Binary Materials Composed of Transition metals coordinated to the Organic Acceptor TCNQ

presented by

Shannon A. O'Kane

has been accepted towards fulfillment
of the requirements for

Masters degree in Chemistry

Kim R. Dunbar

Major professor

Date December 15, 1999

SYNTHESIS AND CHARACTERIZATION OF BINARY MATERIALS COMPOSED OF TRANSITION METALS COORDINATED TO THE ORGANIC ACCEPTOR TCNQ

By

Shannon A. O'Kane

A THESIS

Submitted to
Michigan State University
In partial fulfillment of the requirements
For the degree of

MASTER OF SCIENCE

Department of Chemistry

1999

S
M
C

In the

molecule 7,7,8

research in the

metal TTF-TC

however, that

with a transiti

cyanide accep

polymers in v

DCNQI in

benzoquinone

metal/DCNQI

and $TCNQF_4$

characterizati

divalent ions

Ag(I) with TC

earlier worke

solvent in dic

ABSTRACT

SYNTHESIS AND CHARACTERIZATION OF BINARY MATERIALS COMPOSED OF TRANSITION METALS COORDINATED TO THE ORGANIC ACCEPTOR TCNQ

By
Shannon A. O'Kane

In the early 1960's, the surprising discovery of conducting salts based on the molecule 7,7,8,8-tetracyanoquinodimethane, (TCNQ), paved the way for an explosion of research in the area of "all organic" conductors, the prototype of which is the organic metal TTF-TCNQ where TTF is tetrathiafulvalene. It has only been in recent years, however, that we and others have replaced the donor portion of these charge-transfer salts with a transition metal that is coordinated directly to the nitrile groups of an organo-cyanide acceptor. A foremost illustration of this point is the $Cu(DCNQI)_2$ series of polymers in which mixed-valence Cu(I,II) ions are coordinated to the dicyano units of DCNQI in a three-dimensional fashion (DCNQI = N,N'-dicyano-1,4-benzoquinonediimine). The interesting properties that were observed for the binary metal/DCNQI system prompted our group to investigate similar materials with TCNQ and $TCNQF_4$. This thesis details a series of in-depth studies involving the syntheses, characterization and structural studies of binary TCNQ materials of Ag(I) and the divalent ions of the first-row transition metals, Mn, Fe, Co, and Ni. The chemistry of Ag(I) with $TCNQF_4$ is also described. The main issue in this research, which had eluded earlier workers in the field, is the role of polymorphism and coordinated/interstitial solvent in dictating the purity and properties of M(TCNQ) and $M(TCNQ)_2$ phases.

ACKNOWLEDGMENTS

There are several people who played an integral role in helping me achieve this degree. First and foremost, I would like to thank my advisor, Professor Kim Dunbar, for encouraging my desire to learn and helping me strive to become a better chemist. I would also like to thank her for understanding my decision to obtain this degree. To my "magnetic" co-worker, Rodolphe, I would like to express my appreciation for performing the magnetic measurements, and being another "advisor" who cares about the achievement of his fellow students. Several previous TCNQ project group members namely, Robert Heintz, Hanhua Zhao, Xiang Ouyang, and Guilio Grandinetti, were major contributors to this project. I would like to thank Hanhua Zhao especially for introducing me to the project and teaching me proper synthetic techniques. Many people in the lab, especially Paul and Matt, were very helpful in solving everyday problems and inquiries. This thesis is in memory of Professor Jerry Cowen, our collaborator from the Department of Physics, who contributed valuable background experiments as well as information about the complex magnetic properties of the TCNQ compounds. Most importantly, though, was the emotional support and encouragement that I received from my fiancé, Jeremy, and my friend, Amanda. They kept me laughing, but also focused on the task at hand.

TABLE OF CONTENTS

LIST OF TABLES

LIST OF FIGURES

LIST OF ABBREVIATIONS

Å	Angstrom
δ	bending mode
β	Beta
br	broad
μ	bridging ligand
cm^{-1}	Wavenumber
°C	degree Celsius
ν	frequency (stretching)
g	gram
h	hour
I	insoluble
IR	infrared
m	medium
mL	milliliter
mmol	millimole
mol	mole
π	pi
s	strong
S	soluble
V	volume
w	weak

w/w	weight by weight
X	MeOH or H_2O

Chapter I:

Introduction

Introduction

The recognition of the superconductivity of Hg in 1911, led McCoy and Moore to predict the future synthesis of "synthetic metals".[1] It was theorized that these organic materials would exhibit metallic behavior, namely, an increase in electrical conductivity with decreasing temperature. Upon comparison to their metal counterparts researchers envisioned that the main advantages of these materials would be ease of synthesis at lower temperatures and the ability to be tailored for specific properties which alone makes them worthy of study. The beginning of a realization of this dream occurred in the early 1960's when Melby and coworkers[2] discovered the semiconducting properties of alkali salts of the electron acceptor, TCNQ, 7,7,8,8- tetracyanoquinodimethane, in its reduced form.

During the past four decades a great deal of research has focused on the synthesis of organic superconductors[3] and charge-transfer salts.[4] Only recently have chemists broadened their scope of interest to include the incorporation of paramagnetic transition metal centers for the purpose of obtaining interesting magnetic[5] and conducting[6] properties. After several decades of exhaustive exploration of organic donor and acceptor derivatives, a new trend has emerged in the synthesis of new conductors. The incorporation of an inorganic component provides a new use for the electron acceptor, namely, as a ligand that coordinates to the metal. The resulting materials that form by direct bonding of metals and organic acceptors have opened up a vast new synthetic arena and brought magnetism to the forefront of research interest.

TCNQ, An Electron Acceptor

Several characteristics of 7,7,8,8-tetracyanoquinodimethane, TCNQ, render it an ideal ligand for use in the synthesis of magnetic and conducting materials.[7] TCNQ is a powerful electron acceptor and it forms a very stable radical anion. This is due to the presence of four cyano withdrawing groups, the molecule's planarity, and its high symmetry. TCNQ can coordinate to metals through the nitrogen lone pairs on the cyano groups or through the π-system, although the latter is rare. Various coordination modes have been identified which indicate that TCNQ is a very versatile bridging ligand capable of producing one- , two-, and three-dimensional solids. One of the most important characteristics of TCNQ is its ability to participate in π–stacking. The delocalization of the electrons through the overlapping π-systems has been shown to increase the charge-transfer in these materials in one-dimension. Furthermore, the accessibility of three oxidation states of the ligand, namely, $TCNQ^{0}$, $TCNQ^{-1}$ and $TCNQ^{-2}$, allow for diversity in synthesis and properties due to the possibility of forming mixed-valence compounds. Finally, the interaction of the S = ½ spin state of the reduced form of this ligand with the spin on the metals result in the generation of interesting conducting and magnetic properties.

The synthesis of alkali metal or other organic cation salts of TCNQ resulted in identification of two distinct structures.[2] The first is a 1:1 composition with the formula $M^{+}TCNQ^{-}$, M = alkali metal. The second incorporates neutral TCNQ within the structure and is therefore a 1:2 composition with the formula $M^{+}TCNQ^{-}(TCNQ)$. The representative formulae indicate that a complete charge-transfer to the acceptor has occurred within both structures. The formula differences led to marked differences in

electrical conductivity; the former exhibits a high electrical resitivity of 10^4-10^9 ohm cm, whereas in the salt that contains neutral TCNQ, the resistivity is lowered to 0.01-100 ohm cm.[4] In comparison, a metallic conductor exhibits a resistivity of 10^{-6} ohm cm.

Other electron acceptors have been also used to prepare charge-transfer compounds; these are currently being used to synthesize conducting and magnetic materials in our laboratories. Schematic diagrams of TCNE (tetracyanoethylene), DCNQI (N,N'-dicyano-1,4-benzoquinonediimine), TCNQ and TCNQ derivatives are shown in Figure 1. A close relative to TCNQ is TCNE, which can undergo reduction by

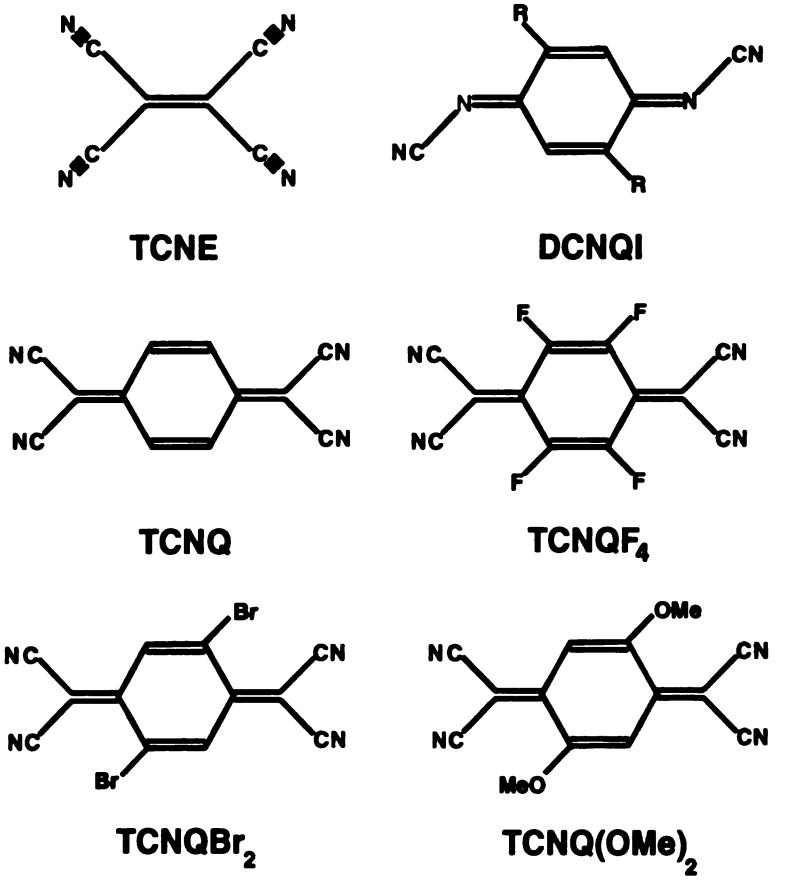

Figure 1. Illustration of a variety of electron acceptors.

one or two electrons, and is known to coordinate to metals through the four cyano groups. Another new class of electron acceptors dicyanoquinodiimines, DCNQI, are similar in their redox properties to TCNQ, but only two coordination sites are available.[6] Further expansion of the field of electron acceptors has occurred through derivatization of the TCNQ molecule. In 1975, derivatives of TCNQ were synthesized by Wheland; these are based on the addition of electron withdrawing halogens (e.g. $TCNQF_4$ or $TCNQ(Br)_2$) or electron donating groups (e.g. $TCNQ(OMe)_2$).[8]

Definition of Terms

Conducting charge-transfer salts are composed of highly ordered donors and acceptors in which at least one component is in the form of a radical species. Conductivity, or delocalization of electrons, is the result of favorable intermolecular orbital interactions in the solid state. The occupancy of the conduction band is, however, also critical for determining this property. Band theory states that a transfer of electrons from the valence (filled) to the conduction (empty) band must occur in order for conductivity to be favorable. Therefore, if there is a sufficiently large energy gap between the bands, the material is an insulator due to the lack of energy available to promote electrons. As the gap decreases, electrons are able to be thermally excited to the HOMO band (conduction) and the material is an intrinsic semiconductor. Metallic behavior requires partially filled bands in which electrons are promoted to infinitely higher energy levels. The Fermi level is the highest occupied state and the mobility of electrons at this level dictates the physical properties of the metal.[9]

Since conductivity is temperature dependent, the critical temperature is important in describing the properties of a charge-transfer complex. Measuring a conductor's resistivity, ρ, is another method of characterization used to describe the ability for current to pass through a substance. Metals have a low resistivity (e.g.10^{-6} ohm cm) whereas an insulator exhibits a high resistivity ~ 10^{10} ohm cm.[4] Organic and inorganic semiconductors fall between those of metals and insulators, having resitivities ranging from 10^4 to 10^8 ohm cm.[4]

The physical property of magnetism, like conductivity, is based on the intrinsic behavior of the material. There are five possible types of magnetic behavior observed in solids, and their appreciation is important for a general understanding of the factors involved in magnetic design. A solid that lacks unpaired electrons is termed diamagnetic, while paramagnetism is observed in solids that have unpaired electrons that interact weakly with a magnetic field. The other three main types of magnetic behavior, ferromagnetism, antiferromagnetism, and ferrimagnetism, are different than the latter in that they are characterized by strong interactions and by cooperative (or bulk) properties. A ferromagnetic ordering occurs when all of the spins in a solid are aligned in a parallel fashion (↑↑). If the spins in the solid are all anitparallel (↑↓) throughout the material, the ordering is classified as being of the antiferromagnetic type. Finally, the phenomenon by which spins order antiferromagnetically but with a net spin (↑↓) remaining is termed *ferri*magnetic.

The coupling constant J, describes the isotropic interaction between two spins S_1 and S_2, and is defined by the spin Hamiltonian, $H = -2J(S_1 \cdot S_2)$.[11] The energy separation between the singlet and the triplet states is J. In ferromagnetically coupled spins, J>0

(triplet ground state), while with antiferromagnetically coupled spins, J<0 (singlet ground state). If the orbitals containing the unpaired electron(s) are orthogonal to each other and Hund's rule keeps the spins parallel, then ferromagnetic coupling between the spins occurs. If there is direct orbital overlap, however, the antiparallel alignment will be favored. In order to achieve a ferromagnetic interaction, spins in orthogonal orbitals must be in the same spatial region (adjacent sites).[12] Ferrimagnetism is achieved when the local antiferromagnetic interactions do not have spins of equal magnitude.

When considering magnetic materials, three factors are useful in describing a magnet.[13] The first is the critical temperature, T_c, which is the temperature at which a magnetic ordering occurs within a system. The second is the saturation magetization or the amount of permanent magnetization that a material can store. Finally, a coercive field defines the magnetic field that must be applied to restore the magnet to its original condition. The latter is important for instance in the resistance of data loss that is stored in magnetic materials.

Organic Conductors

The discovery in the early 1960's that TCNQ salts are organic semiconductors led to almost four decades of intense investigation of electron donors and acceptors.[2] The ultimate goal is the synthesis of highly conducting, especially superconducting, materials. Alkali TCNQ salts such as K^+ are remarkable in that they exhibit room temperature conductivities in the range, $5 \times 10^{-4}\ \Omega^{-1}\ cm^{-1}$, which is a huge increase (4 -10 orders of magnitude) over previous organic materials.[14] After this discovery there was a renewed

interest in TCNQ salts. It was discovered that the high conductivity is due to the stacking of the planar molecules, with segregated stacks of cations and anions. The overlap of the π systems increases the charge-transfer properties with conductivity occurring only along the direction of the stack.

The synthesis of TTF in 1970 introduced a new class of organic donors that contain electron rich sulfur atoms.[15,16] Coppens found that TTF radicals arrange in stacks similar to TCNQ,[17] and that TTF salts[15,16,18] are highly conductive as well ($\sigma = 0.2\ \Omega^{-1}\ cm^{-1}$ at 300K). The combination of TTF and TCNQ seemed to be an obvious method for forming a highly conducting charge-transfer material due to the small difference in redox potentials between the two molecules. Indeed, this proved to be true, as it was found that a solid with partially oxidized TTF and partially reduced TCNQ ions formed an organic metal that exhibited a metallic conductivity (σ) of $\sigma = 10^4\ \Omega^{-1}\ cm^{-1}$ near 60 K.[19] Below this temperature, a phase transition from a metal to a semiconducting state occurs.

Derivatization of the TTF donor contributed to an increase in the number of conducting salts that exhibit charge-transfer properties. TSF-TCNQ, (TSF = tetraselenafulvalene) was the first derivative synthesized by replacing the sulfur atoms with selenium, and, as expected, the high metallic conductivity surpassed that of TTF-TCNQ by two hundred ohms. Furthermore, the conducting state is significantly more stable (> 40K).[20] Other derivatives with selenium, HMTSF-TCNQ[21] (HMTSF, hexamethylene-tetraselenafulvalene) and tetraselenafulvalene (TMTSF) salts[22], also show metallic behavior. In particular, the charge transfer salt, $(TMTSF)_2[PF_6]$, is the first organic metal to exhibit superconductivity at T_c = 0.9K (P = 12 kbar). The use of

pressure suppresses the metal–to–insulator transition that usually occurs, thus allowing metallic behavior to occur at higher critical temperatures.[23]

In the early 1980's, a new electron donor, namely bis(ethylenedithio)tetrathiafulvalene (BEDT-TTF) was discovered to form two-dimensional charge-transfer salts making them distinct from other TTF derivatives. This dimensionality is due to short inter-stacking sulfur interactions in two-dimensions, which surprinsingly leads to superconducting behavior.[24] Two examples of these materials are (BEDT-TTF)ReO_4[24a] and $Cu[N(CN)_2]X$ where X= Br or Cl.[24d] The last example is particularly notable as compounds which superconduct at the highest critical temperature known for organic superconductors (T_c = 11.6 K at ambient pressure and 12.5 K at 0.3 kbar respectively).

Molecular-based Magnets

The introduction of a paramgnetic metal component into charge-transfer materials allows for exploration in the promising field of molecule-based magnets. Over the past thirty years, notable breakthroughs have been reported by Olivier Kahn, who synthesized the first molecular, ferrimagnetic chain based on Mn(II)Cu(II) centers,[25] and by Miller *et al.*, who discovered the first organic–based molecular magnet, namely $[Fe(Cp^*)_2]^{+\cdot}[TCNE]^{-\cdot}$.[26] The latter forms a mixed stack arrangement and exhibits ferromagnetism below 4.8 K. Shortly after this discovery, other first row transition metal Cp* donors were used to prepare ferromagnetic charge-transfer materials when combined with acceptors such as TCNQ, bis(dithiolato)-metalates, and $C_4(CN)_6$.[28] One example,

$[(C_5Me_5)_2Mn][TCNQ]$, exhibits ferromagnetism at a T_c of 6.2 K which was considered to be a breakthrough at the time.[28f] In the ten years since this discovery, however, rapid developments have occurred in the area of higher T_c molecule-based magnets. In fact, there are now room temperature and above room temperature magnets based on molecular precursors.

Complexes That Contain Covalently Linked Donors and Acceptors

A different approach to the design of magnetic and conducting materials is the assembly of open-shell metal centers and organic radicals into inorganic/organic "hybrid" structures.[5a,6,29] The σ-coordination opens up the possibility for acceptors, such as TCNQ and TCNE, to undergo charge-transfer reactions with electron rich organometallic species e.g. $(C_5R_5)(CO)_2Mn(THF)$ where R = H, CH_3.[30] One mode of binding, specifically the σ-η^1 mode, was first identified in the complexes $[Ru(PPh_3)_2(TCNQ)]$ and $[Cu(pdto)(TCNQ)]_2$ (pdto = 1,8-di-z-pyridyl-3,6-dithiaoctane).[31] Other examples include $[Ru_2(CO)_5(\mu\text{-}L)_2(\eta^1\text{-}TCNX)](TCNX)$ (X = E,Q) which contain both inner and outer sphere TCNQ or TCNE.[32]

One of the intriguing findings that has emerged from the coordination of organocyanide acceptors with transition metals is an accidental discovery made by Manriquez and Miller *et al.* The reaction of $V(C_6H_6)_2$ and TCNE was found to yield an insoluble, amorphous solid formulated as $V(TCNE)_2 \cdot 1/2(CH_2Cl_2)$. Reported to be a room-temperature ferrimagnet, this compound is thought to contain σ-coordinated reduced TCNE as deduced by infrared spectroscopy.[5a] Numerous examples of

complexes that contain σ-coordinated TCNE have appeared in the literature,[30,32,33] several of which have been structurally characterized by X-ray crystallography.[34] The majority of these products exhibit either σ-η^1 or σ-μ-η^2 coordination modes within a linear chain structural motif. Two such examples are the ferromagnetic salt, [MnTPP][TCNE] (TPP = meso-tetra-phenylporphinato) and $[M(hfacac)_2][TCNE]$ (M = Co, Cu; hfacac = hexafluoroacetylacetonate). Also, a two-dimensional structure was reported to consist of σ-μ-η^4-TCNE units linking $Rh_2(O_2CCF_3)_4$ through the axial Rh sites, although these compounds are not of any magnetic interest.[34f]

An excellent illustration of the design of highly conducting covalent solids with σ- as well as dπ-pπ interactions between metal and organic constituents is the class of compounds, $Cu(R,R'\text{-}DCNQI)_2$ (DCNQI = N,N' –dicyanoquinonediimine, R,R' = halide, alkyl group or alkoxide groups).[6] X-ray studies of these compounds reveal DCNQI molecules that form one-dimensional columns connected to each other by tetrahedral mixed-valence $Cu^{+/2+}$ cations. The high conductivity that results is mainly attributed to the DCNQI-DCNQI stacking within these structures.

Conducting Metal/TCNQ Materials

The DCNQI compounds are not the only structures composed solely of metal cations and electron acceptor anions. Alkali metal/TCNQ complexes[35] exhibit electrical conductivities on the order of 10^{-2} to 10^{-5} Ω^{-1} cm^{-1}.[36] This class of compounds has been structurally characterized and the direction of conductivity is ascertained to be parallel to the stacks of TCNQ molecules. Surprisingly, there are noticeable structural differences

in this fam

modes of r

each cubic C

structures the r

octahedral coor

only six nitrile

distances betwe

in this family of compounds. One of the most important is the three TCNQ stacking modes of ring overlap, which are shown in Figure 2. Four TCNQ molecules surround

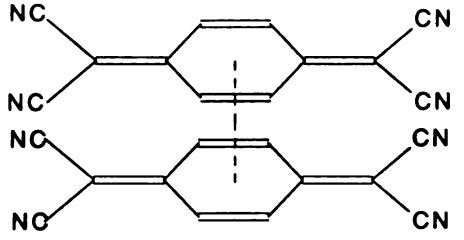

(a) ring- ring (eclipsed)

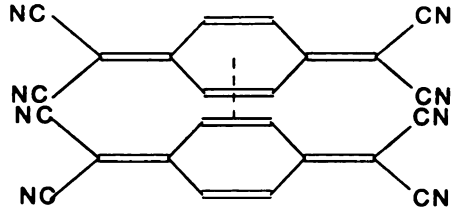

(b) ring - edge

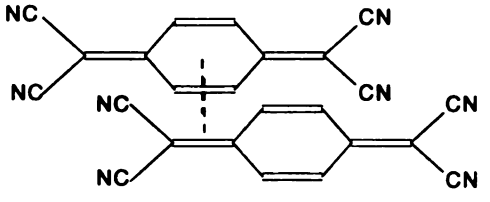

(c) ring - external bond

Figure 2. Different stacking modes of TCNQ rings.

each cubic Cs^+ cation in $Cs_2(TCNQ)_3$,[35a] while in the Rb(TCNQ) and K(TCNQ) structures the metal cation is surrounded by eight nitrile groups.[35b,f] For Na(TCNQ), an octahedral coordination is exhibited around the metal with the cation being surrounded by only six nitrile groups.[35e] Another structural differences includes variation of stacking distances between TCNQ molecules which range from 3.2 to 3.6 Å.[35] These differences

can be dir

alkali meta

Mo

conducting

$TCNQ^-$ an

a 1:1 ratio o

metal into a

field to a de

Al electrode

critical thres

which it rem

high resista

original me

shown in E

photoelectr

molecule ir

[Cu

The

subtle chan

properties o

transformati

at longer dip

can be directly correlated to the reported differences in electrical conductivities for the alkali metal/TCNQ salts.

More to the point of the present work, the material Cu(TCNQ),[37] whose conducting properties have been the subject of intense debate, exhibits σ-coordination of $TCNQ^-$ anions to the metal center. As the formula indicates, Cu(TCNQ) is composed of a 1:1 ratio of metal and ligand. The compound was first prepared as a film by dipping Cu metal into a solution of neutral TCNQ. It was reported that the application of an electric field to a device consisting of a thin film of Cu(TCNQ) sandwiched between a Cu and an Al electrode induces a switching of the material from a high to a low resistance state at a critical threshold potential.[37a] Furthermore, this device displays a memory effect in which it remains in a low resistant state for a period of time before returning to a state of high resistance.[37b-f] Variations in film design affect the conducting properties. The original mechanism proposed by Potember *et al.*, the discoverers of this phenomenon, is shown in Eq 1. Numerous techniques including Raman, infrared, auger, and X-ray photoelectron spectroscopies have been used to probe the electronic state of the TCNQ molecule in the films.

$$[Cu^+(TCNQ^-)]_n \quad \leftrightarrow \quad [Cu^0]_x + [TCNQ^0]_x + [Cu^+(TCNQ^-)]_{n-x} \qquad \text{(Eq.1)}$$

The scientific findings surrounding this controversy led our group to suspect that subtle changes in film preparation were responsible for the differences in the electrical properties of the Cu(TCNQ) films. SEM images provided by Hipps *et al.* revealed that a transformation from a needle morphology to a more mosaic plate-like phase was evident at longer dipping times.[37u] These results suggested to us that there are two polymorphs of

Cu(TCNQ

data as a m

found that

redissolve

displayed i

and spectro

illustrate th

transformat

Figure 3.

Cu(TCNQ), thus we began an extensive study to ascertain structural and spectroscopic data as a means to explain the conducting behavior. Using bulk synthetic methods, it was found that needles of Cu(TCNQ) phase I form at short reaction times (2 min) and then redissolve to form platelets of Cu(TCNQ) phase II.[38] SEM images of these phases are displayed in Figure 3. These compounds have been characterized by several structural and spectroscopic methods (XPS, IR). X-ray powder diffraction was also used to illustrate the sequential conversion of phase I to phase II over several hours. The transformation is shown in Figure 4.

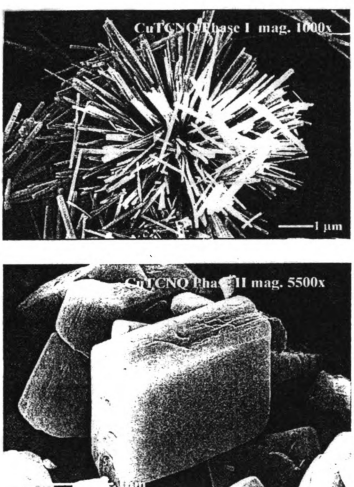

Figure 3. SEM images of Cu(TCNQ) phase I (top) and phase II (bottom) illustrating the morphological differences.[38]

Figu

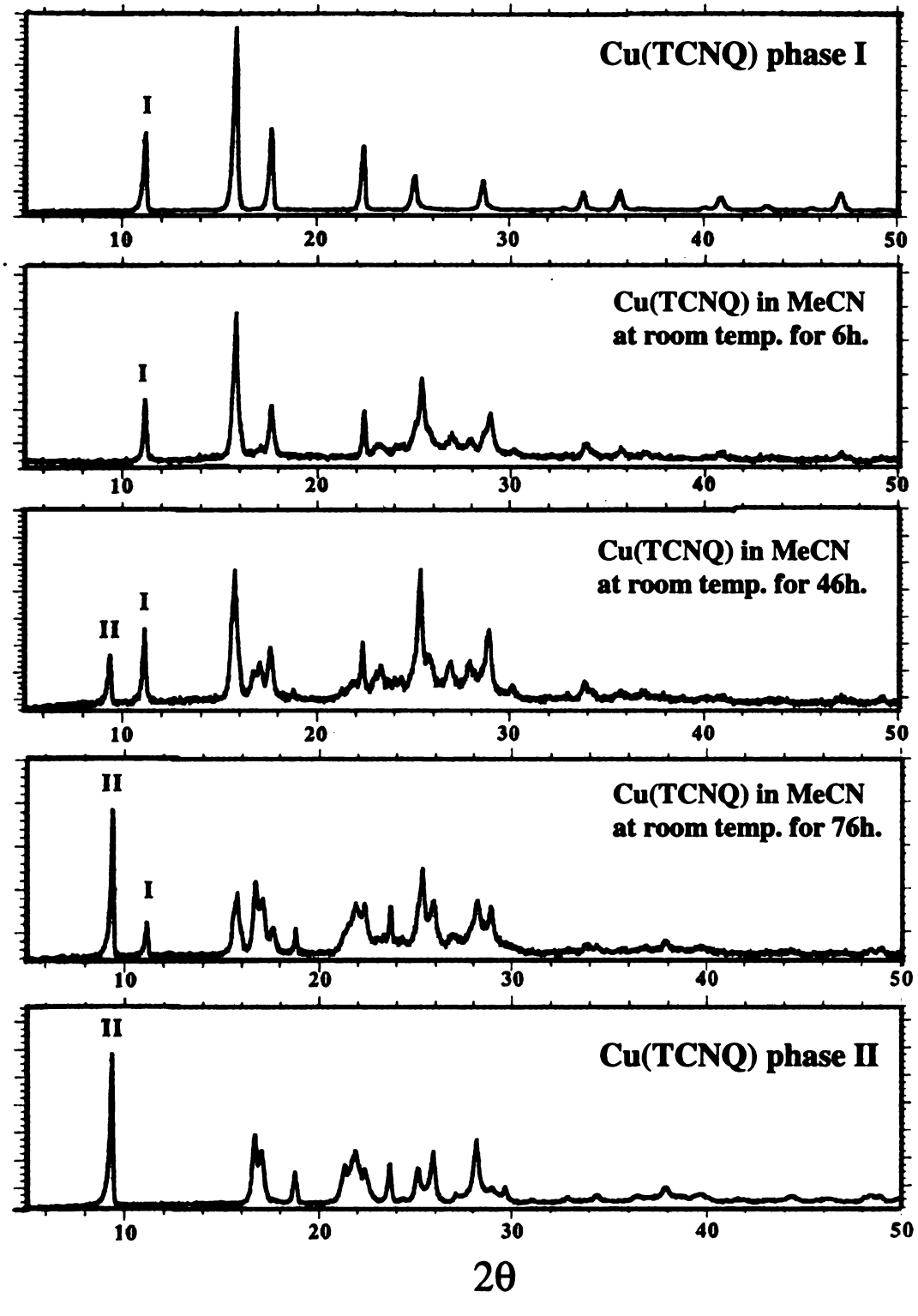

Figure 4. X-ray powder diffraction patterns of the conversion of Cu(TCNQ) phase I to phase II at varying time intervals.[38] (Hanhua Zhao)

During the course of the controversial studies of Cu(TCNQ), a similar compound, Ag(TCNQ), was structurally characterized and subjected to magnetic measurements.[39] Crystals grown by electrochemical means exhibit a structure similar to phase I of Cu(TCNQ), in that a pseudo four-fold coordination of TCNQ is exhibited about the metal ion. The distorted tetrahedral coordination, depicted in Figure 5, is similar to that found in $Cs_2(TCNQ)_3$. Along the *a* axis, there are two independent parallel stacks of TCNQ molecules. The conductivity for Ag(TCNQ) is 3.6 X 10-4 Ω^{-1} cm^{-1}, which is much lower than that of Cu(TCNQ). The magnetic behavior was reported to follow Curie paramagnetism. Only one phase of Ag(TCNQ) has been reported, although polymorphism should be possible due to its structural similarity to Cu(TCNQ).

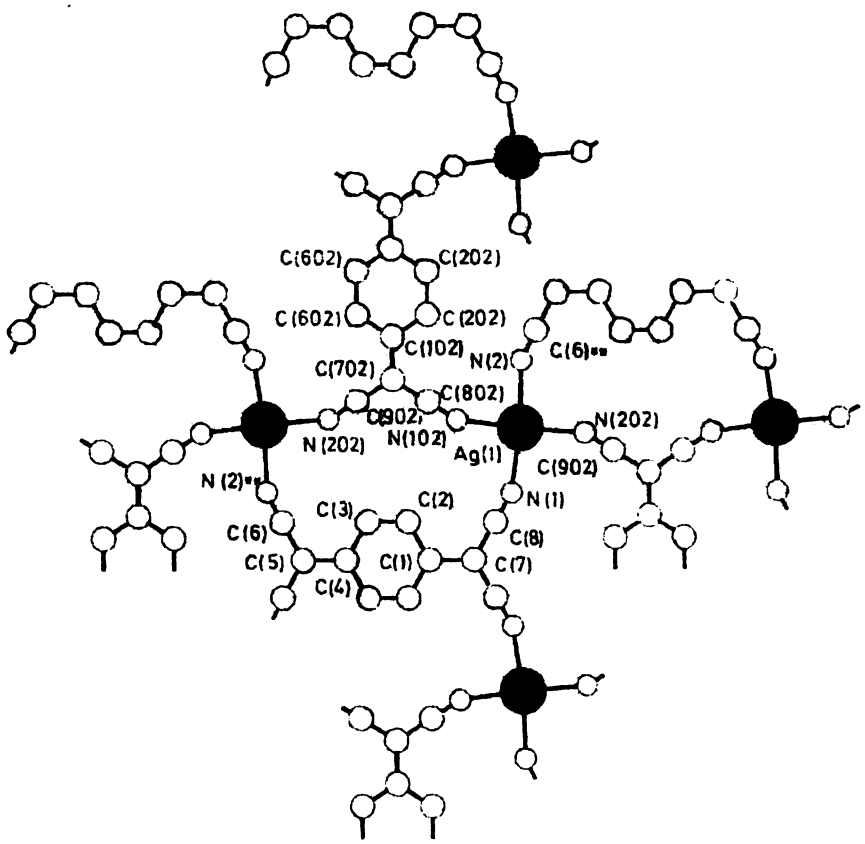

Figure 5. The coordination environment of Ag(TCNQ).[39]

The focus of this project is the design and synthesis of "hybrid" polymeric materials using transition metals and TCNQ with the intention of studying their magnetic properties. In chapter II, the synthesis and characterization of the two phases of Ag(TCNQ), one of them previously known, as well as the structural characterization of the novel $Ag(TCNQF_4)$ material will be presented. Chapter III details the further expansion of the use of the $TCNQ^-$ ligand with divalent first row transition metals (M^{2+}= Mn, Fe, Co, and Ni). These were targeted due to the presence of multiple unpaired electrons being available to interact with the S = 1/2 spin state of $TCNQ^-$. The final chapter, Chapter IV, focuses on the development of procedures for the isolation of the two components of these bulk products. The previously reported bulk product, $Mn(TCNQ)_2(MeOH)_2$, was investigated in an effort to separate the two crystalline phases, $[Mn(TCNQ)(TCNQ\text{-}TCNQ)_{0.5}(MeOH)_2]_\infty$ and an "all σ-dimer phase", $[Mn(TCNQ\text{-}TCNQ)(MeOH)_4]_\infty$. Additionally, the bulk phase $Mn(TCNQ)_2(H_2O)_2$ phase was checked for multiple phases and it was found that a second phase is produced in addition to the reported one. Furthermore, the possible synthetic conversion of three similar bulk products $Mn(TCNQ)_2(MeOH)_2$ and $Mn(TCNQ)_2(H_2O)_2$ to the magnetic material, $Mn(TCNQ)_2$ will be discussed.

References:

1. McCoy, H. N.; Moore, W. C. *J. Am. Chem. Soc.* **1911**, *33*, 273.
2. Acker, D. S.; Harder, R. J.; Hertler, W. R.; Mahler, W.; Melby, L. R.; Bensin, R. E.; Mochel, W. E. *J. Am. Chem. Soc.* **1960**, *82*, 6408.
3. (a) Jérome, D. *Science* **1991**, *252*, 1509. (b) Torrance, J. B. *Acc. Chem. Res.* **1979**, *12*, 79. (c) Bryce, M. R. *Chem. Soc. Rev.* **1991**, *20*, 355. (d) Williams, J. M.; Schultz, A. J.; Geiser, U.; Carlson, K. D.; Kini, A. M.; Wang, H. H.; Kwok, W. - K.; Wangbo, M. - H.; Schirber, J. E. *Science*, **1991**, *252*, 1501.
4. Melby, L. R.; Harder, R. J.; Hertler, W. R.; Mahler, W.; Benson, R. E.; Mochel, W. E. *J. Am. Chem. Soc.* **1962**, *84*, 3374.
5. (a) Manriquez, J. M.; Yee, G. T.; McLean, S.; Epstein, A. J.; Miller, J. S. *Science* **1991**, *252*, 1415. (b) Tamaki, H.; Zhuang, Z. J.; Matsumoto, N.; Kida, S.; Koikawa, M.; Achiwa, N.; Hashimoto, Y.; Okawa, H. *J. Am. Chem. Soc.* **1992**, *114*, 6974. (c) Stumpf, H. O.; Pei, Y.; Kahn, O.; Sletten, J.; Renard, J. P. *J. Am. Chem. Soc.* **1993**, *115*, 6738. (d) Inoue, K.; Iwamura, H. J. *J. Am. Chem. Soc.* **1994**, *116*, 3173. (e) Ohba, M.; Maruono, N.; Okawa, H.; Enoki, T.; Latour, J.- M. *J. Am. Chem. Soc.* **1994**, *116*, 11566. (f) Kahn, O. In *Molecular Magnetism: From Molecular Assemblies to the Devices*; NATO ASI Series E321; Coronado, E.; Delhaes, P.; Gatteschi, D.; Miller, J. S., Eds; Kluwer: Dordrecht, 1996; p. 243-288. (g) Decurtins, S.; Schmalle, H. W.; Schneuwly, P.; Zheng, L. - M.; Ensling, J.; Hauser, A. *Inorg. Chem.* **1995**, *34*, 5501. (h) Miyasaka, H.; Matsumoto, N.; Okawa, H.; Re, N.; Gallo, E.; Floriani, C. *Angew. Chem., Int. Ed. Engl.* **1995**, *34*, 1446. (i) Ohba, M.; Okawa, H.; Ito, T.; Ohto, A. J. *J. Am. Chem. Soc., Chem. Commun.* **1995**, 1545. (j) Michaut, C.; Ouahab, L.; Bergerat, P.; Kahn, O.; Bousseksou, A. *J. Am. Chem. Soc.* **1996**, *118*, 3610. (k) de Munno, G.; Poerio, T.; Viau, G.; Julve, M.; Loret, F.; Journaux, Y.; Riviere, E. *Chem. Commun.* **1996**, 2587.
6. (a) Aumüller, A.; Erk, P.; Klebe, G.; Hünig, S.; von Schütz, J.; Werner, H. *Angew. Chem., Int. Ed. Engl.* **1986**, *25*, 740. (b) Aumüller, A.; Erk, P.; Hünig, S. *Mol. Cryst. Liq. Cryst.* **1988**, *156*, 215. (c) Aumüller, A.; Erk, P.; Hünig, S. *Mol. Cryst. Liq.*

Cryst. Inc. Nonlin. Opt. **1988**, *156*, 215. (d) Erk, P.; Gross, H. - J.; Hünig, U. L.; Meixner, H.; Werner, H. - P.; von Schütz, J. U.; Wolr, H. C. *Angew. Chem., Int. Ed. Engl.* **1989**, *28*, 1245. (e) Kato, R.; Kobayashi, H.; Kobayashi, A. *J. Am. Chem. Soc.* **1989**, *111*, 5224. (f) Sinzger, K.; Hünig, S.; Jopp, M.; Bauer, D.; Beitsch, W.; von Schütz, J. U.; Wolf, H. C.; Kremer, R. K.; Metzenthin, T.; Bau, R.; Khan, S. I.; Lindbaum, A.; Lengauer, C. L.; Tillmanns, E. *J. Am. Chem. Soc.* **1989**, *115*, 7696. Aumüller, A.; Erk, P.; Hünig, S.; Hädicke, E.; Peters, K.; von Schnering, H. G. *Chem. Ber.* **1991**, *124*, 2001.

7. Kaim, W.; Moscherosch, M. *Coor. Chem. Rev.* **1994**, *129*, 157.
8. Wheland, R. C.; Martin, E. L. *J. Org. Chem.* **1975**, *40*, 3101.
9. Bryce, M. R. *Chem. Soc. Rev.* **1991**, *20*, 355.
10. Bardeen, J.; Cooper, L. N.; Schrieffer, J. R. *Phys. Rev.* **1957**, *108*, 1175.
11. There are different conventions used in the description of magnetic interaction. See, for example, (a) Carlin, R. L. *Magnetochemistry*, Springer-Verlag: Berlin Heidelberg, Chapter 5, **1986**. (b) Mattis, D. C. *The Theory of Magnetism*, Springer-Verlag: New York, **1981**; Vol. 1. The convention in this thesis follows the convention used in reference (a).
12. (a) Kahn, O. *Structure and Bonding*, **1987**, *68*, 89. (b) Kahn, O. *Angew. Chem., Int. Ed.* **1985**, *24*, 834.
13. Miller, J. S.; Epstein, A. J. *Chemistry & Industry* **1996**, 49.
14. Torrance, J. B. *J. Am. Chem. Soc.* **1979**, *12*, 79.
15. Wudl, F.; Smith, G. M.; Hufnagel, E. J. *J. Chem. Soc., Chem. Commun.* **1970**, 1453.
16. Hünig, S.; Kiesslich, G.; Scheutzow, D.; Zahradnik, R.; Carsky, P. *Int. J. Sulfur Chem. Part C.* **1971**, 109.
17. Coppens, P. *J. Chem. Soc., Chem. Commun.* **1971**, 889.
18. Wudl, F.; Wobschall, D.; Hefnagel, E. J. *J. Am. Chem. Soc.* **1972**, *94*, 670.
19. (a)Ferraris, J.; Cowan, D. O.; Walatka, V. V.; Perlstein, J. H. *J. Am. Chem. Soc.* **1973**, *95*, 948. (b)Coleman, L. B.; Cohen, M. J.; Sandman, D. J.; Yamagishi, F. G.; Garito, A. F.; Heger, A. J. *J. Solid State Commun.* **1973**, *12*, 1125.
20. Engler, E. M.; Patel, V. V. *J. Am. Chem. Soc.* **1974**, *96*, 7376.
21. Bloch, A. N.; Cowan, D. O.; Benchgaard, K.; Pyke, R. E.; Banks, R. H. *Phys. Rev.*

Lett. **1975**, *34*, 1561.

22. (a) Jérome, D.; Manzand, A.; Ribault, M.; Benchgaard, K. *J. Phys. Lett.* **1980**, L95. (b)Benchgaard, K.; Jacobsen, C. S.; Mortensen, K.; Pendersen, H. J.; Thorup, N. *Solid State Commun.* **1980**, *33*, 119.
23. (a) Wudl, F.; Thomas, G. A.; Nalewajek, D.; Hauser, J. J.; Lee, P. A.; Poehler, T. O. *Phys. Rev. Lett.* **1980**, *45*, 829. (b) Scott, J. C.; Pendersen, H. J.; Benchgaard, K. *Phys. Rev. Lett.* **1980**, *45*, 2125.
24. (a) Parkin, S. S. P.; Engler, E. M.; Schumaker, R. R.; Laiger, R.; Lee, V. Y.; Scott, J. C.; Greene, R. L. *Phys. Rev. Lett.* **1983**, *50*, 270. (b) Yagubskii, E. B.; Schegolev, I. F.; Laukhin, V. N.; Karatsovnik, P. A.; Karatsovnik, M. V.; Zvarykina, A. V.; Buravov, L. I. *J.E.T.P. Lett. (Engl. Trans.)* **1984**, *39*, 12. (c) Schirber, J. E.; Azevado, L. J.; Kwak, J. K.; Venturini, E. L.; Leung, P. C. W.; Beno, M. A.; Wang, H. H.; Williams, J. M. *Phys. Rev. B.* **1986**, *33*, 1987. (d) Williams, J. M.; Kini, A. M.; Wang, H. H.; Carlson, K. D.; Geiser, U.; Montgomery, L. K.; Pyrka, G. J.; Watkins, D. M.; Kommers, J. K.; Boryschuk, S. J.; Crouch, A. V.; Kwok, W. K.; Schirber, J. E.; Overmeyer, D. L.; Jung, D.; Whangbo, M. - H. *Inorg. Chem.* **1990**, *29*, 3274.
25. Pei, Y.; Verdaguer, M.; Sletten, J.; Renard, J. P. *J. Am. Chem. Soc.* **1986**, *108*, 7428.
26. Miller, J. S.; Calabrese, J. C.; Epstein, A. J.; Bigelow, W.; Zhang, J. H.; Reiff, W. M. *J. Chem. Soc., Chem. Commun.* **1986**, 1026.
27. (a) Miller, J. S.; Epstein, A. J. *J. Am. Chem. Soc.* **1987**, *109*, 3850. (b) Kollmar, C.; Kahn, O. *Acc. Chem. Res.* **1993**, *26*, 259.
28. (a) Miller, J. S.; Zhang, J. H.; Reiff, W. M. *J. Am. Chem. Soc.* **1987**, *109*, 4584. (b) Miller, J. S.; Epstein, A. J.; Reiff, W. M. *Science* **1988**, *240*, 40. (c) Miller, J. S.; Epstein, A. J.; Reiff, W. M. *Acc. Chem. Res.* **1988**, *21*, 114. (d) Miller, J. S.; Calabrese, J. C.; Epstein, A. J. *Inorg. Chem.* **1989**, *28*, 4230. (e) Miller, J. S.; Glatzhofer, D. T.; O'Hare, D. M.; Reiff, W. M.; Chakraborty, A.; Epstein, A. J. *Inorg. Chem.* **1989**, *28*, 2930. (f) Broderick, W. E.; Thompson, J. A.; Day, E. P.; Hoffman, B. M. *Science* **1990**, *249*, 401.
29. (a) Cayton, R. H.; Chisholm, M. H.; Darrington, F. D. *Angew. Chem., Int. Ed. Engl.* **1990**, *29*, 1481. (b) Stoner, T. C.; Dallinger, R. F.; Hopkins, M. D.; *J. Am. Chem. Soc.* **1990**, *112*, 5651. (c) Bartley, S. L.; Dunbar, K. R. *Angew. Chem., Int. Ed. Engl.*

1991, *103*, 447. (d) Cayton, R. H.; Chisholm, M. H.; Huffman, J. C.; Lobkovsky, E. B. *J. Am. Chem. Soc.* **1991**, *113*, 8709. (e) Huckett, S. C.; Arrington, C. A.; Burns, C. J.; Clark, D. L.; Swanson, B. I. *Synt. Met.* **1991**, *41-43*, 2769. (f) Dunbar, K. R. *J. Cluster Science* **1994**, *5*, 125. (g) Dunbar, K. R.; Ouyang, X. *Mol. Cryst. Liq. Cryst.* **1995**, *273*, 21.

30. (a) Gross, R.; Kaim, W. *Angew. Chem., Int. Ed. Engl.* **1987**, *26*, 251. (b) Olbrich-Deussner, B.; Gross, R.; Kaim, W. *J. Organomet. Chem.* **1989**, *366*, 155. (c) Gross-Lannert, R.; Kaim, W.; Olbrich-Deussner, B. *Inorg. Chem.* **1990**, *29*, 5046. (d) Schewenderski, B.; Kaim, W.; Olbrich-Deussner, B.; Roth, T. *J. Organomet. Chem.* **1992**, *440*, 145.
31. (a) Ballester, L.; Barrel, M. C.; Gutiérrez, A.; Jiménez-Aparicio, R.; Martínez-Muyo, J. M.; Perpiñan, M. F.; Monge, M. A.; Ruíz-Valero, C. *J. Chem. Soc., Chem. Commun.* **1991**, 1396. (b) Humphrey, D. G.; Fallon, G. D.; Murray, K. S. *J. Chem. Soc., Chem. Commun.* **1998**, 1356.
32. (a) Bell, S. E.; Field, J. S.; Haines, R. J.; Moscherosch, M.; Matheis, W.; Kaim, W. *Inorg. Chem.* **1992**, *31*, 3269. (b) Bell, S. E.; Field, J. S.; Haines, R. J.; Sundermeyer, J. *J. Organomet. Chem.* **1992**, *427*, C1.
33. (a) Demerseman, B.; Pankowske, M.; Bouquet, G; Bigorgne, M.; *J. Organomet. Chem.* **1976**, *117*, C10. (b) Ittel, S. D.; Tolman, C. A.; Krusic, P. J.; English, A. D.; Jesson, J. P. *Inorg. Chem.* **1978**, *17*, 3432. (c) Booth, B. L.; McAuliffe, C. A.; Stanley, G. L.; *J. Chem. Soc. Dalton Trans.* **1982**, 535. (d) Rockenbauer, A.; Speier, G.; Szabo, L. *Inorg. Chim. Acta* **1992**, *201*, 5.
34. (a) Ewan, A.; McQueen, D.; Blake, A. J.; Stephenson, T. A.; Schroder, M.; Yellowlees, L. J. *J. Chem. Soc., Chem. Commun.* **1988**, 1533. (b) Braunwarth, H.; Huttner, G.; Zsolnai, L. *J. Organomet. Chem.* **1989**, *372*, C23. (c) Bunn, A. G.; Carroll, P. J.; Wayland, B. B. *Inorg. Chem.* **1992**, *31*, 1297. (d) Miller J. S.; Calabrese, J. C.; McLean, R. S.; Epstein, A. J. *Adv. Mater.* **1992**, *4*, 498. (e) Yee, G. T.; Calabrese, J. C.; Vazquez, C.; Miller, J. S. *Inorg. Chem.* **1993**, *32*, 377. (f) Cotton, F. A.; Kim, Y.; Ren, T. *Ployhedron* **1993**, *12*, 607.
35. (a) Fritchie, C. J., Jr.; Arthur, P. *Acta Crystallogr.* **1966**, *21*, 139. (b) Hoekstra, A.; Spoelder, T.; Vos, A. *Acta Crystallogr.* **1972**, *B28*, 14. (c) Konno, M.; Saito, Y. *Acta*

Crystallogr. **1974**, *B30*, 1294. (d) Murakami, M.; Yoshimura, S. *Bull. Chem. Soc. Jpn.* **1975**, *48*, 157. (e) Konno, M.; Saito, Y. *Acta Crystallogr.* **1975**, *B31*, 2007. (f) Konno, M.; Ishii, T.; Saito, Y. *Acta Crystallogr.* **1977**, *B33*, 763.

36. Siemons, W. J.; Bierstedt, P. E.; Kepler, R. G. *J. Chem. Phys.* **1963**, *39*, 3523.
37. (a) Potember, R. S.; Poehler, T. O.; Cowan, D. O. *Appl. Phys. Lett.* **1979**, *34*, 405. (b) Potember, R. S.; Poehler, T. O.; Rappa, A.; Cowan, D. O.; Bloch, A. N. *J. Am. Chem. Soc.* **1980**, *102*, 3659. (c) Potember, R. S.; Poehler, T. O.; Cowan, D. O.; Brant, P.; Carter, F. L.; Bloch, A. N. *Chem. Scr.* **1981**, *17*, 219. (d) Kamistos, E. I.; Risen, W. M., Jr. *Solid State Commun.* **1982**, *42*, 561. (e) Potember, R. S.; Poehler, T. O.; Cowan, D. O.; Carter, F. L.; Brant, P. I. In *Molecular Electronic Devices*; Carter, F. L., Ed.; Marcel Dekker: New York, 1982; p. 73. (f) Potember, R. S.; Poehler, T. O.; Benson, R. C. *Appl. Phys. Lett.* **1982**, *41*, 548. (g) Potember, R. S.; Poehler, T. O.; Rappa, A.; Cowan, D. O.; Bloch, A. N. *Synth. Met.* **1982**, *4*, 371. (h) Kamitsos, E. I.; Risen, W. M. *Solid State Commun.* **1983**, 45, 165. (i) Kamitsos, E. I.; Risen, W. M.*J. Chem. Phys.* **1983**, 79, 477. (j) Kamitsos, E. I.; Risen, W. M. Jr. *J. Chem. Phys.* **1983**, 79, 5808. (k) Benson, R. C.; Hoffman, R. C.; Potember, R. S.; Bourkoff, E.; Poehler, T. O. *Appl. Phys. Lett.* **1983**, *41*, 548. (l) Poehler, T. O.; Potember, R. S.; Hoffman, R.; Benson, R. C.; *Mol. Cryst. Liq. Cryst.* **1984**, *107*, 91. (m) Kamistos, E. I.; Risen, W. M., Jr. Mol. *Cryst. Liq. Cryst.* **1986**, *134*, 31. (n) Potember, R. S.; Poehler, T. O.; Hoffman, R. C.; Speck, K. R.; Benson, R. C. In *Molecular Electronic Devices II*; Carter, F. L., Ed.; Marcel Dekker: New York, 1987; p. 91 (o) Wakida, S.; Ujihira, Y. *J. Appl. Phys.* **1988**, *27*, 1314. (p) Hoffman, R. C.; Potember, R. S. *Appl. Opt.* **1989**, *28* (7), 1417. (q) Duan, H.; Mays, M. D.; Cowan, D. O.; Kruger, J. *Synth. Met.* **1989**, *28*, C675. (r) Sato, C.; Wakamatsu, S.; Tadokoro, K.; Ishii, K. *J. Appl. Phys.* **1990**, *68* (12) 6535. (s)Yamaguchi, S.; Viands, C. A.; Potember, R. S. *J. Vac. Sci. Technol.* **1991**, *9*, 1129. (t) Hua, Z, Y.; Chen, G. R. *Vacuum* **1992**, *43*, 1019. (u) Hoagland, J. J.; Wang, X. D.; Hipps, K. W. *Chem. Mater.* **1993**, *5*, 54. (v) Liu, S. G.; Liu, Y. Q.; Wu, P. J.; Zhu, D. B. *Chem. Mater.* **1996**, *8*, 2779. (w) Liu, S. G.; Liu, Y. Q.; Zhu, D. B. *Thin Solid Films* **1996**, *280*, 271. (x) Sun, S. Q.; Wu, P. J.; Zhu, D. B. *Solid State Commun.* **1996**, *99*, 237. (y)

Liu, S. G.; Liu, Y. Q.; Wu, P. J.; Zhu, D. B.; Tian, H.; Chen, K. C. *Thin Solid Films* **1996**, *289*, 300.

38. Heintz, R. A.; Zhao, H.; Ouyang, X.; Grandinetti, G.; Cowen, J.; Dunbar, K. R. *Inorg. Chem.* **1999**, *38*, 144.
39. Shields, L. *J. Chem. Soc., Faraday Trans. 2* **1985**, *81*, 1.
40. Zhao, H.; Heintz, R. A.; Ouyang, X.; Dunbar, K. R. *Chem. Mater.* **1999**, *11*, 736.

Chapter II

Novel Polymeric Crystalline Phases of Ag(TCNQ) and Ag(TCNQF$_4$): Structures and Magnetic Studies

Introduction

The use of transition metal precursors as building blocks in coordination compounds allows for impressive structural diversity and opens up a wealth of potential applications for porous[1], magnetic[2], and conducting[3] solids.[1-5] In many cases, knowledge of the geometry of the ligand and the coordination environment of the metal has allowed synthetic chemists to design new strategies and to predict the resulting structural architecture. This concept works well when polymorphism is not an issue, but this is unfortunately not the case with π-stacked charge-transfer materials. Conducting charge transfer materials composed of stacks of donor cations and organic radical acceptors such

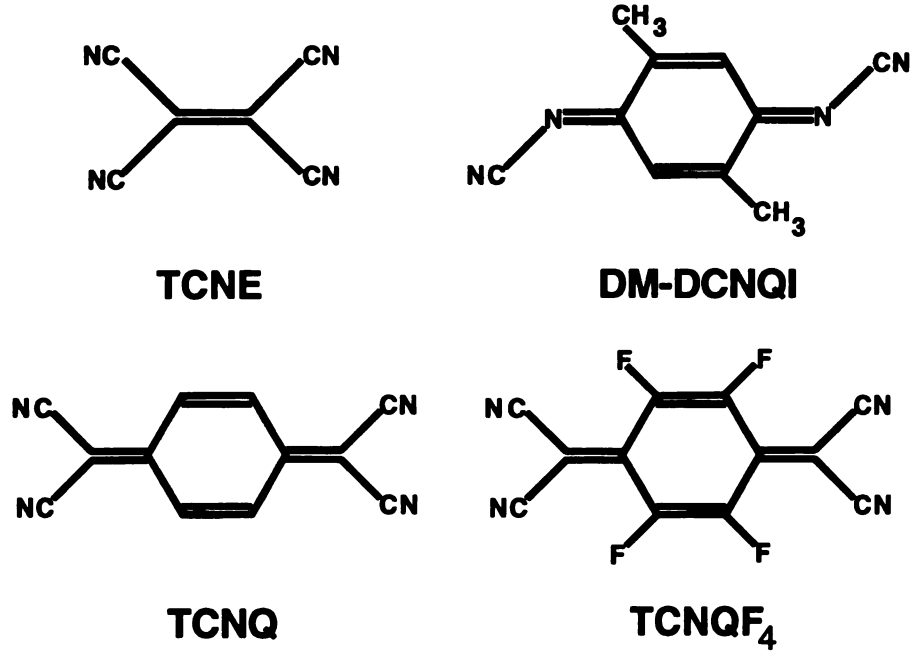

Figure 6. Organonitrile acceptor molecules used as ligands in metallopolymers.

as those exhibited in Figure 6 have been under investigation for over forty years, yet there is still an element of structural serendipity that cannot be denied.[3,5] In addition to classical organic or organometallic donor/acceptor salts that involve π-stacks, polymeric materials composed of a metal ion directly bonded to the organic radical may be envisioned. Such direct bonding between the metal donor and the organic acceptor allows for a combination of the unique characteristics of the transition metal (optical, magnetic, *etc.*,) with the conducting properties of organic radical stacks.[5a,c-h,j,m-p,6] A foremost example of this approach is the use of 2,5-DM-DCNQI (Figure 6b) with Cu (I,II) in the assembly of tetrahedral metal based, three-dimensional networks.[3a] The mixed-valence material, $Cu(DM\text{-}DCNQI)_2$, exhibits an extraordinarily high metallic conductivity ($5x10^5$ S cm^{-1} at 3.5 K) which is related to the presence of the 1-D stacked DCNQI radicals as well as to interactions of the metal with the ligand via metal d and ligand p orbital overlap. The latter interactions serve to increase the dimensionality of the system and lead to increased conductivities in two-dimensions. The $Cu(DCNQI)_2$ system is an excellent example of how inorganic/organic hybrid materials of the coordination polymer type can be competitive in the area of highly conducting materials.[3]

The incorporation of "bare" metal ions into networks with organic acceptors spawned technological development of binary metal/TCNQ films that behave as switches. Two of the most well-investigated materials in this regard are Cu(TCNQ) ($TCNQ^-$ = 7,7,8,8-tetra-cyanoquinodimethanide) and Ag(TCNQ) which exhibit electric-field-induced bistable switching under certain conditions.[7,8] Specifically, the application of an electric field across a thin film of these materials leads to an observable "switching" from a high- to a low-resistance state (Figure 7) at a critical threshold potential.[8a] For over

twenty years there has been intense debate in the literature concerning the mechanism of the switching as well as the role of film growth conditions on the resulting properties. Earlier this year, our group reported the X-ray structures of two different forms of Cu(TCNQ) with very different magnetic and conducting

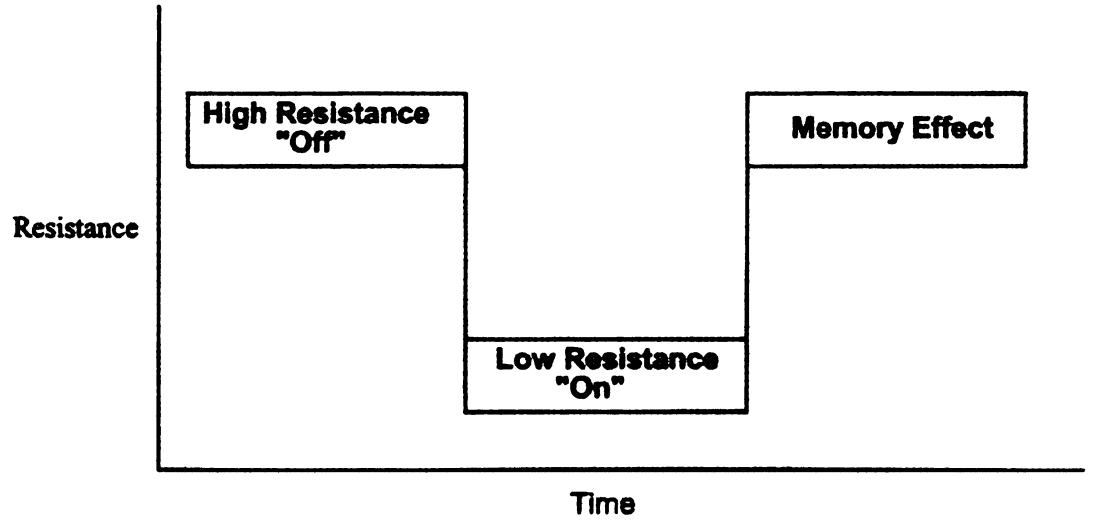

Figure 7. Schematic drawing showing the change of resistance over time for Cu(TCNQ) films.

properties.[9] This unrecognized polymorphism in the Cu system is unfortunate, as it led to many years of fruitless work on mixtures of two compounds. Clearly, further evaluation of other metal/TCNQ materials is in order. A search of the literature revealed that the switching behavior of both Cu and *Ag* devices has been studied at the same time, but that Ag(TCNQ) films have not been scrutinized as carefully as the Cu(TCNQ) system. In terms of structural evidence, however, until recently the Ag analog was better characterized. In 1985, Shields reported the single-crystal X-ray structure of a Ag(TCNQ) crystal obtained by electrochemical synthesis.[7] No reports of powder data or comments on the singularity of the electrochemical form of Ag(TCNQ) have appeared

since this time, however, therefore it is logical to ask if the reported form of Ag(TCNQ) is the only stable phase. In this paper we explore the issue of polymorphism in Ag(TCNQ) and in the corresponding Ag($TCNQF_4$) material. A combination of infrared spectroscopy, electron microscopy, X-ray crystallography, and magnetic susceptibility methods were used to characterize the new compounds.

Experimental

A. Synthesis

Reactions were carried out under a dinitrogen atmosphere unless otherwise indicated. Acetonitrile was dried over 3 Å molecular sieves and distilled under a nitrogen atmosphere prior to use. Ag(BF_4) was purchased from Aldrich Chemical Company, and TCNQ was purchased from TCI Chemical Company and recrystallized from hot acetonitrile. The salt [*n*-Bu_4N][TCNQ][14] and neutral $TCNQF_4$[15] were prepared according to literature methods, while preparation of the reduced anion salts, Li($TCNQF_4$) and [*n*-Bu_4N][$TCNQF_4$] were adapted from the original preparations of the corresponding TCNQ salts. Since Ag cation salts are prone to decomposition to metallic Ag, reaction flasks were covered with aluminum foil prior to and during reactions to prevent light induced reduction to Ag^+ to Ag.

a) Bulk Synthesis of Ag(TCNQ) Phase I, (1).

$Ag(BF_4)$ (0.20 g, 1.03 mmol) was dissolved in 20 mL of acetonitrile and filtered through Celite under a nitrogen atmosphere. Separately, [*n*-Bu_4N][TCNQ] (0.405 g, 0.906 mmol) was dissolved in 20 mL of acetonitrile and slowly added to the $Ag(BF_4)$ solution. A blue-purple microcrystalline product precipitated immediately, and, after two minutes, it was collected by filtration, washed with 10 mL of acetonitrile followed by 20 mL of diethyl ether and dried *in vacuo*; yield 0.254 mg, 90%. Anal. Calcd for $C_{12}H_4N_4Ag$: C, 46.19; H, 1.29; N, 17.95; Found: C, 45.38; H, 1.32; N, 17.51. Characteristic IR data (Nujol mull, KBr plates, cm^{-1}): ν(C≡N), 2199s, 2194sh, 2184s, 2161s; ν(C=C), 1507s; δ(C-H), 824s.

b) Bulk Synthesis of Ag(TCNQ) Phase II, (2) from Ag metal.

Ag powder (0.18 g, 1.67 mmol) was suspended in 150 mL of acetonitrile, TCNQ (1 g, 4.89 mmol) was added, and the mixture was stirred in the dark for 2 days. After filtration, the reddish purple microcrystalline product was washed with acetonitrile and suspended in a 150 mL TCNQ/acetonitrile solution (0.5 g, 2.44 mmol) to remove any unreacted Ag metal. After additional days of stirring in the dark, the solution was decanted to remove any small particles suspended in the solution. The product was washed repeatedly with acetonitrile, filtered and dried *in vacuo*; yield 0.45 g, 86.5%. Anal. Calcd for $C_{12}H_4N_4Ag$: C, 46.19; H, 1.29; N, 17.95; Found: C, 45.94; H, 1.38; N, 17.84. Characteristic IR data (Nujol mull, KBr plates, cm^{-1}): ν(C≡N), 2202sh, 2185s, 2170s, 2131sh; ν(C=C), 1505s; δ(C-H), 820s.

c) Synthesis of [*n*-Bu_4N][TCNQ] (3).

A quantity of Li(TCNQ) (1.48 g, 0.007 mol) was dissolved in 100 mL of hot distilled water. In a separate flask an excess of [*n*-Bu_4N]I (5.2 g, 0.0140 mol) was dissolved in 600 mL of boiling distilled water. Upon the addition of Li(TCNQ) to the [*n*-Bu_4N]I solution, an instantaneous reaction ensued with the precipitation of a dark purple solid. The stirred solution was warmed for one hour, after which time the product was collected by vacuum filtration. The dark purple powder was washed with several aliquots of hot water followed by diethyl ether, and dried *in vacuo*: yield, 3.1 g (99%). The product was recrystallized as follows. The crude product was dissolved in a minimal volume of dichloromethane (~100 mL), and the solution was dried with anhydrous magnesium sulfate. After filtration, the solution was reduced in volume (~30 mL), and an equivalent volume of hexanes was added to induce crystallization. After the excess dichloromethane had been evaporated, the dark purple crystalline product was collected by vacuum filtration, washed with copious quantities of hexanes and dried *in vacuo*: yield, 2.96 g, (95%). Anal. Calcd for $C_{28}H_{36}N_5$: C, 75.29; H, 9.03; N, 15.68; Found: C, 73.95; H, 9.52; N, 15.32. Characteristic IR data (Nujol mull, KBr plates, cm^{-1}): ν(C≡N), 2187 sh, 2181 s, 2160 sh, 2157 s; ν(C=C), 1507 s; δ(C-H), 824 m.

d) Synthesis of [*n*-Bu_4N][$TCNQF_4$] (4).

[*n*-Bu_4N]I (1.69 g, 0.458 mmol) was dissolved in 200 mL of hot distilled water. Subsequently, Li[$TCNQF_4$] (0.650 g, 0.230 mmol) was dissolved in 50 mL of distilled

water. Upon addition of the Li[TCNQF$_4$] solution to the [*n*-Bu$_4$N]I solution, a dark purple microcrystalline product immediately precipitated. After one hour of stirring, the product was collected by filtration. The crude product was dissolved in methylene chloride, dried with magnesium sulfate, and the solution was filtered. The volume was reduced by rotoevaporation, and 40 mL of hexanes was added to induce precipitation of the product. Crystals of [*n*-Bu$_4$N][TCNQF$_4$] suitable for X-ray structural determination were obtained directly from this procedure. To recover more product, the methylene chloride filtrate was then evaporated which gave an additional crop of dark purple crystals of [*n*-Bu$_4$N][TCNQF$_4$]. These were collected by filtration, washed with hexanes and dried *in vacuo*; yield 1.02 g, 86%. Anal. Calcd for $C_{28}N_5H_{36}F_4$: C, 64.84; H, 7.00; N, 13.50; Found: C, 64.11; H, 7.63; N, 12.36. Characteristic IR data (Nujol mull, KBr plates, cm^{-1}): ν(C≡N), 2197s, 2174s, 2154s, 2134sh; ν(C=C), 1506 sh, 1498 s.

e) Bulk Synthesis of Ag(TCNQF$_4$) (5).

Ag(BF$_4$) (0.135g, 0.693 mmol) was dissolved in 20 mL of acetonitrile and filtered through Celite, and, separately, [*n*-Bu$_4$N][TCNQF$_4$] (0.363, 0.70 mmol) was dissolved in 20 mL of acetonitrile. Both solutions were chilled to –20 °C and the solution of [*n*-Bu$_4$N][TCNQF$_4$] was added to Ag(BF$_4$) and stirred for two minutes. A dark blue purple microcrystalline powder was collected by filtration, washed with 10 mL of acetonitrile, followed by 20 mL of diethyl ether, and dried *in vacuo*; yield 0.238 g (92%). Anal. Calcd for $C_{12}F_4N_4Ag$: C, 37.53; H, 0.0; N, 14.95; Found: C, 37.12; H, 0.01; N, 14.92.

Characteristic IR data (Nujol mull, KBr plates, cm^{-1}): ν(C≡N), 2220s, 2213s, 2197s; ν(C=C), 1501s; ν(C-F), 1208m, 1154w.

B. Structural Studies

a) X-ray Structural Determination of [*n*-Bu_4N][$TCNQF_4$] (4).

A typical needle crystal of dimensions 0.80 × 0.12 × 0.10 mm^3 was mounted on the end of a glass fiber with silicone grease. A full sphere of data was collected at 173±(2) K for a [*n*-Bu_4N][$TCNQF_4$] crystal on a Siemens SMART 1K CCD area detector diffractometer with a graphite monochromated Mo Kα radiation (λ_α = 0.71073 Å). The frames were integrated in the Siemens SAINT software package, and the data were corrected for absorption using the SADABS program. The data were integrated in a $P2_1/n$ monoclinic cell setting a = 7.4244(15) Å, b = 20.212(4) Å, c = 19.758(4) Å, β = 97.32(3)°. The structure was solved using the SHELXS program, and refinement was carried out by full matrix least-squares calculations on F^2 using the SHELXL - 97 program. All the atoms were refined anisotropically to give final residuals of R1 = 0.0507 and a wR2 of 0.0946 at a resolution of 0.75 Å. The final refinement was based on 479 parameters and 35072 reflections, 7113 of which were unique. The highest peak in the final difference map was 0.224 $e^-/Å^3$.

b) X-ray Structural Determination of Ag($TCNQF_4$) (5).

A typical rectangular platelet crystal of dimensions 0.31 × 0.16 × 0.08 mm^3 was mounted on the end of a glass fiber with silicone grease. A hemisphere of data was

collected at 173±(2) K for a Ag(TCNQF$_4$) crystal on a Siemens SMART 1K CCD area detector diffractometer with a graphite monochromated Mo Kα radiation (λ_α = 0.71073 Å). The frames were integrated with the Siemens SAINT software package, and the data were corrected for absorption using the SADABS program. The data were integrated in a C2/c monoclinic cell setting a = 13.429(3) Å, b = 6.9331(14) Å, c = 25.735(5) Å, β = 116.66(3)°. The structure was solved using the SHELXS program and refinement was carried out by full matrix least-squares calculations on F^2 using the SHELXL-97 program. All the atoms were refined anisotropically to give final residuals of R1 = 0.0225 and a wR2 of 0.0586 at a resolution of 0.75 Å. The final refinement was based on 191 parameters and 6416 reflections, 2526 of which were unique. The highest peak in the final difference map was 0.811 $e^-/Å^3$.

C. Physical Measurements.

Infrared spectra were recorded as Nujol mulls on KBr plates using a Nicolet IR/42 FT-IR spectrometer. Field Emission Scanning Electron Microscopy (FESEM) measurements were performed on a Hitachi Ltd., Model S-4700II with a Tungsten filament housed in the W.M. Keck Microfabrication Facility located in the Department of Physics & Astronomy at Michigan State University. X-ray powder diffraction patterns were collected on a Rigaku RU200B X-ray powder diffractometer with Cu Kα radiation. The variable temperature magnetic susceptibility data were collected in the range 2-300 K using a Quantum Design, Model MPMS-5 SQUID magnetometer housed in the Physics & Astronomy Department at Michigan State University. The data were corrected for the

diamagnetism of the sample as evaluated from the Pascal constants[16] and for the sample holder.

Results and Discussion

The controversy over the phenomenon of the bistable switching ability of Cu(TCNQ) films[8a], along with our recent verification of two distinct Cu(TCNQ) phases[9] prompted us to study other related metal/TCNQ systems. Reports of switching behavior for devices containing Ag and organic acceptors[8b,g,n] such as $TCNQF_4$, 2,5-dimethoxy-7,7,8,8-tetracyanoquinodimethane ($TCNQ(OMe)_2$), 11,11,12,12-tetracyano-2,6-napthoquinodimethane (TNAP), and tetracyanoethylene (TCNE) point to this metal as a logical choice for synthetic and structural studies. To date, single crystal X-ray data have been published for one phase of Ag(TCNQ) phase II which was grown using electrochemical methods.[8] Since the stoichiometry of Ag(TCNQ) is identical to Cu(TCNQ), namely 1:1, it seemed a likely prospect to exhibit more than one polymorph as well. Indeed, during our investigation of the bulk synthesis of Ag(TCNQ) another phase was discovered, referred to as phase I, the existence of which is supported by X-ray powder diffraction, spectroscopic, and magnetic measurements. The original phase of Ag(TCNQ) discovered by Shields is designated as Phase II. Unlike the Cu(TCNQ) phases, which exhibit very different morphologies, both phases of Ag(TCNQ) exhibit similar needle morphologies. Powder diffraction reveals that the structures are different

and indexing reveals that phase I is tetragonal as opposed to phase II which is orthorhombic.

In addition to sorting out the polymorphism of the Ag(TCNQ) materials, we also extended this chemistry to $TCNQF_4$ ($TCNQF_4$: 2,3,5,6-tetrafluoro-7,7,8,8-tetracyanoquinodimethanide). Although there are several reports of structural[10], magnetic[11], and spectroscopic[12] studies of $TCNQF_4$ charge transfer salts in the literature, the present work constitutes the first structurally characterized metal/$TCNQF_4$ polymer. Analysis of the solid-state structure of $Ag(TCNQF_4)$ indicates that it is distinctly different from either phase of Ag(TCNQ) or the alkali metal TCNQ salts[13]. Interestingly, there appears to be only one phase of $Ag(TCNQF_4)$ which one obtains regardless of reaction conditions.

The starting material, $[n\text{-}Bu_4N][TCNQF_4]$, was also subjected to X-ray studies in order to compare the stacking motif of the $TCNQF_4$ anions in this simple organic salt with the patterns found in the Ag polymers.

A. Synthesis of Bulk Phases

The aims of this study were (1) to determine whether a second Ag(TCNQ) polymorph exists and (2) to obtain pure samples of the materials for physical properties measurements. In accord with the literature report, we verified that samples of Ag(TCNQ) can be prepared in bulk using electrochemical methods with Ag metal. (Eq. 1)

$$Ag + TCNQ \rightarrow Ag(TCNQ) \qquad \text{(Eq. 1)}$$

A more direct route is a simple metathesis reaction as shown in Eq. 2. This method is advantageous for several reasons: the metal and ligand are in the desired oxidation states,

the reagents are completely soluble, and the product precipitates upon formation which allows it to be separated from soluble by-products. Furthermore, this reaction leads to essentially quantitative yields.

$$Ag(BF_4) + [n\text{-}Bu_4N][TCNQ] \rightarrow Ag(TCNQ)\,(s) + [n\text{-}Bu_4N][BF_4] \qquad \text{(Eq. 2)}$$

Variations in reaction times and temperatures do not significantly alter the outcome of the reaction in Eq. 2. The favored product is the previously unrecognized phase of Ag(TCNQ) phase I (**1**). With very long reaction times and a large volume of solvent it is possible to pass from phase I to phase II, but the process is not clean, as large quantities of Ag metal are also formed in the process. It appears that the conversion involves a decomposition of phase I to Ag metal and neutral TCNQ, which then react to form phase II *in situ*. Isolation of pure phase II is not feasible by this method. The best route to phase II is, in fact, the direct reaction of Ag(s) and neutral TCNQ. (Eq. 3)

$$Ag\,(s) + TCNQ \rightarrow Ag(TCNQ)\,(s)\,(\mathbf{2}) \qquad \text{(Eq. 3)}$$

Interestingly, only one phase of $Ag(TCNQF_4)$ (**4**) appears to exist. Reaction conditions were varied in a manner similar to the Ag(TCNQ) chemistry, but all reactions yielded only one phase. Furthermore, slow electrolysis of $TCNQF_4$ at a Ag electrode yielded crystals whose structure is identical to that of the bulk product as judged by powder X-ray methods.

B. Infrared Spectroscopy

Infrared spectroscopy is a useful technique for characterizing TCNQ charge transfer salts, especially with respect to distinguishing the presence of TCNQ in it's neutral versus reduced forms.[5f] As expected, the IR spectra of the two phases of Ag(TCNQ) are similar, owing to their structural similarities and their basic formulation as compounds of $TCNQ^-$. Table 1 summarizes the pertinent data for compounds (**1** - **5**). In the ν(C≡N) region, several stretching modes indicate the presence of $TCNQ^-$. Ag(TCNQ) phase I exhibits strong, broad absorptions at 2199, 2194, 2187, and 2162 cm^{-1} while Ag(TCNQ) phase II shows a similar pattern but at slightly lower frequencies, *viz.*, 2202, 2185, 2170, 2131 cm^{-1}. These features are lower in energy than the ν(C≡N) stretch of neutral TCNQ which occurs at 2222 cm^{-1}, and are characteristic of $TCNQ^-$. $Ag(TCNQF_4)$ exhibits strong absorptions at 2220, 2212, 2197 cm^{-1} in accord with data for salts containing $TCNQF_4^-$.[18] Neutral $TCNQF_4$ occurs at 2227 cm^{-1}.[15] The ν(C=C) stretching region is characteristic for the TCNQ phenyl ring. The π-bond delocalization in the ring results in one strong (C=C) stretch ranging from 1500-1510 cm^{-1} for $TCNQ^-$. Ag(TCNQ) (phases I and II) and $Ag(TCNQF_4)$ spectra exhibit ν(C=C) features at 1507, 1505, and 1501 cm^{-1} respectively. The δ(C-H) bending mode is also a sensitive indicator of the presence of $TCNQ^-$, $TCNQ^{2-}$, and mixed-valence stacks of $TCNQ^-/TCNQ$.[19] Ag(TCNQ) phases I exhibits a weak absorption at 824 cm^{-1} while phase II exhibits a lower energy mode at 820 cm^{-1}. Both frequencies are within the range reported for reduced TCNQ. The absence of peaks corresponding to bound acetonitrile or $[BF_4]^-$ anions indicate that the material is composed solely of Ag+ and $TCNQ^-$ ions.

Table 1. IR data for Cu(TCNQ), Ag(TCNQ), Ag($TCNQF_4$), [*n*-Bu_4N][TCNQ], and [*n*-Bu_4N][$TCNQF_4$].

IR SPECTRAL DATA				
COMPOUND	ν(C≡N) (cm^{-1})	ν(C=C) (cm^{-1})	δ(C-H) (cm^{-1})	Refs.
Cu(TCNQ)				
phase I	2199 s, br; 2172 s	___	825 s	9
phase II	2211 s, 2172 s	___	825 s	9
Ag(TCNQ)	2199 s, 2194 sh, 2184 s,	1507 s	824 s	this work
phase I	2161 s			
phase II	2202 sh, 2185s, 2170 s,	1505 s	820 s	this work
	2131 sh			
Ag($TCNQF_4$)	2220 s, 2213 s, 2197 s	1501 s	___	this work
[*n*-Bu_4N][TCNQ]	2188 sh, 2180 s, 2162s ,	1507 s	824 s	this work
	2157 s			
[*n*-Bu_4N][$TCNQF_4$]	2197 s, 2174 s, 2157 s,	1506 sh,	___	this work
	2134 sh	1498 s		

C. Structural Studies

A determination of the solid-state structures of the metal/TCNQ materials is crucial to fully understanding their unusual switching behavior. Despite several attempts to obtain single crystals of Ag(TCNQ) phase I (**1**), small crystal size and/or twinning prevented a crystal structure analysis. X-ray powder diffraction, however, was very useful for discerning the differences between phase I and phase II. X-ray quality crystals of Ag($TCNQF_4$) (**5**) and the starting material, [*n*-Bu_4N][$TCNQF_4$] (**4**), was isolated and the data are presented here.

a) Field Emission Scanning Electron Microscopy (FESEM)

Microscopy techniques were very useful for viewing the morphological differences in the two phases of Cu(TCNQ).[9] FESEM images of Ag(TCNQ) phase I and II (shown in Figures 8 and 9 respectively) indicate that both exhibit needle-like morphologies, although it is clear that phase II is much more crystalline. The images of single crystals of $Ag(TCNQF_4)$ and $[n\text{-}Bu_4N][TCNQF_4]$ are illustrated in Figure 10. The rectangular morphology of $Ag(TCNQF_4)$ is distinct from the needle morphology of $[n\text{-}Bu_4N][TCNQF_4]$. Both crystals are large in size and thus diffract well. The single crystal of $Ag(TCNQF_4)$ is a representative size for those obtained through electrocrystallization, while the crystal of $[n\text{-}Bu_4N][TCNQF_4]$ is representative of those obtained in the bulk synthesis. Unfortunately, one must be careful when choosing crystals for X-ray analysis. It is apparent, especially with the crystal of $[n\text{-}Bu_4N][TCNQF_4]$, that a surface unevenness or growth of "daughter" crystals on the surface causes problems in data collection. A smooth, nicely shaped crystal is more suitable for structural analysis.

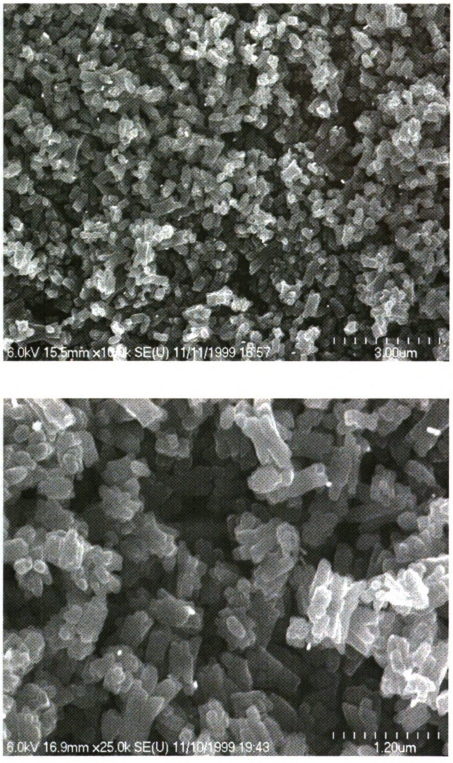

Figure 8. FESEM photographs of Ag(TCNQ) phase I at various magnifications.

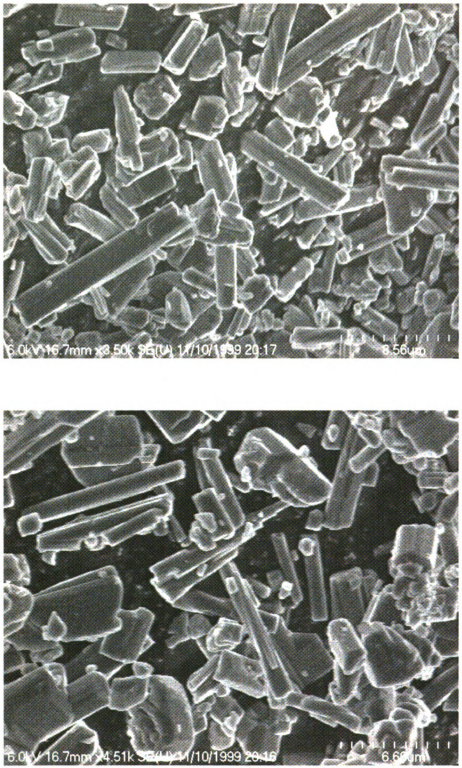

Figure 9. FESEM photographs of Ag(TCNQ) phase II at various magnifications.

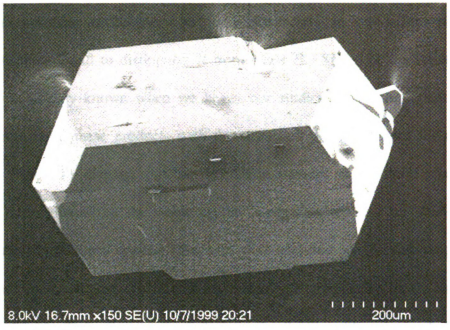

$Ag(TCNQF_4)$

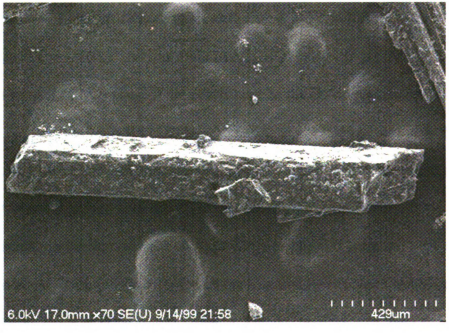

$[n\text{-}Bu_4N][TCNQF_4]$

Figure 10. FESEM images of $Ag(TCNQF_4)$ and $[n\text{-}Bu_4N][TCNQF_4]$.

b) Powder X-ray Diffraction of Chemically Prepared Phases.

X-ray powder diffraction was used extensively in our efforts to identify Ag(TCNQ) phase I and to distinguish it from phase II. Since the crystal structure of phase II was already known when we began our studies, it was important for us to compare both bulk phase products with the simulated powder pattern for the known material. Figure 11 displays powder diffraction patterns of the bulk phases and a simulated pattern based on the single crystal X-ray data reported by Shields for the electrochemically obtained crystals. Samples were analyzed using a step program (12 s per 0.02° at 2Θ) on a Rigaku RU200B X-ray powder diffractometer with Cu Kα radiation ($\lambda\alpha$ = 1.54050 Å). The patterns were indexed using the Treor90 program.[20] This led to the tetragonal cell with a = b = 12.1422Å, c = 17.0498Å , and V = 2513.70Å^3 for Ag(TCNQ) phase I and an orthorhombic cell with a = 17.4448Å, b = 16.5790Å , c = 7.2892Å, and V = 2108Å^3 for the bulk Ag(TCNQ) phase II product . The indexed parameters for Ag(TCNQ) phase II are comparable to the lattice parameters published for the Ag(TCNQ) crystal (a = 6.975Å, b = 16.686Å, c = 17.455Å, and V = 2031.5Å^3).[7] These results support the fact that the two phases are not the same, and that the bulk Ag(TCNQ) phase II pattern corresponds to that of the crystal structure.

Attempts to convert phase I of Ag(TCNQ) to phase II were not very successful. These experiments were originally based on the idea that these phases would be related to each as found for Cu(TCNQ), *viz.*, that a kinetic product can be converted to a thermodynamic product with heating in solution, but there is no evidence that this is the case for Ag(TCNQ). As indicated by the powder data in Figure 12, a mixture is obtained

and it appears that phase I (which is only slightly soluble) does not readily convert to phase II, except by formation of Ag metal and neutral TCNQ.

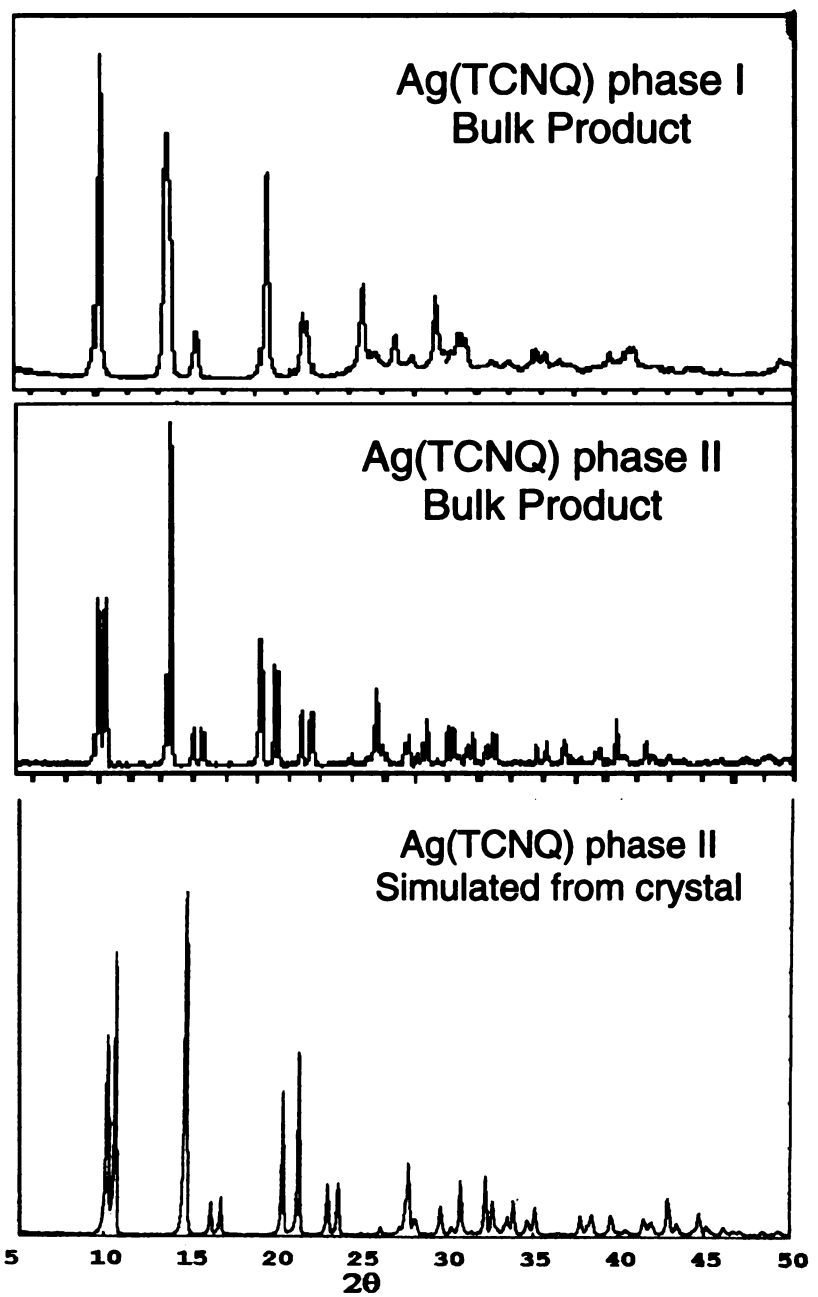

Figure 11. Powder patterns for the two phases of Ag(TCNQ) and a simulation of electrochemically prepared Ag(TCNQ) from the literature.

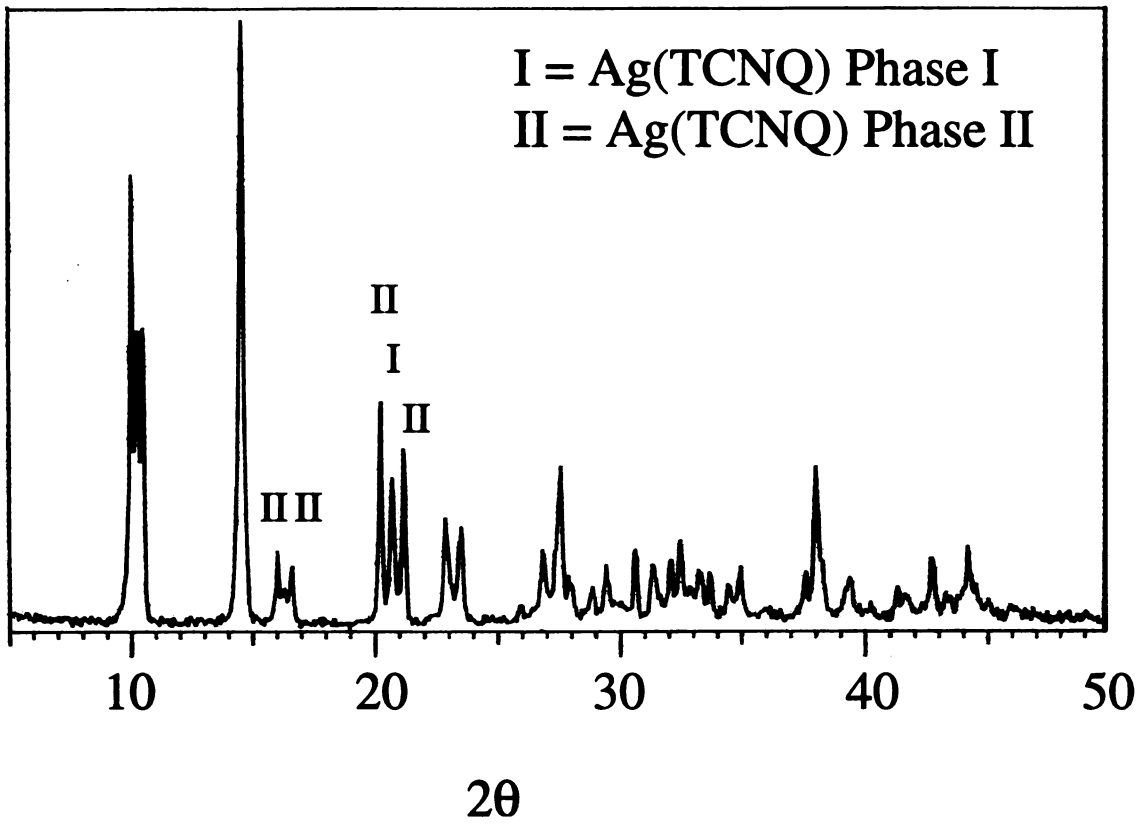

Figure 12. Powder diffraction pattern illustrating the attempted conversion of Ag(TCNQ) phase I to phase II.

This conclusion is based on the observation that suspensions of Ag(TCNQ) phase I in acetonitrile that are not heated and which are protected from light do not convert to phase II. On the other hand, if the solutions of phase I are warmed *and* exposed to light, phase II and Ag metal are formed as deduced from powder X-ray data. In light of our findings, it is not possible to cite either of the two phases as being the kinetic or thermodynamic product. It may be that low solubility prevents the conversion of phase I to phase II, or it may simply be that phase II forms only by direct reaction of Ag metal and TCNQ.

As a final comparison of the various structures possible for 1:1 binary M(TCNX) materials, we examined the powder diffraction pattern of $Ag(TCNQF_4)$ illustrated in

Figure 13. A comparison is made to Ag(TCNQ) phase II which reveals that they are not isostructural compounds. Indeed this was verified by single crystal X-ray methods as well. The pattern also shows that $Ag(TCNQF_4)$ is highly crystalline and diffracts well even at high angles.

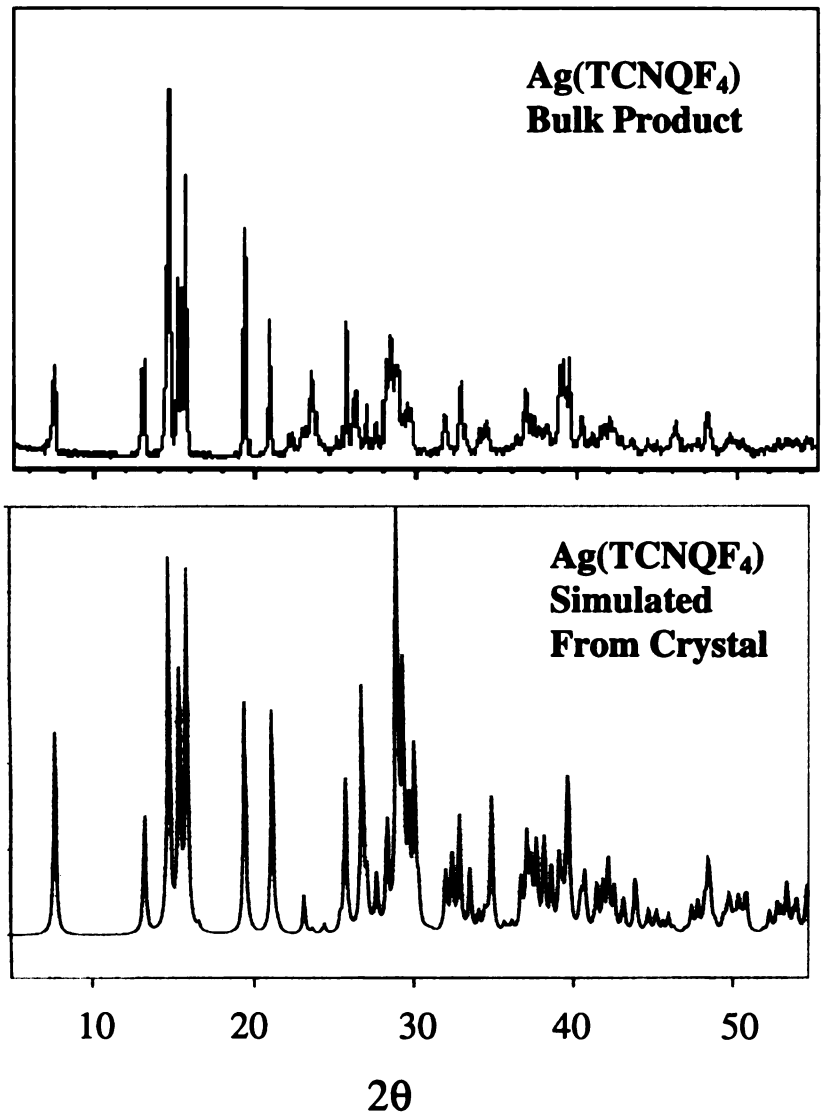

Figure 13. Comparison of the powder diffraction patterns of $Ag(TCNQF_4)$ and the simulated powder diffraction pattern from the $Ag(TCNQF_4)$ crystal structure.

c)Single Crystal Diffraction Studies

(i) Single Crystal Growth

Numerous attempts to grow sufficiently large single crystals of Ag(TCNQ) phase I (**1**), including slow diffusion in solvents and gels as well as bulk electrolysis, were unsuccessful. Tiny crystals were obtained in some cases, but they were invariably plagued with twinning or weak diffraction problems. On the other hand, crystals of $Ag(TCNQF_4)$ were easily obtained by electrocrystallization in a manner similar to what was employed by Shields to prepare crystals of Ag(TCNQ) phase II (**2**). Electrochemical reduction of $TCNQF_4$ was carried out at room temperature by slow reduction of $TCNQF_4$ at a Ag electrode (1mm in diameter and 15 mm long) in a two-compartment electrolysis cell filled with 20 mL of acetonitrile, which functioned as the solvent and the supporting electrolyte. The largest crystals were obtained with 15 mg of $TCNQF_4$ and a constant current of 3 μA. The light yellow solution turned dark green with concomitant deposition of crystals on the Ag electrode. After a period of 2 weeks (corresponding to the consumption of 80% of $TCNQF_4$), crystals were collected and washed with acetonitrile, and dried *in vacuo*. X-ray quality crystals of $[n\text{-}Bu_4N][TCNQF_4]$ were obtained directly from the bulk product.

(ii) Structural analysis of $Ag(TCNQF_4)$.

The structure was solved using direct methods. A total of 2526 unique reflections were refined isotropically on F^2 to R1(wR2) = 0.0225 (0.0586). Surprisingly, the $Ag(TCNQF_4)$ structure is not isostructural to Ag(TCNQ) phase II. A pseudotetrahedral geometry (Figure14) is invoked about the silver atoms due to the four-fold coordination

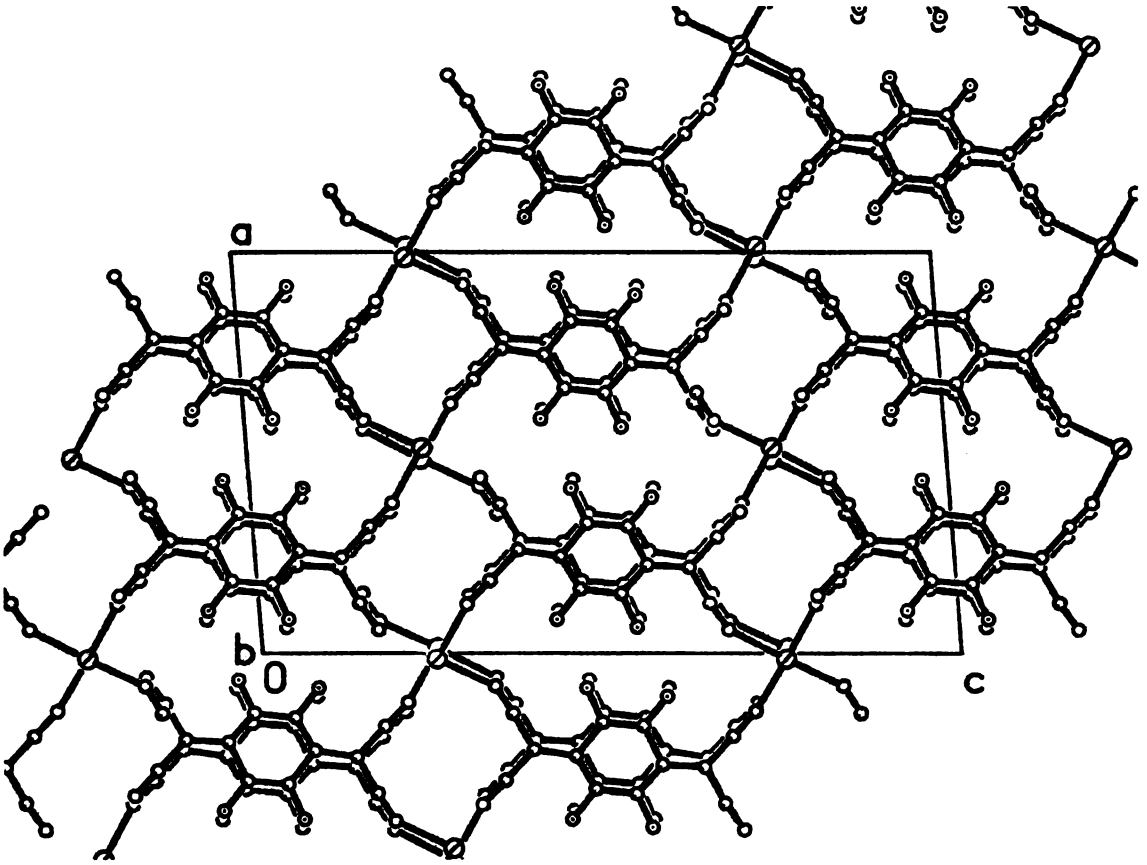

Figure 14. Four-fold coordination within $Ag(TCNQF_4)$.

of the $TCNQF_4^-$ ligands. The N-Ag–N angles range between 97.84° and 130.96° and indicate that the structure is highly distorted. This tetrahedral geometry is characteristic of Ag(TCNQ) phase II[7] and $Cs_2(TCNQ)_3$[13a], and is unlike the coordination of Na^+ [13c], K^+ [13f], or Rb^+ [13b] in the alkali metal family salts of $TCNQ^{-1}$. In Figure 14 it is also evident that the $TCNQF_4$ ligands are almost perfectly eclipsed which results in a high degree of ligand dimerization. $Ag(TCNQF_4)$ is distinct in that adjacent $TCNQF_4^-$ stacks are not rotated 90° with respect to each other, which is a common feature in binary metal/TCNQ salts[7,13]. Instead the two-fold rotation axis generates layers of parallel $TCNQF_4$ anions which form columnated stacks along the *b* axis (Figure 15). Within these stacks, a pattern of dimers

emerges with two average interplanar distances, namely, 3.11 and 3.33 Å. These distances are not only less then the van der Waals distance of 3.4 Å for carbon

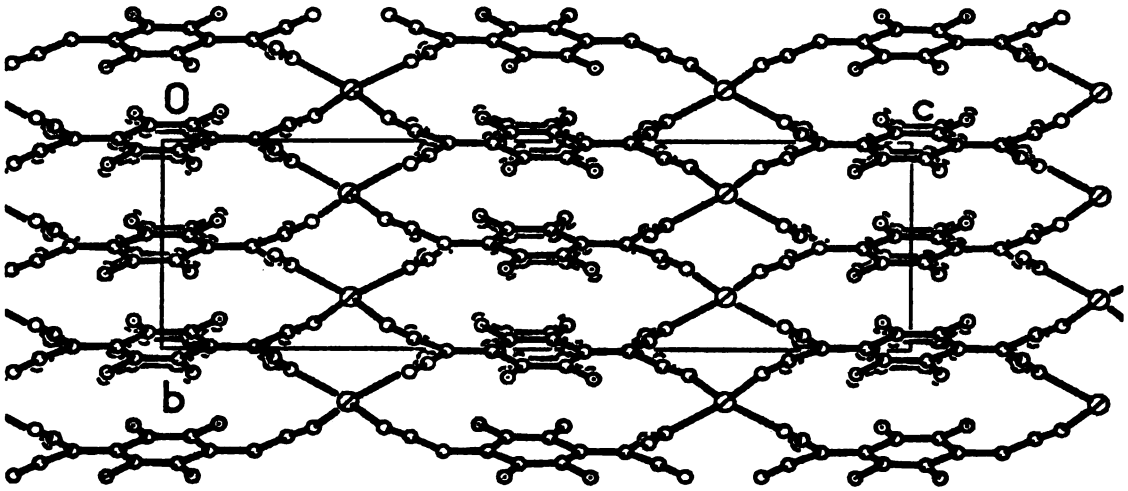

Figure 15. Ligand π-stacking along the *b* axis in $Ag(TCNQF_4)$.

atoms, but are the shortest values for any M(TCNQ) salt (M = Ag or alkali metal). It is important to point out that since this is the first $M(TCNQF_4)$ compound to be structurally characterized, one is limited to making comparisons to TCNQ structures. The only structure with a comparable short intra-layer stacking distance (between two TCNQ ligands) is $Mn(TCNQ)_2(H_2O)_2$ which is 3.05 Å.[21] The short distances in the $Ag(TCNQF_4)$ structure are attributed to the presence of strong electron withdrawing fluorine groups on the benzene ring which are known to lead to increased dimerization of $TCNQF_4$ even in solution.

(iii) Structural Analysis of [*n*-Bu_4N][$TCNQF_4$].

Crystals of this starting material were obtained from the bulk synthesis in which a slow precipitation was induced by addition of hexanes. This structure was solved in the monoclinic space group, $P2_1/n$, using direct methods. A total of 7113 unique reflections were refined isotropically on F^2 to R1(wR2) = 0.0507(0.0948). This structure consists of a diagonal stacking pattern for the $TCNQF_4^-$ molecules which are arranged parallel to the *a* axis. Stacking distances of 3.09Å and 3.73 Å indicate that a dimerization occurs only within pairs of $TCNQF_4$ anions. This distance is shorter than the Van der Waals distance of 3.4 Å for carbon atoms as well as those reported for other simple ammonium TCNQ salts.[22] This is the first simple ammonium salt reported for $TCNQF_4$, thus a comparison to other $TCNQF_4$ structures is not possible.

D. Magnetic Behavior

According to the solid-state structures which indicate that the $TCNQ^{-1}$ anions in the two Ag(TCNQ) polymorphs are strongly dimerized, magnetic susceptibility measurements (Figure 16) reveal only temperature independent paramagnetism of 1.9 10^{-3} (phase II) and 1.4 10^{-3} emu CGS/mol (phase I). A small Curie contribution at low temperatures is a signature of defects (or S = ½ paramagnetic impurities) in the samples and is typical of $TCNQ^{-1}$ materials (Table II). Similar behavior was observed for Ag($TCNQF_4$) (Figure 16) with a t.i.p. of 0.9 10^{-3} emu CGS/mol. In all these Ag compounds, the strongly dimerized nature of the organic acceptor is such that the thermal population of the triplet state (S = 1) cannot be observed in the accessible temperature

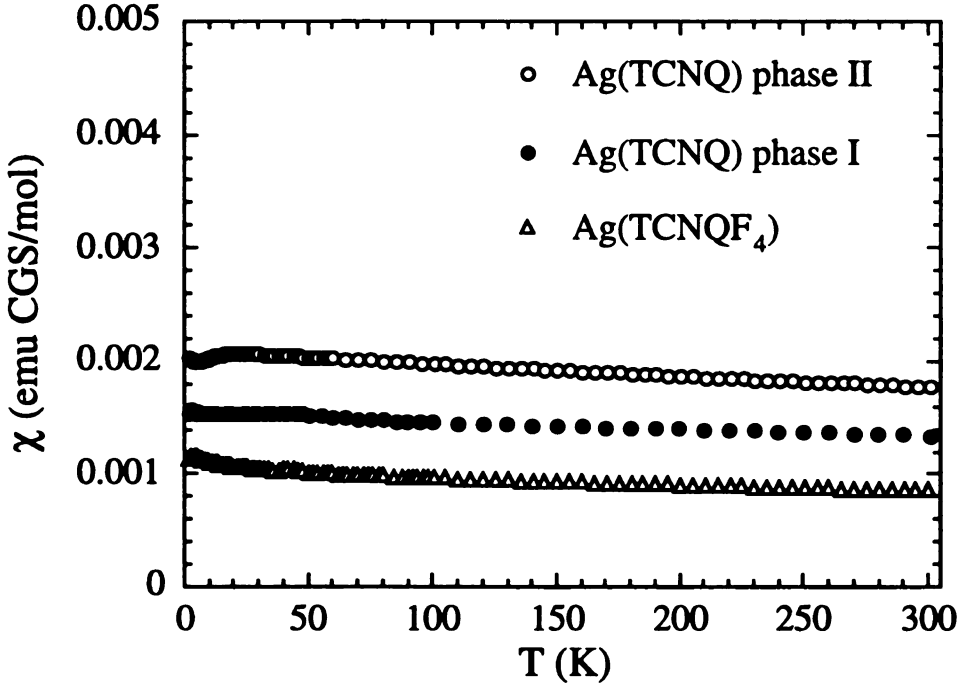

Figure 16. Temperature plots of the magnetic susceptibility for Ag(TCNQ) phase I (at 5000 G) and II (at 1000 G) and Ag(TCNQF$_4$) (at 1000 G).

Table 2. Magnetic parameters for the Ag(TCNQ) family and Ag(TCNQF$_4$). C_b is the Curie constant of the impurity, and should be 0.375 for one spin S = ½. In parenthesis is given the molar percentage of spin 1/2 present in the sample.

	TIP (emu CGS/mol) (290 K)	C_b (emu CGS.K/mol)
Ag(TCNQ) phase I	0.0013 (2)	0.0072 (1.9%)
Ag(TCNQ) phase II	0.0018 (2)	0.0009 (0.2%)
Ag(TCNQ F$_4$)	0.0010 (2)	0.0082 (2.2%)

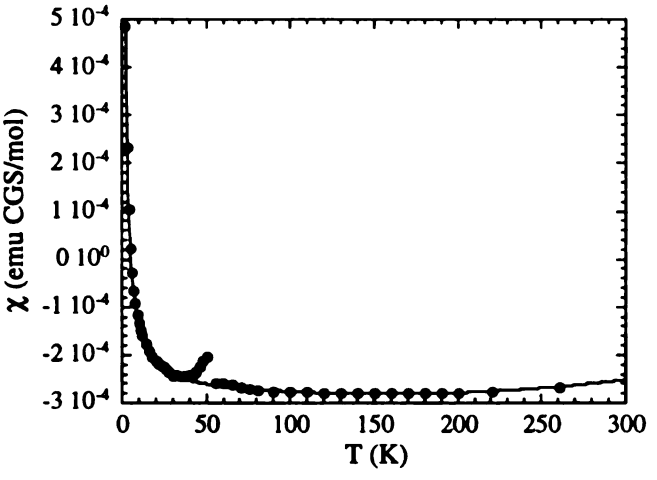

Figure 17. Temperature dependence of the magnetic susceptibility for [*n*-Bu_4N][TCNQ] (at 5000 G). The bump between 40 and 50 K is due to the presence of oxygen. The black line is the best fit obtained with a dimer model of spin = ½.[23]

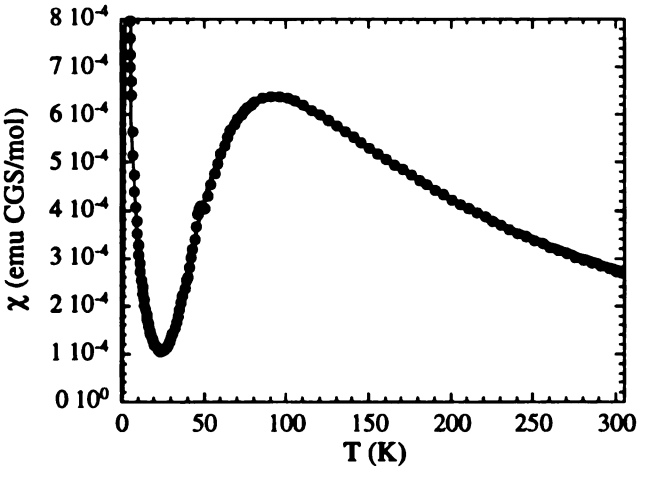

Figure 18. Temperature dependence of the magnetic susceptibility for [*n*-Bu_4N][$TCNQF_4$] (at 1000 G). The black line is the best fit obtained with a dimer model of spin = ½.[23]

range. Interestingly, the salts [*n*-Bu_4N][TCNQ] and [*n*-Bu_4N][$TCNQF_4$] exhibit different magnetic behavior. (Figures 17 and 18). The magnetic susceptibility studies reveal a diamagnetic ground state (S=0) which, is also signature of the organic acceptor dimerization, but in these cases the triplet state (S=1) is thermally accessible with an energy gap of 1380 K and 152 K for [*n*-Bu_4N][TCNQ] and [*n*-Bu_4N][$TCNQF_4$] respectively[23]. In figure 17, the negative values that are constant through most of the temperature range represent the magnitude of the diamagnetic correction.

Conclusion

This study supports the existence of two distinct polymorphs of Ag(TCNQ). This conclusion is based on synthetic, spectroscopic, and structural data. Both phases can be synthesized in bulk using two separate synthetic methods. This distinguishes them from the two polymorphs of Cu(TCNQ) which are connected by a direct kinetic/thermodynamic relationship. A bulk sample of AgTCNQ phase II prepared from Ag powder and TCNQ is identical to the electrochemically prepared crystal by Shields as verified by X-ray powder diffraction. The conversion of Ag(TCNQ) phase I to phase II is possible, but it requires heat and/or light which produces silver metal. It seems unlikely that a direct conversion of soluble Ag^+ ions and $TCNQ^{-1}$ is occurring.

The use of the stronger electron acceptor $TCNQF_4$ has allowed us to expand our structural database for metal/TCNQ binary phases. The structure of Ag($TCNQF_4$) is the first of it's kind with a metal bound to $[TCNQF_4]^{-1}$, and the material exhibits much more strongly dimerized anions than $TCNQ^{-1}$ salts of alkali metal salts. The stacking

interactions are exceedingly short, which is undoubtedly related to the electron withdrawing fluorine groups on the π–delocalized ring. A slipped ring-external bond stacking mode is apparent in the structure of [*n*-Bu_4N][$TCNQF_4$] which is also evident in other organic cation TCNQ salts. The stacking distance within a $TCNQF_4$ dimer, however, is shorter than the corresponding distances observed for ammonium cation salts of TCNQ. The synthesis of other metal-based $TCNQF_4$ compounds will be continued in the future, along with a further expansion into the use of other organic acceptor ligands such as dibromo- and dimethoxy- TCNQ.

References

1. (a) Gardner, G. B.; Venkataraman, D.; Moore, J. S.; Lee, S. *Nature* **1995**, *374*, 792-795. (b) Yaghi, O. M.; Li, G.; Li, H. *Nature* **1995**, *378*, 703. (c) Yaghi, O. M.; Li, H. *J. Am. Chem. Soc.* **1995**, *117*, 10401. (d) Venkataraman, D.; Gardner, G. B.; Lee, S.; Moore, J. S. *J. Am. Chem. Soc.* **1995**, *117*, 11601. (e) Whiteford, J. A.; Rachlin, E. M.; Stang, P. J. *Angew. Chem., Int. Ed. Engl.* **1996**, *35*, 2524. (f) Yaghi, O. M.; Li, H. *J. Am. Chem. Soc.* **1996**, *118*, 295. (g) Yaghi, O. M.; Li, H.; Groy, T. L. *J. Am. Chem. Soc.* **1996**, *118*, 9096. (h) Olenyuk, B.; Whiteford, J. A.; Stang, P. J. *J. Am. Chem. Soc.* **1996**, *118*, 8221.
2. (a) Manriquez, J. M.; Yee, G. T.; McLean, S.; Epstein, A. J.; Miller, J. S. *Science* **1991**, *252*, 1415. (b) Tamaki, H.; Zhuang, Z. J.; Matsumoto, N.; Kida, S.; Koikawa, M.; Achiwa, N.; Hashimoto, Y.; Okawa, H. *J. Am. Chem. Soc.* **1992**, *114*, 6974. (c) Stumpf, H. O.; Pei, Y.; Kahn, O.; Sletten, J.; Renard, J. P. *J. Am. Chem. Soc.* **1993**, *115*, 6738. (d) Inoue, K.; Iwamura, H. J. *J. Am. Chem. Soc.* **1994**, *116*, 3173. (e) Ohba, M.; Maruono, N.; Okawa, H.; Enoki, T.; Latour, J.-M. *J. Am. Chem. Soc.* **1994**, *116*, 11566. (f) Kahn, O. In *Molecular Magnetism: From Molecular Assemblies to the Devices*; NATO ASI Series E321; Coronado, E.; Delhaès, P.; Gatteschi, D.; Miller, J.S., Eds; Kluwer: Dordrecht, 1996; pp. 243-288. (g) Decurtins, S.; Schmalle, H. W.; Schneuwly, P.; Zheng, L.-M.; Ensling, J.; Hauser, A. *Inorg. Chem.* **1995**, *34*, 5501. (h) Miyasaka, H.; Matsumoto, N.; Okawa, H.; Re, N.; Gallo, E.; Floriani, C. *Angew. Chem., Int. Ed. Engl.* **1995**, *34*, 1446. (i) Ohba, M.; Okawa, H.; Ito, T.; Ohto, A. J. *J. Am. Chem. Soc., Chem. Commun.* **1995**, 1545. (j) Michaut, C.; Ouahab, L.; Bergerat, P.; Kahn, O.; Bousseksou, A. *J. Am. Chem. Soc.* **1996**, *118*, 3610. (k) de Munno, G.; Poerio, T.; Viau, G.; Julve, M.; Lloret, F.; Journaux, Y.; Riviere, E. *Chem. Commun.* **1996**, 2587.
3. (a) Aumüller, A.; Erk, P.; Klebe, G.; Hünig, S.; von Schütz, J.; Werner, H. *Angew. Chem., Int. Ed. Engl.* **1986**, *25*, 740. (b) Aumüller, A.; Erk, P.; Hünig, S. *Mol. Cryst. Liq. Cryst.* **1988**, *156*, 215. (c) Erk, P.; Gross, H.-J.; Hünig, U. L.; Meixner, H.; Werner, H. - P.; von Schütz, J. U.; Wolr, H. C. *Angew. Chem., Int. Ed. Engl.* **1989**, *28*, 1245. (d) Kato, R.; Kobayashi, H.; Kobayashi, A. *J. Am. Chem. Soc.* **1989**, *111*, 5224. (e) Aumüller, A.; Erk, P.; Hünig, S.; Hädicke, E.; Peters, K.; von

Schnering, H.G. *Chem. Ber.* **1991**, *124*, 2001. (f) Sinzger, K.; Hünig, S.; Jopp, M.; Bauer, D.; Beitsch, W.; von Schütz, J. U.; Wolf, H. C.; Kremer, R. K.; Metzenthin, T.; Bau, R.; Khan, S. I.; Lindbaum, A.; Lengauer, C. L.; Tillmanns, E. *J. Am. Chem. Soc.* **1989**, *115*, 7696.

4. See for example: (a) Fagan, P J.; Ward, M. D.; Calabrese, J.C. *J. Am. Chem. Soc.* **1989**, *111*, 1698. (b) Iwamaoto, T. in *Inclusion Compounds: Inorganic and Physical Aspects of Inclusion*; Iwamoto, T., Atwood, J. L., Davies, J. E. D., MacNicol, D. D., Eds.; Oxford University Press: Oxford, 1991; Vol. 5, Chapter 6, p. 177. (c) Robson, R.; Abrahms, B. F.; Batten, S. R.; Gable, R. W.; Hoskins, B. F.; Liu, J. in *Supramolecular Architecture*, Bein, T., Ed.; American Chemical Society: Washington, DC, 1992; p. 256. (d) Tannenbaum, R. *Chem. Mater.* **1994**, *6*, 550. (e) Constable, E. C. *Prog. Inorg. Chem.* **1994**, *42*, 67. (f) Lu, J.' Harrison, W. T. A.; Jacobson, A. J. *Angew. Chem., Int. Ed. Engl.* **1995**, *24*, 2557. (g) Dunbar, K. R.; Heintz, R. A. *Prog. Inorg. Chem.* **1996**, *35*, 4449. (i) Whiteford, J. A.; Rachlin, E. M.; Stang, P. J. *Angew. Chem., Int. Ed. Engl.* **1996**, *35*, 2524. (j) Sharma, C. V. K.; Zaworotko, M. J. *Chem. Commun.* **1996**, 2655. (k) Hirsch, K. A.; Wilson, S. R.; Moore, J. S. *Inorg. Chem.* **1997**, *36*, 2960.

5. (a) Lacroix, P.; Kahn, O.; Gliezes, A.; Valade, L.; Cassoux, P.; *Nouv. J. Chim.* **1985**, 643. (b) Gross, R.; Kaim, W.; *Angew. Chem., Int. Ed. Engl.* **1987**, *26*, 251. (c) Humphrey, D. G.; Fallon, G. D.; Murray, K. S. *J. Chem. Soc., Chem. Commun.* (d) Bartley, S. L.; Dunbar, K. R. *Angew. Chem., Int. Ed. Engl.* **1991**, *30*, 448. (e) Ballester, L.; Barral, M.; Gutiérrez, A.; Jiménez-Apararicio, R.; Martinez-Muyo, J.; Perpiñan, M.; Monge, M.; Ruiz-Valero, C. *J. Chem. Soc., Chem. Commun.* **1991**, 1396. (f) Cornelissen, J. P.; van Diemen, J. H.; Groeneveld, L. R.; Haasnoot, J. G.; Spek, A. L.; Reedijk, J. *Inorg. Chem.* **1992**, *31*, 198. (g) Oshio, H.; Ino, E.; Mogi, I.; Ito, T. *Inorg. Chem.* **1993**, *33*, 5697. (h) Ballester, L.; Barral, M.; Gutiérrez, A.; Perpiñan, M.; Monge, M.; Ruiz-Valero, C.; Sánchez-Pélaez, A. *Inorg. Chem.* **1994**, *33*, 2142. (i) Dunbar, K. R.; Ouyang, X. *Mol. Cryst. Liq. Cryst. Sci. Technol.* **1995**, *273*, 21. (j) Oshio, H.; Ino, E.; Ito, T.; Maeda, Y. *Bull. Chem. Soc. Jpn.* **1995**, *68*, 889. (k) Dunbar, K. R.; *Angew. Chem.* **1996**, *35*, 1659. (l) Decurtins, S.; Dunbar, K. R.; Gomez-Garcia, C. J.; Mallah, T.; Raptis, R.G.; Talham, D.; Veciana, J. in *Molecular Magnetism: From Molecular Assemblies to the Devices*; NATO ASI

Series E321; Coronado, E.; Delhaès, P., Gatteschi, D., Miller J. S., Eds.; Kluwer: Dordrecht, 1996; 571. (m) Dunbar, K. R.; Ouyang, X. *Chem. Commun.* **1996**, 2427. (n) Zhao, H.; Heintz, R. A.; Rogers, R. D.; Dunbar, K. R. *J. Am. Chem. Soc.* **1996**, *118*, 12844. (o) Dunbar, K. R.; Ouyang, X. *Inorg. Chem.* **1996**, *35*, 7188. (p) Azcondo, M. T.; Ballester, C. J.; Gutiérrez,, A.; Perpiñan, M.; Amador, U.; Ruiz-Valero, C.; Bellitto, C. *J. Chem. Soc., Dalton Trans.* **1996**, 3015.

6. For an excellent review on the subject of σ coordination to TCNX molecules, see: Kaim, W.; Moscherosch, M. *Coord. Chem. Rev.* **1994**, *129*, 157.
7. Structure of Ag(TCNQ): Shields, L. *J. Chem. Soc., Faraday Trans. 2* **1985**, *81*, 1.
8. (a) Potember, R. S.; Poehler, T. O.; Cowan, D. O. *Appl. Phys. Lett.* **1979**, *34*, 405. (b) Potember, R. S.; Poehler, T. O.; Rappa, A.; Cowan, D. O.; Bloch, A. N. *J. Am. Chem. Soc.* **1980**, *102*, 3659. (c) Potember, R. S.; Poehler, T. O.; Cowan, D. O.; Brant, P.; Carter, F. L.; Bloch, A. N. *Chem. Scr.* **1981**, *17*, 219. (d) Kamistos, E. I.; Risen, W. M., Jr. *Solid State Commun.* **1982**, *42*, 561. (e) Potember, R. S.; Poehler, T. O.; Cowan, D. O.; Carter, F. L.; Brant, P. I. In *Molecular Electronic Devices*; Carter, F. L., Ed.; Marcel Dekker: New York, 1982; p. 73. (f) Potember, R. S.; Poehler, T. O.; Benson, R. C. *Appl. Phys. Lett.* **1982**, *41*, 548. (g) Potember, R. S.; Poehler, T. O.; Rappa, A.; Cowen, D. O.; Bloch, A. N. *Synth. Met.* **1982**, *4*, 371. (h) Kamitsos, E. I.; Risen, W. M. *Solid State Commun.* **1983**, 45, 165. (i) Kamitsos, E. I.; Risen, W. M.*J. Chem. Phys.* **1983**, 79, 477. (j) Kamitsos, E. I.; Risen, W. M. Jr. *J. Chem. Phys.* **1983**, 79, 5808. (k) Benson, R. C.; Hoffman, R. C.; Potember, R. S.; Bourkoff, E.; Poehler, T. O. *Appl. Phys. Lett.* **1983**, *41*, 548. (l) Poehler, T. O.; Potember, R. S.; Hoffman, R.; Benson, R. C.; *Mol. Cryst. Liq. Cryst.* **1984**, *107*, 91. (m) Kamistos, E. I.; Risen, W. M., Jr. Mol. *Cryst. Liq. Cryst.* **1986**, *134*, 31. (n) Potember, R. S.; Poehler, T. O.; Hoffman, R. C.; Speck, K. R.; Benson, R. C. In *Molecular Electronic Devices II*; Carter, F. L., Ed.; Marcel Dekker: New York, 1987; p. 91 (o) Wakida, S.; Ujihira, Y. *J. Appl. Phys.* **1988**, *27*, 1314. (p) Hoffman, R. C.; Potember, R. S. *Appl. Opt.* **1989**, *28* (7), 1417. (q) Duan, H.; Mays, M. D.; Cowan, D. O.; Kruger, J. *Synth. Met.* **1989**, *28*, C675. (r) Sato, C.; Wakamatsu, S.; Tadokoro, K.; Ishii, K. *J. Appl. Phys.* **1990**, *68* (12) 6535. (s)Yamaguchi, S.; Viands, C. A.; Potember, R. S. *J. Vac. Sci. Technol.* **1991**, *9*, 1129. (t) Hua, Z, Y.; Chen, G. R. *Vacuum* **1992**, *43*, 1019. (u) Hoagland, J. J.; Wang, X. D.; Hipps, K.

W. *Chem. Mater.* **1993**, *5*, 54. (v) Liu, S. G.; Liu, Y. Q.; Wu, P. J.; Zhu, D. B. *Chem. Mater.* **1996**, *8*, 2779. (w) Liu, S. G.; Liu, Y. Q.; Zhu, D. B. *Thin Solid Films* **1996**, *280*, 271. (x) Sun, S. Q.; Wu, P. J.; Zhu, D. B. *Solid State Commun.* **1996**, *99*, 237. (y) Liu, S. G.; Liu, Y. Q.; Wu, P. J.; Zhu, D. B.; Tian, H.; Chen, K. C. *Thin Solid Films* **1996**, *289*, 300.

9. Heintz, R. A.; Zhao, H.; Ouyang, X.; Grandinetti, G.; Cowen, J.; Dunbar, K. R. *Inorg. Chem.* **1999**, *38*, 144.

10. (a) Emge, T. J.; Bryden, W. A.; Wiygul, F. M.; Cowan, D. O.; Kistenmacher, T. J. *J. Chem. Phys.* **1982**, *77*, 3188. (b) Metzger, R. A.; Heimer, N. E.; Gundel, D.; Sixi, H.; Harms, R.H.; Keller, H.J.; Nöthe, D.; Wehe, D. *J. Chem. Phys.* **1982**, *77*, 6203. (c) Wiygul, F. M.; Emge, T.J.; Kistenmacher, T.J. *Mol. Cryst. Liq. Cryst.* **1982**, *90*, 163. (d) Emge, T. J.; Cowan, D. O.; Bloch, A. N.; Kistenmacher, T. J. *Mol. Cryst. Liq. Cryst.* **1983**, *95*, 191.

11. (a) Jones, M. T.; Maruo, T.; Jansen, S.; Roble, J.; Rataiczak, R. D. *Mol. Cryst. Liq. Cryst.*, **1986**, *134*, 21. (b) Maruo, T.; Rataiczak, R. D.; Jones, M. T. *Mol. Phys.* **1991**, *73*, 1365. (c) Sugano, T.; Fukasawa, T.; Kinoshita, M. *Synth. Met.* **1991**, *41*, 3281. (d) Agostini, G.; Corvaja, C.; Giacometti, G.; Pasimeni, L. *Chem. Phys.* **1993**, *173*, 177. (e) Otsubo, T.; Kono, Y.; Hozo, N.; Miyamoto, H.; Aso, Y.; Ogura, F.; Tanaka, T.; Sawada, M. *Bull. Chem. Soc. Jpn.* **1993**, *66*, 2033. (f) Nishikawa, H.; Kawakami, K.; Fujiwara, H.; Uehara, T.; Misaki, Y.; Yamabe, T. *Synth. Met.* **1993**, *56*, 1983. (g) Nakamura, Y.; Iwamura, H. *Bull. Chem. Soc. Jpn.* **1993**, *66*, 3724. (h) Sugimoto, T.; Tsujii, M.; Murahashi, E.; Makatsuji, H.; Yamauchi, J.; Fujita, H.; Kai, Y.; Hosoito, N. *Mol. Cryst. Liq. Cryst.* **1993**, *232*, 117.

12. (a) Meneghetti, M.; Girlando, A.; Pecile, C. *J. Chem. Phys.* **1985**, *83*, 3134. (b) Meneghetti, M.; Pecile, C. *J. Chem. Phys.* **1986**, *84*, 4149. (c) Meneghetti, M.; Bozio, R.; Pecile, C. *Synth. Met.* **1987**, *19*, 451. (d) Meneghetti, M.; Bozio, R. *J. Chem. Phys.* **1988**, *89*, 2704.

13. (a) Fritchie, C. J., Jr.; Arthur, P. *Acta Crystallogr.* **1966**, *21*, 139. (b) Hoekstra, A.; Spoelder, T.; Vos, A. *Acta Crystallogr.* **1972**, *B28*, 14. (c) Konno, M.; Saito, Y. *Acta Crystallogr.* **1974**, *B30*, 1294. (d) Murakami, M.; Yoshimura, S. *Bull. Chem. Soc. Jpn.* **1975**, *48*, 157. (e) Konno, M.; Saito, Y. *Acta Crystallogr.* **1975**, *B31*, 2007. (f) Konno, M.; Ishii, T.; Saito, Y. *Acta Crystallogr.* **1977**, *B33*, 763.

14. Melby, L. R.; Harder, R. J.; Hertler, W. R.; Mahler, W.; Benson, R. E.; Mochel W. E. *J. Am. Chem. Soc.* **1962**, *84*, 3374.

15. Wheland, R. C.; Martin, E. L. *J. Org. Chem.* **1975**, *40* (21), 3101.

16. Boudreaux, E. A.; Mulay, J. N. *Theory and Applications of Molecular Paramagnetism*, Eds., J. Wiley & Sons: New York, **1976**.

17. (a) Lunille, B.; Pecile, C. *J. Chem. Phys.* **1970**, *52*, 2375. (b) Bozio, R.; Girlando, A.; Pecile, C. *J. Chem. Soc., Faraday Trans. 2* **1975**, *71*, 1237. (c) Van Duyne, R. P.; Suchanski, M. R.; Lakovits, J. M.; Siedle, A. R.; Parks, K. D.; Cotton, T. M. *J. Am. Chem. Soc.* **1979**, *101*, 2832. (d) Chappell, J. S.; Bloch, A. N.; Bryden, A.; Maxfiled, M.; Poehler, T. O.; Cowan, D. O. *J. Am. Chem. Soc.* **1981**, *103*, 2442. (e) Farges, J. P.; Brau, A; Dupuis, P. *Solid State Commun.* **1985**, *54* (6), 531. (f) Inoue, M.; Inoue, M. B. *J. Chem. Soc., Faraday Trans. 2* **1985**, *81*, 539. (g) Inoue, M.; Inoue, M. B. *Inorg. Chem.* **1986**, *25*, 37. (h) Inoue, M.; Inoue, M. B.; Fernando, Q.; Nebesny, K. W. *J. Phys. Chem.* **1987**, *91*, 527. (i) Pukaki, W.; Pawlak, M.; Graja, A.; Lequan, M.; Lequan, R. M. *Inorg. Chem.* **1987**, *26*, 1328.

18. (a) Meneghetti, M.; Pecile, C. *J. Chem. Phys.* **1986**, *84* (8), 4149. (b) Meneghetti, M.; Bozio, R.; Pecile, C. *Synth. Met.* **1987**, *19*, 451. (c) Meneghetti, M.; Bozio, R. *J. Chem. Phys.* **1988**, *5*, 2704. (d) Chiang, L. Y.; Goshorn, D. P. *Mol. Cryst. Liq. Cryst.* **1989**, *26*, 229.

19. (a) Yashihiro, Y.; Furukawa, Y.; Kobayashi, A.; Tasumi, M.; Kato, R.; Kobayashi, H. *J. Chem. Phys.* **1994**, *100*, 2449. (b) Kobayashi, A.; Kato, R.; Kobayashi, H.; Mori, T.; Inokuchi, H. *Solid State Commun.* **1987**, *64*, 45. (c) Willett, R. D.; Long, G. Personal communication.

20. Werner, P.E.*J. Appl. Cryst.* **1985**, *18*, 367. TREOR program was adapted to PC and PROSZKI system at Jaqielloniam University 1989.

21. Zhao, H.; Heintz, R. A.; Ouyang, X.; Dunbar, K. R. *Chem. Mater.* **1999**, *11*, 736.

22. (a) Kobayashi, H.; Danno, T.; Saito, Y. *Acta Crystallogr.* **1973**, *B29*, 2693. (b) Kobayashi, H. *Acta. Crystallogr.* **1978**, *B34*, 2818. (c) Fihol, A.; Rovira, M.; Hauw, C.; Gaultier, J.; Chasseau, D.; Dupuis, P. *Acta Crystallogr.* **1979**, *B35*, 1652. (d) Shibaeva, R. P.; Kaminskii, V. F.; Simonov, M. A. *Cryst. Struct. Commun.* **1980**, *9*, 655.

23. We fit our experimental data using the Bleaney-Bowers formula and a Curie law for S=1/2, equation 1 where N is the number of TCNQ or $TCNQF_4$ coupled into dimer, N' is the number of molecules with an unpaired spin, μ_B is the Bohr magneton, and the g -factor is assumed to be equal to 2 (usual for TCNQ compounds):

$$\chi_p = \frac{2Ng^2\mu_B^2}{kT}\left(\frac{1}{3+\exp[-2J/(kT)]}\right)+\left(\frac{N'g^2\mu_B^2}{4kT}\right)$$

Chapter III

Synthesis and Characterization of Paramagnetic Metal/TCNQ Compounds: The $M(TCNQ)_2$ Family

Introduction

Charge-transfer materials have been under intense investigation for the past four decades. This research has resulted in the identification of a wide variety of conducting salts containing organocyanide acceptors such as TCNQ.[1] The conducting ability of these materials is attributed to the stacking arrangement of the planar organic radicals within these charge-transfer materials which allows for a continuous π-pathway for communication. The nature of the stacking has been noted to dramatically affect the magnetic and charge-transport properties. For example, the well known [TTF][TCNQ] salt crystallizes as segregated stacks of donors and acceptors and exhibits high electrical conductivity, whereas integrated stacks of alternating donors and acceptors exhibit interesting optical and magnetic properties.[2]

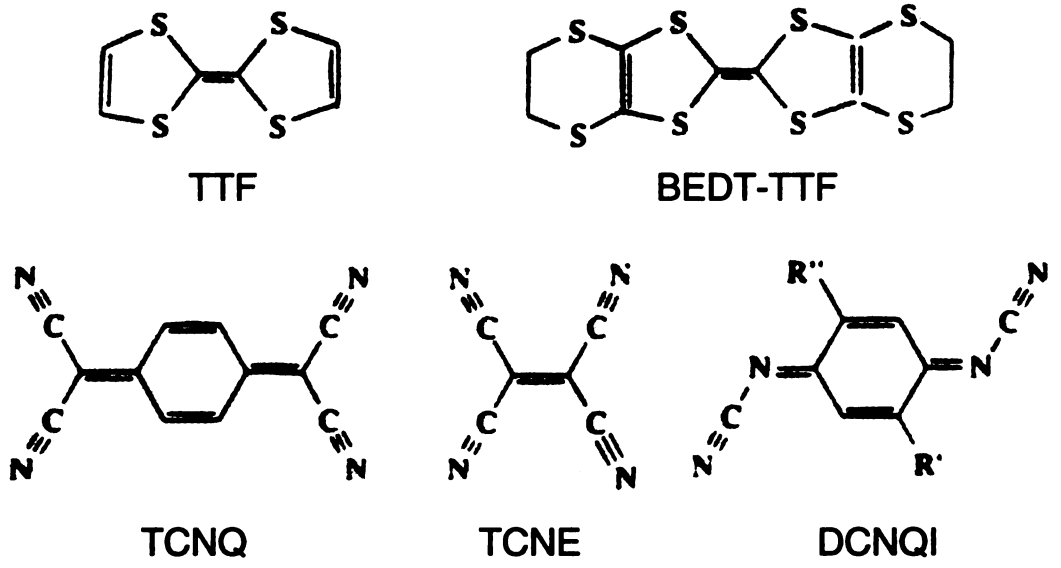

Figure 19. Schematic diagrams of organic donors and acceptors used in charge-transfer materials.

Recently, researchers have expanded the field of donor-acceptor chemistry by incorporating molecules of the types depicted in Figure 19 into multi-dimensional framework solids that contain a paramagnetic inorganic component.[3] This approach appears to be very promising, indeed materials containing BEDT-TTF ions and paramagnetic metal anions have been found to exhibit highly conducting and even superconducting properties![4] In terms of magnetic materials, one can envision the direct coordination of paramagnetic metal cations to open-shell organic acceptor anions such as $TCNQ^-$ (7,7,8,8-tetracyanoquinodimethane)[5], $TCNE^-$ (tetracyanoethylene)[6], and $DCNQI^-$ (N,N'-dicyanoquinodiimine)[7]. In this way, multi-dimensional inorganic/organic polymers can be produced by taking advantage of the π-stacking ability of TCNQ, and, at the same time, imparting new properties based on the presence of unpaired electrons on the metals. The most well known examples of this strategy are: (1) metallic polymers of Cu with DCNQI,[7] (2) electrically bistable conducting materials of Cu and Ag with TCNQ,[8] and (3) a room-temperature bulk ferromagnet of V with TCNE.[6a] In all cases, the organic molecules in the structures are in the radical anion (-1) or mixed valence (0/-1) states.

Although TCNQ radicals are more stable than TCNE, and the compound has been known since the early 1960's, little is known about the chemistry of TCNQ as a ligand for paramagnetic transition metals. Furthermore, only several structures were known when studies commenced in or laboratories in the early 1990's. This chapter describes the syntheses and characterization of $M(TCNQ)_2$ compounds, prepared from reactions of first row transition metals, Mn (**1**), Fe (**2**), Co (**3**), and Ni (**4**) with $TCNQ^-$. These materials are binary compounds composed solely of metals and organic acceptor with no

co-ligands and can therefore be classified as true "inorganic/organic hybrid" materials. Their simplicity makes them attractive candidates for study, but a major disadvantage of working with these compounds is that they are notoriously difficult to crystallize. Not surprisingly, structural information, which is of central importance for our complete understanding of the magnetic properties of these materials, is sorely lacking. Fortunately, other means of characterization such as powder X-ray diffraction and infrared spectroscopy have allowed for educated guesses about the nature of these materials. These details are useful when examining their magnetic properties, which has been carried out in detail by both d.c. and a.c methods.

Experimental Section

A. General Considerations

All reactions were carried out under a nitrogen atmosphere using standard Schlenk-line techniques. Acetonitrile was dried over 3Å molecular sieves and distilled under a nitrogen atmosphere prior to use. Diethyl ether was dried and distilled over Na/K amalgam. TCNQ was purchased from TCI Chemical Company and recrystallized from hot acetonitrile. LiI and $[Bu_4N]I$ was purchased from Aldrich Chemical Company; $[n\text{-}Bu_4N]I$ was recrystallized from hot water. The divalent metal $[BF_4]^-$ anion salts, $[M(MeCN)_{4,6}][BF_4]_2$, where M = Mn, Fe, Co, and Ni, were prepared as described in the literature.[10]

B. Synthesis

Although the literature outlines general synthetic methods for the syntheses of both Li(TCNQ) and [*n*-Bu_4N][TCNQ],[1b] a more detailed description of their preparation and characterization is provided here for convenience.

(a) Preparation of Li(TCNQ)

A typical bulk preparation requires a 3:2 ratio of LiI (1.50 g, 0.0112 mol) and TCNQ (1.53 g, 0.0075 mol) respectively. Under a nitrogen atmosphere, LiI was dissolved in 40 mL of acetonitrile whereas TCNQ was dissolved in 400 mL of boiling acetonitrile in a 1-L beaker. The solution of LiI was transferred via cannula into the solution of TCNQ and a dark purple precipitate formed immediately. The solution was cooled to allow for full precipitation of the product. The product was recovered by vacuum filtration, washed with 50 mL of acetonitrile and 100 mL of diethyl ether, and dried *in vacuo*: yield 1.48 g (94%). Anal. Calcd for $C_{12}H_4N_4Li$: C, 68.3; H, 1.9; N, 26.5; Found: C, 68.09; H, 1.87; N, 26.25. Characteristic IR data (Nujol mull, KBr plates, cm^{-1}): ν(C≡N), 2211 s, 2196 s, 2180 sh 2154 s; ν(C=C), 1507 s; δ(C-H), 826 m.

(b) Preparation of [*n*-Bu_4N][TCNQ]

A quantity of Li(TCNQ) (1.48 g, 0.007 mol) was dissolved in 100 mL of hot distilled water, and, in a separate flask, an excess of [*n*-Bu_4N]I (5.2 g, 0.0140 mol) was dissolved in 600 mL of boiling distilled water. Upon the addition of Li(TCNQ) to [*n*-Bu_4N]I, a dark purple precipitate formed immediately. The stirred solution was kept warm for 1 h after which time the product was collected by vacuum filtration. The

resulting dark purple powder was washed with several additions of hot water, followed by diethyl ether, and finally dried *in vacuo*: yield, 3.1 g (99%). The product was recrystallized as follows. The crude product was dissolved in a minimal volume of dichloromethane (~100 mL), and the solution was dried with anhydrous magnesium sulfate. After filtration, the solution was reduced in volume to ~30 mL, and an equivalent volume of hexanes was added to induce crystallization. After the excess dichloromethane was evaporated, the dark purple crystalline product was collected by vacuum filtration, washed with copious amounts of hexanes and dried *in vacuo*: yield, 2.96 g, (95%). Anal. Calcd for $C_{28}H_{36}N_5$: C, 75.29; H, 9.03; N, 15.68; Found: C, 73.95; H, 9.52; N, 15.32. Characteristic IR data (Nujol mull, KBr plates, cm^{-1}): ν(C≡N), 2187 sh, 2181 s, 2160 sh, 2157 s; ν(C=C), 1507 s; δ(C-H), 824 m.

(c) Synthesis of $M(TCNQ)_2$ compounds, where M = Mn (1), Fe (2), and Co (3).

A quantity of [*n*-Bu_4N][TCNQ] (0.455 g, 1.02 mmol) was dissolved in 20 mL of acetonitrile to give a green solution, which was transferred via cannula into respective 20 mL volume acetonitrile solutions of $[Mn(MeCN)_4][BF_4]_2$ (0.200 g, 0.51 mmol), $[Fe(MeCN)_6][BF_4]_2$ (0.242 g, 0.51 mmol), and $[Co(MeCN)_6][BF_4]_2$ (0.244g, 0.51 mmol). A dark purple precipitate formed immediately in all three cases, with no visible changes occurring during the twenty-minute reaction time. The precipitates were collected by filtration under nitrogen, washed with 10 mL of acetonitrile followed by of 20 mL diethyl ether, and dried *in vacuo*: yield: (1), 0.223 g, 95%; (2), 0.224 g, 95%; (3), 0.220 g, 93%. Analytical data: Calcd for $C_{24}H_8MnN_8$: C, 62.20; H, 1.74; N, 24.19. Found: C, 61.71; H, 1.90; N, 21.38. Calcd for $C_{24}H_8FeN_8$: C, 62.10; H, 1.74; N, 24.14. Found: C, 60.78; H,

2.26 ; N, 22.54. Calcd for $C_{24}H_8CoN_8$: C, 61.68; H, 1.73; N, 23.98. Found: C, 59.87; H, 2.27; N, 21.49. Characteristic IR data (Nujol mull, KBr plates, cm^{-1}): $Mn(TCNQ)_2$: ν(C≡N), 2205 s, 2187 s, 2137 sh; ν(C=C), 1505 s; δ(C-H), 826 m. $Fe(TCNQ)_2$: ν(C≡N), 2217 s, 2187 s, 2142 sh; ν(C=C), 1505 s; δ(C-H), 827 m. $Co(TCNQ)_2$: ν(C≡N), 2217 s, 2188 s 2137 sh; ν(C=C), 1505 s; δ(C-H), 827 m.

(d) Synthesis of $Ni(TCNQ)_2$ (4).

A quantity of [*n*-Bu_4N][TCNQ] (0.455 g, 1.02 mmol) was dissolved in 30 mL of acetonitrile to give a green solution which was slowly added to a 30 mL acetonitrile solution of $[Ni(MeCN)_6][BF_4]_2$ (0.244 g, 0.51 mmol). The resulting reaction solution was allowed to stir for 3 hours in order to bypass a green kinetic intermediate before going on to form the desired dark purple product. The product was collected by filtration under nitrogen, washed with acetonitrile (10 mL) followed by diethyl ether (20 mL) and dried *in vacuo*. Yield: 0.223 g, 94%. Calcd for $C_{24}H_8NiN_8$: C, 61.72; H, 1.73; N, 23.99;. Found: C, 60.02; H, 2.21; N, 23.06. Characteristic IR data (Nujol mull, KBr plates, cm^{-1}): ν(C≡N), 2224 s, 2208 s, 2192 s, 2155 sh; ν(C=C), 1503 s; δ(C-H), 829 m.

C. Single Crystal Growth

Several methods of crystallization, including slow diffusion of reactants in solvents[11] and gels,[12] were used in attempts to isolate single crystals of the $M(TCNQ)_2$ compounds (**1** - **4**) (Figure 20). Each method is described in detail along with the outcome. As a preface, it should be noted that these compounds are exceedingly insoluble in acetonitrile and thus great care was taken to prevent rapid precipitation of the

products. Their nearly total insolubility seriously hinders crystallization, as crystal growth requires time in solution for a crystal to heal defects and to grow to an appreciable size.

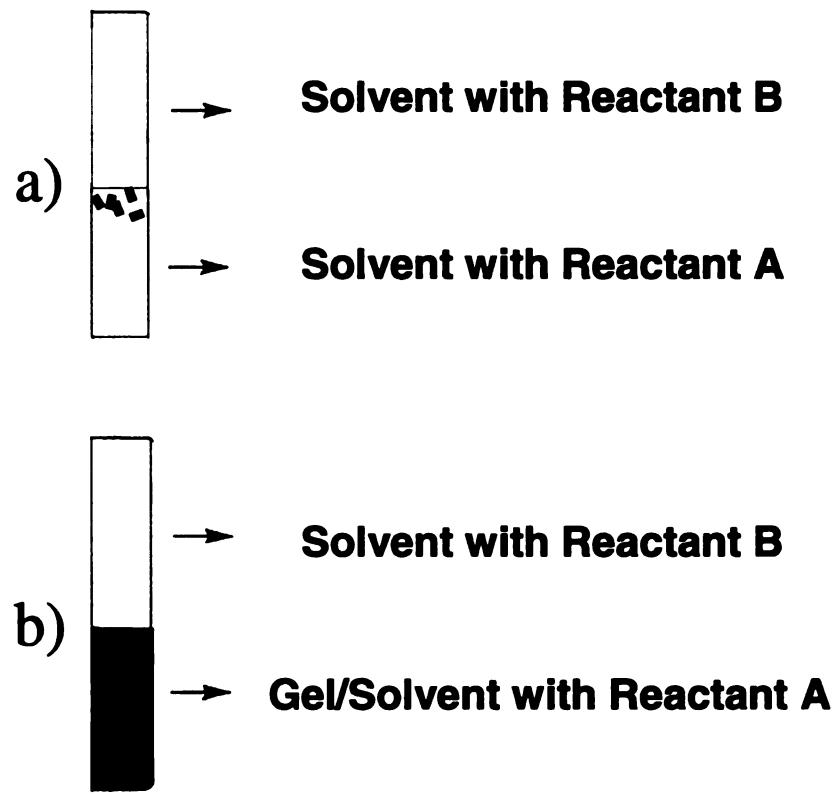

Figure 20. Slow diffusion of (a) solvent layers and (b) solvent/gel layers.

(a) Slow Diffusion of Reactants in Solvents

This was the first method used in attempts to crystallize compounds (**1** - **4**). The general procedure involves careful layering of a solution of [*n*-Bu_4N][TCNQ] over a layer of the metal containing salt with both of the reagents being dissolved in CH_3CN. This leads to the formation of the product at the interface (Figure 20a).[11] Metal solvated

solutions were layered on the bottom of the tube because they are often more dense in solution compared to the $TCNQ^{-1}$ solutions. Several factors were used to slow the process of product formation. A lower concentration of reactants (50 mg of metal solvated in 100 mL) obviously reduces the tendency for immediate precipitation of the product at the interface, and a smaller diameter tube size (6-mm diameter) further slows the diffusion of the reactants. Different solvents with higher densities than acetonitrile, such as methylene chloride, were used in the metal component layer to further slow the diffusion of the layers as well. Finally, once the tubes were layered they were placed in a refrigerator to take advantage of the temperature effect on diffusion rates of solvents. Inevitably, powders or films were obtained at the interface in all tubes, underscoring the extreme insolubility of these compounds.

(b) Incorporation of Gels

As it became clear that slow diffusion of solvent layers was not producing the desired result, gels were incorporated into the metal layer as a means to severely limit the diffusion of reactants (Figure 20b).[12] A solvent solubility study was performed to determine the most versatile gel (Table 3). PMMA, (poly-methylmethacrylate), was determined to be the better than PEO, (poly-ethyleneoxide),[12e] or Sephadax.[12a] Different gel percentages were used to vary the diffusion rates; the higher the gel concentration, the more viscous the solution and therefore the slower the diffusion rate. Gel percentages are based on w/w %;[12d] for instance, a 9% gel is composed of 9 g PMMA/ 91 g of solvent totaling 100 g or 100%.

Table 3. Solubility studies of various gels where S = soluble and I = insoluble. Heat was used with gels that did not readily dissolve.

Solvent	PEO	w/heat	PMMA	w/ heat	Sephadex	w/ heat
Methylene Chloride	S	–	S	–	I	I
Benzene	I	S	S	–	I	I
Tetrahydrofuran	I	S	S	–	I	I
Acetone	S	–	S	–	I	I
Acetonitrile	S	–	S	–	I	I
Methanol	I	I	I	I	I	I
Ethanol	I	I	I	I	I	I
Ether	I	I	I	I	I	I
Hexanes	I	I	I	I	I	I
Toluene	I	S	S	–	Partially	–

(c) A Typical Setup

For a 5% gel, approximately 1 g of PMMA was added to a Schlenk flask and placed under vacuum. Under nitrogen, an appropriate quantity of $Mn[MeCN]_4[BF_4]_2$ (0.100 g) was added. A total acetonitrile volume of 20 mL was added under nitrogen, and the solution was stirred until the gel completely dissolved. Often slight application of heat was necessary to achieve complete dissolution of the gel. Approximately 2 mL of the metal solution was added to the tube via a cannula, followed by slow addition of the same volume of a solution containing 0.227 g of [*n*-Bu_4N][TCNQ]. Gel conditions were varied in order to optimize crystal growth. The gel percentage was increased to 15 or 20% to increase viscosity, and solvents with a higher density than acetonitrile were used

in the metal layer. Also, cold temperatures were used to further slow diffusion rates. This gel method proved to be the most fruitful because microcrystals were obtained, albeit small and irregular in shape. Unfortunately, the crystals diffracted only weakly, thus indexing was not possible. These results, however, do suggest that gels will be useful for growing crystals of these neutral phase materials. Additional studies in this area will be continued by other group members.

D. Physical Measurements

Infrared spectra were recorded as Nujol mulls on KBr plates in the range 400-4800 cm^{-1} using a Nicolet IR/42 FT-IR spectrometer. Powder X-ray data were collected using a Rigaku RU200B X-ray powder diffractometer with Cu Powder Kα radiation in the range 5-80° in steps of 0.02° in 2Θ. Variable temperature magnetic susceptibility data were collected from 5-300K at fields of 500 or 1000 G using a Quantum Design, Model MPMS SQUID magnetometer housed in the Physics & Astronomy Department at Michigan State University. Field emission scanning electron microscopy measurements (FESEM) were performed on a Hitachi Ltd., Model S-4700II with a Tungsten filament housed in the W.M. Keck Microfabrication Facility located in the Department of Physics & Astronomy at Michigan State University.

Results and Discussion

A. Synthetic Analysis

Reactions of the acetonitrile starting materials $[M(MeCN)_x][BF_4]_2$ (M= Mn, x = 4; Fe, Co, Ni, x = 6) with [*n*-Bu_4N][TCNQ] in acetonitrile led to rapid formation of dark purple crystalline solids (Eq.1).

$$[M(MeCN)_{4,6}][BF_4]_2 + [n\text{-}Bu_4N][TCNQ] \rightarrow M(TCNQ)_2\,(s) + [n\text{-}Bu_4N][BF_4] \quad \text{(Eq. 1)}$$

There is no visible decomposition when these materials are exposed to air, moisture and light. IR spectroscopy, however, indicated that these materials are hygroscopic when exposed to ambient lab atmosphere, and SQUID measurements revealed a detectable decrease in the magnetic susceptibility that can be attributed to air exposure and/or general decomposition over several months. When samples are handled under a nitrogen atmosphere, analytical data for these compounds support the empirical formulae $M(TCNQ)_2$, which is consistent with the charge balance of the divalent metal ions. Unlike previously reported materials of this type, *e.g.*, $M(TCNQ)_2(H_2O)_2$ (M = Mn, Fe, Co and Ni) or $M(TCNQ)(MeOH)_{2,3,4}$ (x = 2, Mn, Fe; x = 3, Co; x = 4, Ni),[13] the present acetonitrile derived materials retain no coordinated solvent molecules according to elemental analysis. Once formed, these compounds are extremely insoluble in common solvents except acids which destroy the materials. Interestingly, and somewhat surprisingly due to their rapid precipitation, $M(TCNQ)_2$ bulk products are microcrystalline and diffract well in powder X-ray experiments.

The choice to react the fully solvated acetonitrile cations that contain the "innocent' $[BF_4]^-$ anion with salts of the coordinating $TCNQ^{-1}$ anion is based on the notion that such metathesis reactions will produce clean, isolable products. By-products remain in solution and are simply washed away from the metal/TCNQ solid; this results

in reproducibly high yields. The main benefit to preparing $M(TCNQ)_2$ products by this approach is that a pre-selected oxidation state of the metal ion is introduced into the material. Other reactions such as oxidation of the metallic form of the element or reduction of neutral TCNQ with metal iodides do not always produce the same results (Eq. 2 and 3). Indeed, these reactions are known to lead to multiple products when more

$$M + nTCNQ \rightarrow M(TCNQ)_n \quad \text{(Eq. 2)}$$

$$3MI + 2nTCNQ \rightarrow 2M(TCNQ)n + MI_3 \quad \text{(Eq. 3)}$$

than one oxidation state is electrochemically accessible for the transition metal. Thus, it is synthetically advantageous to begin with both reactants in their desired oxidation states to insure that the same phase is reproducibly obtained.

The primary synthetic focus of this project was to obtain $M(TCNQ)_2$ products in the highest purity and with the highest ordering temperatures, T_c. To achieve this, it was necessary to carefully monitor and optimize reaction conditions. Several factors such as reaction time and concentration were found to affect the overall magnetic behavior of the resulting products. A time elapsed study, the results of which are listed in Table 4, indicated that the $M(TCNQ)_2$ products degrade from a crystalline to an amorphous phase with increasing reaction times and prolonged contact with the solvent. Elemental analysis results indicated that the optimal time for the reaction is approximately twenty minutes. Increased contact with solution produced average empirical formulae of $M(TCNQ)_x$ ($1 < x < 1.5$) which are further along on the reaction profile than the desired products, and, in fact, may merely represent a mixture of decomposed phases. Analyses of various $Ni(TCNQ)_2$ samples indicate that Ni is unique among the transition metal

series that we studied, in that the desired product does not form at short reaction times. Instead, the final product is formed after approximately three hours of stirring in solution. The conclusion is that increased contact with solution leads to subtle decomposition reactions at the surfaces of the particles, which are accompanied by loss of TCNQ.

Table 4. A study of the effect of reaction time on the composition of $M(TCNQ)_2$ phases using elemental analysis as a test for purity.

Compound/ Sample #	Reaction Time	C%	H%	N%
$Mn(TCNQ)_2$	**Theoretical %**	**62.20**	**1.74**	**24.19**
1	20 min.	61.84	2.25	21.71
2	30 min.	61.26	1.98	22.41
3	1 hour 20 min.	60.18	2.51	21.68
4	13 hours	59.39	2.38	21.87
5	48 hours	55.81	2.06	20.82
6	8 days	53.80	2.13	20.06
7	30 days	51.83	1.59	20.03
$Ni(TCNQ)_2$	**Theoretical %**	**61.72**	**1.73**	**23.99**
1	5min.	51.90	2.27	19.64
2	2 hours	53.46	2.33	19.72
3	3 hours *	60.02	2.21	23.06
4	24 hours	55.21	2.17	20.51

Once the optimal reaction times were found, it was necessary to combine these findings with the optimal concentration. Concentrations of 1.3 mmol in the metal reactant led to products with the highest T_c value when 20 mL of acetonitrile were used as the total reaction volume. Figure 21 summarizes the reaction times and concentrations versus magnetization intensities for samples of four $Mn(TCNQ)_2$. The trend that higher

concentrations lead to increased magnetization reflects the fact the $M(TCNQ)_2$ are apparently dissolving slightly and decomposing even while they are forming. With conditions that favor the decomposition there will be an increase in physical defects that

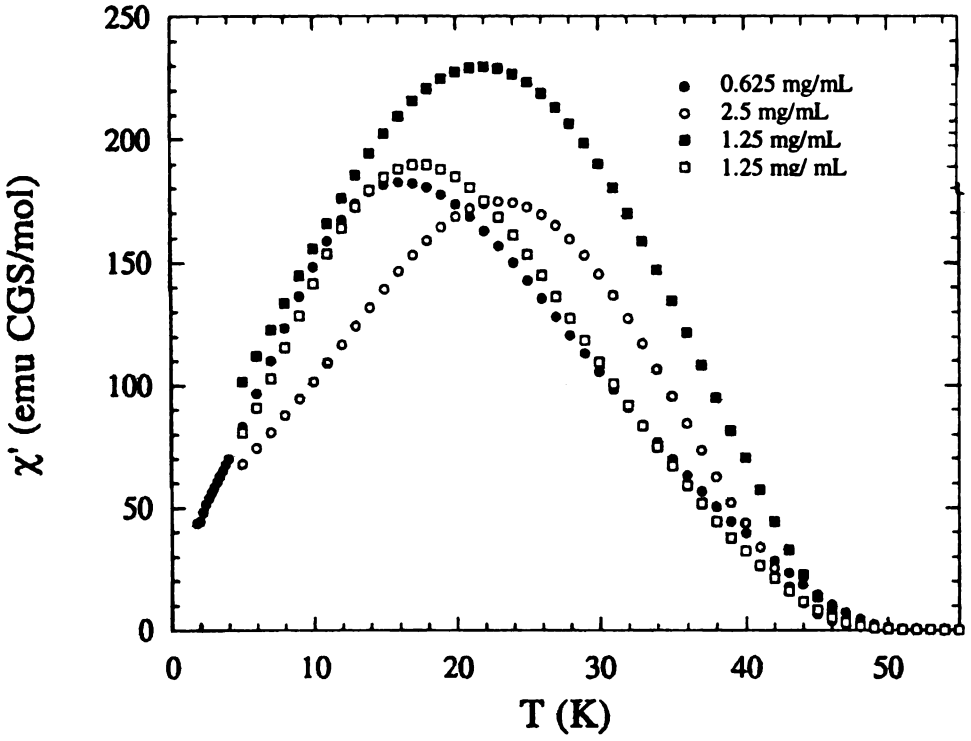

Figure 21. Plots of magnetization versus temperature for four $Mn(TCNQ)_2$ compounds with various reactant and solvent concentrations.

form within the material. An increase of solvent volume (lower concentrations) leads to greater degradation of the product even when the same reaction time is constant. This trend has a limiting concentration, however, beyond which higher reactant concentrations (i.e. 1.25 mg/mL (▪) shown in Figure 21) lead to a lower magnetization value. Finally, as Figure 21 illustrates, magnetic data reproducibility is not possible even when the same conditions are used. In one case, the same reaction conditions led to magnetization values that differed by almost 50 emu CGS/mol! This inconsistency strongly hints at a

dependence of the magnetic properties on particle size which is a parameter that is not easily controlled.

One final comparison (Figure 22) concerns the degradation of the samples over time. Two $Mn(TCNQ)_2$ samples (illustrated as circles) were analyzed at varying time intervals after their isolation in the solid-state (illustrated as squares). In general, as time increased, the magnetic moments decreased. Deliberate exposure to air appeared to hasten the process of decomposition, but this occurred even in samples that were kept under nitrogen in a dry box! The question of how and why the degradation occurs is still not clear, but they are not stable in air or light for long periods of time.

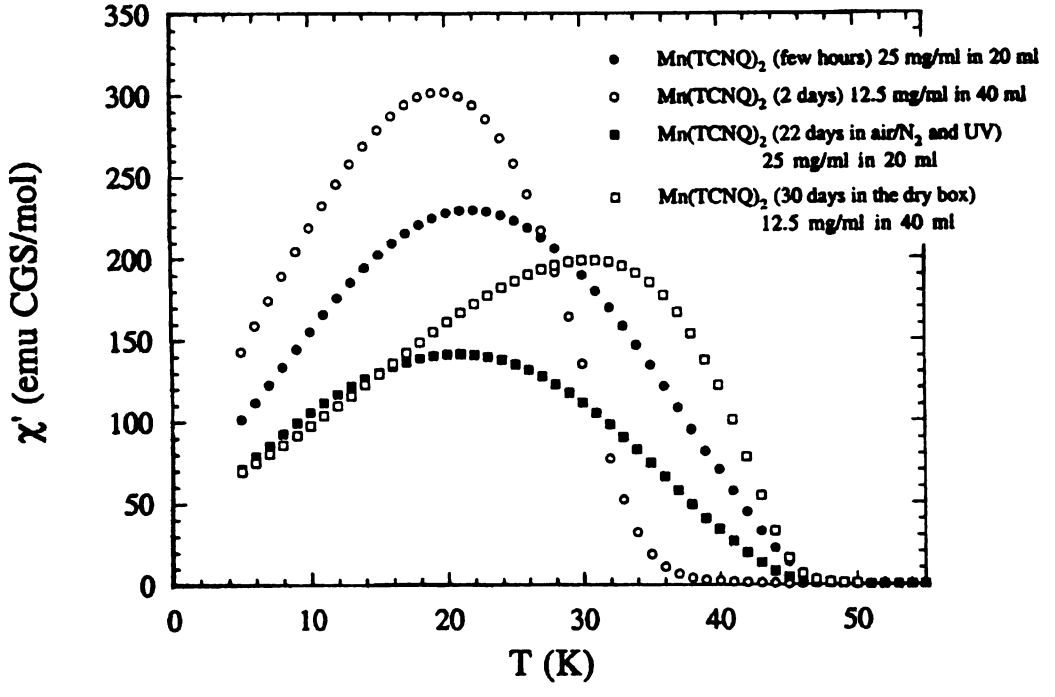

Figure 22. Plots of magnetization versus temperature indicating the "aging process" of the $Mn(TCNQ)_2$ material.

B. Infrared Spectroscopy

This technique proved to be invaluable for the characterization of the $M(TCNQ)_2$ compounds, not only for establishing metal-TCNQ binding, but for addressing structural changes that accompany decomposition. Unfortunately, analysis of the IR data for TCNQ compounds is often difficult due to the extremely versatile nature of the molecule. There are three possible oxidation states, namely $TCNQ^0$, $TCNQ^-$, $TCNQ^{2-}$, multiple isomers for binding the cyano groups such as σ, bridging or dimerized, and in addition, different types of interactions of the TCNQ units themselves (i.e. π-stacked and σ-dimerized).[14] Several research groups have reported the unique infrared bands characteristic of their compounds with the intention of discerning between TCNQ oxidation states and ligand coordination modes in the mid–IR ν(C≡N) region.[5d,f,14,16]

For metal-bound TCNQ, three regions provide important information for assigning charge and discerning the coordination and stacking modes in $TCNQ^{n-}$ salts.[5d,f,15,16] Values in the ν(C≡N) in the region 2100 - 2300 cm^{-1} verify the presence of TCNQ. The ν(C=C) region is characteristic of π-delocalization within the TCNQ ring, and often occurs around 1500 cm^{-1} for $TCNQ^-$. However, there are difficulties with the interpretation of metal-bound TCNQ compounds in these regions of the spectrum, because vibrational stretching modes shift upon coordination. A shift to higher frequencies for ν(C≡N) occurs if TCNQ acts as a σ-donor whereas a shift to lower frequencies indicates a significant TCNQ to metal π-back-bonding.[14] Furthermore, multiple stretches in the ν(C≡N) region render assignments and correlations to other compounds difficult. To alleviate this problem, the δ(C-H) bending region has also been

used because of its' high sensitivity to changes in oxidation state and coordination. In this region, oxidation states are more easily distinguished from each other, for example the neutral TCNQ bending mode occurs at 864 cm^{-1}, while $TCNQ^-$ is in the range 819 - 830 cm^{-1}. Recently, a unique TCNQ dimerized species, referred to as the σ-dimer, $[TCNQ\text{-}TCNQ]^{2-}$, has been identified by our research group to have a δ(C-H) bend occur at 802 cm^{-1}.[5f,16] Since this discovery, the bending mode of TCNQ has become an exceedingly useful tool in the study of metal/TCNQ coordination compounds. For instance, both π-stacked and σ–dimerized forms of reduced TCNQ were found to be present in $[Mn(TCNQ)(TCNQ\text{-}TCNQ)_{0.5}(MeOH)_2]_\infty$ whereas only a σ-dimer is found in the closely related polymeric material, $[Mn(TCNQ\text{-}TCNQ)_2(MeOH)_4]_\infty$.[13] As the number of metal TCNQ coordination compounds increases, a comparative analysis of structural features by infrared spectroscopy becomes possible as in the case of the present set of materials.

Analyses of the infrared spectral data for $M(TCNQ)_2$ compounds (**1** - **4**) indicate that they are similar in structure. A compilation of infrared data is shown in Table 5.

Table 5. Infrared spectroscopic data in the ν(C≡N), ν(C=C), and δ(C-H) regions for $TCNQ^-$ compounds.

Compound	ν(C≡N) (cm^{-1})	ν(C=C) (cm^{-1})	δ(C-H) (cm^{-1})
$Mn(TCNQ)_2$ (**1**)	2205 s, 2187 s, 2137 sh	1505 s	826 m
$Fe(TCNQ)_2$ (**2**)	2217 s, 2187 s, 2142 sh	1505 s	827 m
$Co(TCNQ)_2$ (**3**)	2217 s, 2188 s 2137 sh	1505 s	827 m
$Ni(TCNQ)_2$ (**4**)	2224 s, 2208 s, 2192 s, 2155 sh	1503 s	829 m
TCNQ	2222 s	—	864 s
Li(TCNQ)	2211 s, 2196 s, 2180 sh, 2154 s	1507 s	826 m
[*n*-Bu_4N][TCNQ]	2188 sh, 2180 s, 2162s , 2157 s	1507 s	824 m

In general, there is a notable absence of features that correspond to bound acetonitrile or $[BF_4]^-$ counterions. This is in accord with TCNQ being in its mono-reduced form and acting as the only ligand for the divalent metals. In the ν(C≡N) region of the Mn, Fe and Co compounds there are three stretching modes whereas there are four features in the spectrum of $Ni(TCNQ)_2$. The slight differences may be due, in part, to the presence of an intermediate that is known to form in the $Ni(TCNQ)_2$ reaction or to a solid-state splitting effect not observed in the others. The stretching modes for all four metal compounds are generally lower in energy than the corresponding mode for neutral TCNQ, *viz.*, 2222 cm^{-1}, and are characteristic of $TCNQ^-$. The ν(C=C) stretching region is characteristic for the TCNQ phenyl ring. The π-bond delocalization over the ring results in one strong (C=C) stretching feature that is typically in the range 1500-1510 cm^{-1} for $TCNQ^-$. Compounds (**1** - **3**) exhibit bands at 1505 cm^{-1}, while the (C=C) stretch for **4** is slightly lower in energy at 1503 cm^{-1}. The δ(C-H) bending modes of the four compounds were examined as well. In this region, modes for $TCNQ^-$, $TCNQ^{2-}$, and mixed-valence stacks of $TCNQ^-$ and TCNQ are well-documented.[17] In accord with literature reports for $TCNQ^-$, compounds **1** - **4** exhibit δ(C-H) frequencies between 826 and 829 cm^{-1} which is well within the expected range for mono-reduced TCNQ.

An interesting phenomenon was noted after infrared spectral analysis of $M(TCNQ)_2$ products from reactions that were stirred for longer periods of time. The presence of the unit that we have come to realize is quite prevalent in metal/TCNQ compounds, namely the σ-dimer form $[TCNQ\text{-}TCNQ]^{2-}$, was evident. This surprising occurrence is noted in Figure 23. As indicated in the figure, the feature for $TCNQ^-$ anion

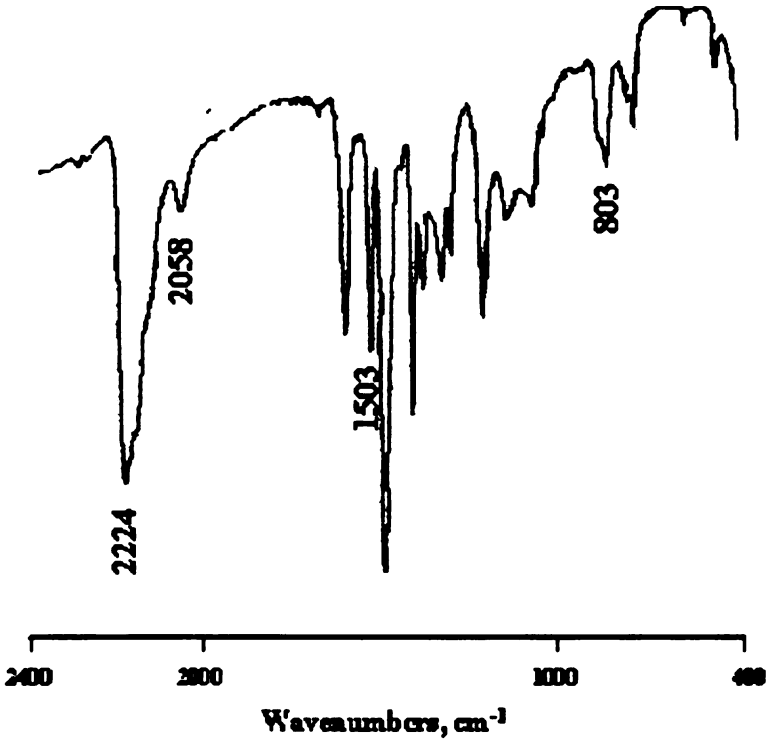

Figure 23. IR spectrum of a bulk sample of $Ni(TCNQ)_2$ indicating presence of a σ-dimer containing phase(s) at 803 cm^{-1}.

is still present, but it diminishes as the σ-dimer structural unit appears as a feature at 803 cm^{-1}. It appears that $M(TCNQ)_2$ is being converted over time to a new phase that contains both reduced and dimerized forms of TCNQ. Alternatively it may be that the new phase is composed solely of σ-dimers represented by the formula, $M[TCNQ\text{-}TCNQ]^{2-}$. This phenomenon occurs in all of the $M(TCNQ)_2$ materials, and even in compounds isolated at shorter reaction times; in the latter cases the 802 cm^{-1} feature is detected as only a very small shoulder.

In summary, infrared spectroscopy has proven to be quite useful for helping to identify the structural components of these $M(TCNQ)_2$ polymers. Although there are

slight differences in the IR data in the family, the striking similarities lend support to the conclusion that they contain the same arrangement and oxidation state of TCNQ.

C. Structural Studies

(a) Field Emission Scanning Electron Microscopy, FESEM

Several important facts emerged from analysis of **1 - 4** by FESEM techniques. One point is that compounds are not as crystalline as the copper and silver TCNQ compounds. Instead of well-defined crystallites, the bulk products contain "spheres" which are often rough and irregular in shape as shown in Figure 24.

Upon examination at higher magnifications it is possible to see that the surface of an individual sphere is very rough and uneven and that there are smaller particles or domains on the surface. In other words, the spherical shapes are secondary and not primary particles. The observations above can be seen more clearly in images obtained using transmission electron microscopy (TEM). In Figure 25, the crystallinity and particle sizes are shown for compounds 1-4. For all compounds except Mn, the particles tend to form homogenous "clusters" throughout the material.

The high surface areas of these solids may very well affect the magnetic behavior due to the large number of physical defects. As mentioned earlier, the magnetic properties are never fully reproducible even when one tries to control the synthetic parameters; the extremely small particle size could be the reason.

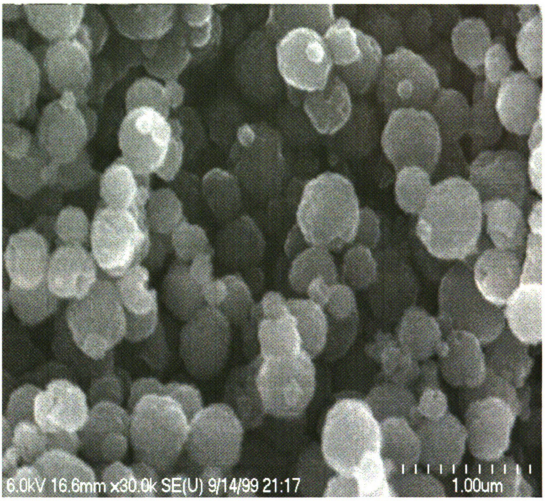

Figure 24. Spherical particles of $Ni(TCNQ)_2$.

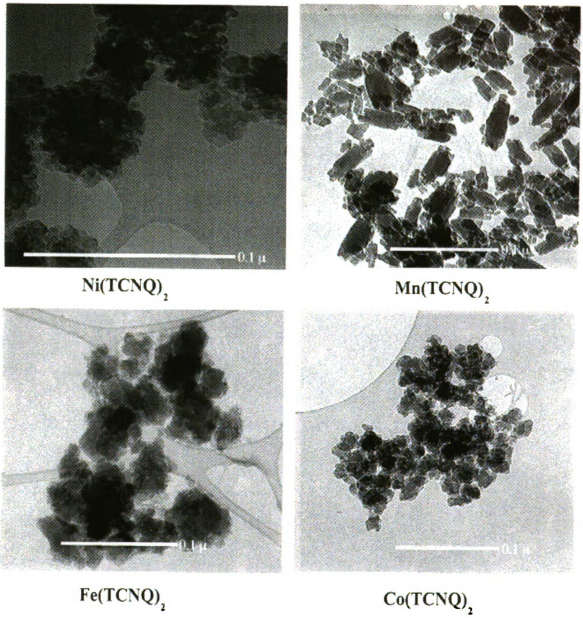

Figure 25. TEM photographs of compounds 1 - 4.

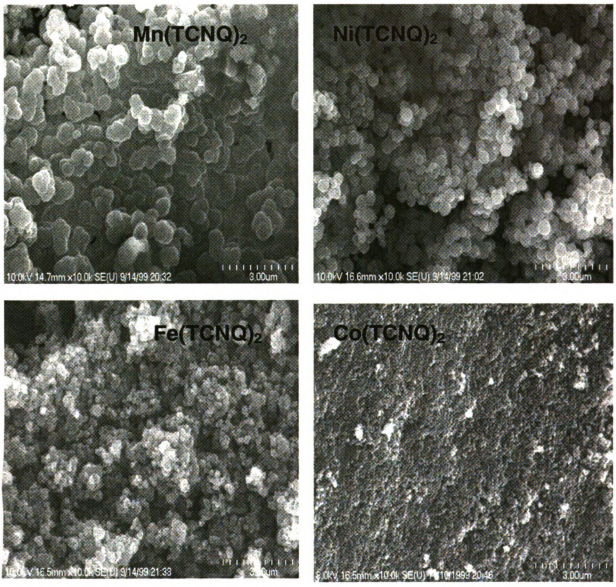

Figure 26. Particle size trend for $M(TCNQ)_2$ compounds at 10k magnification.

It was evident in the images of the $M(TCNQ)_2$ products that there is a particle size trend. In Figure 26, the four compounds were each imaged at a 10k magnification using a 10.0 kV accelerating voltage. The largest particles are found in $Mn(TCNQ)_2$ followed by $Ni(TCNQ)_2$, and finally the Fe and Co analogs whose particles are approximately the same size. This trend correlates with the clarity of the powder patterns for these compounds, in that the larger the particle size, the greater the intensity in the powder X-ray diffraction pattern. The images provide important visual evidence of the high surface area of these compounds and also reveal a homogeneity that is remarkably good. Normally, without any attempts to control particle size, one obtains a distribution of particle sizes. In the $M(TCNQ)_2$ samples nearly every particle is identical, and there is no evidence for more than one phase.

(b) Powder X-ray Diffraction

Bulk microcrystalline products of **1** - **4** yield simple powder patterns as illustrated in Figure 27. Samples were analyzed using a step program (12 s per 0.02° at 2Θ) on a Rigaku RU200B X-ray powder diffractometer with Cu Kα radiation (λ_α = 1.54050 Å), and the patterns were indexed using the Treor90 program.[18] These efforts led to a tetragonal cell with a = 18.8527, b = 15.4499, c = 8.2539 and V = 2404.14 for $Mn(TCNQ)_2$ (**1**). As indicated in the figure, the intensities and peak positions at 2Θ are nearly identical, which provide evidence that the compounds are isostructural. Therefore, the lattice parameters found for $Mn(TCNQ)_2$ should also be similar for the other members of the family.

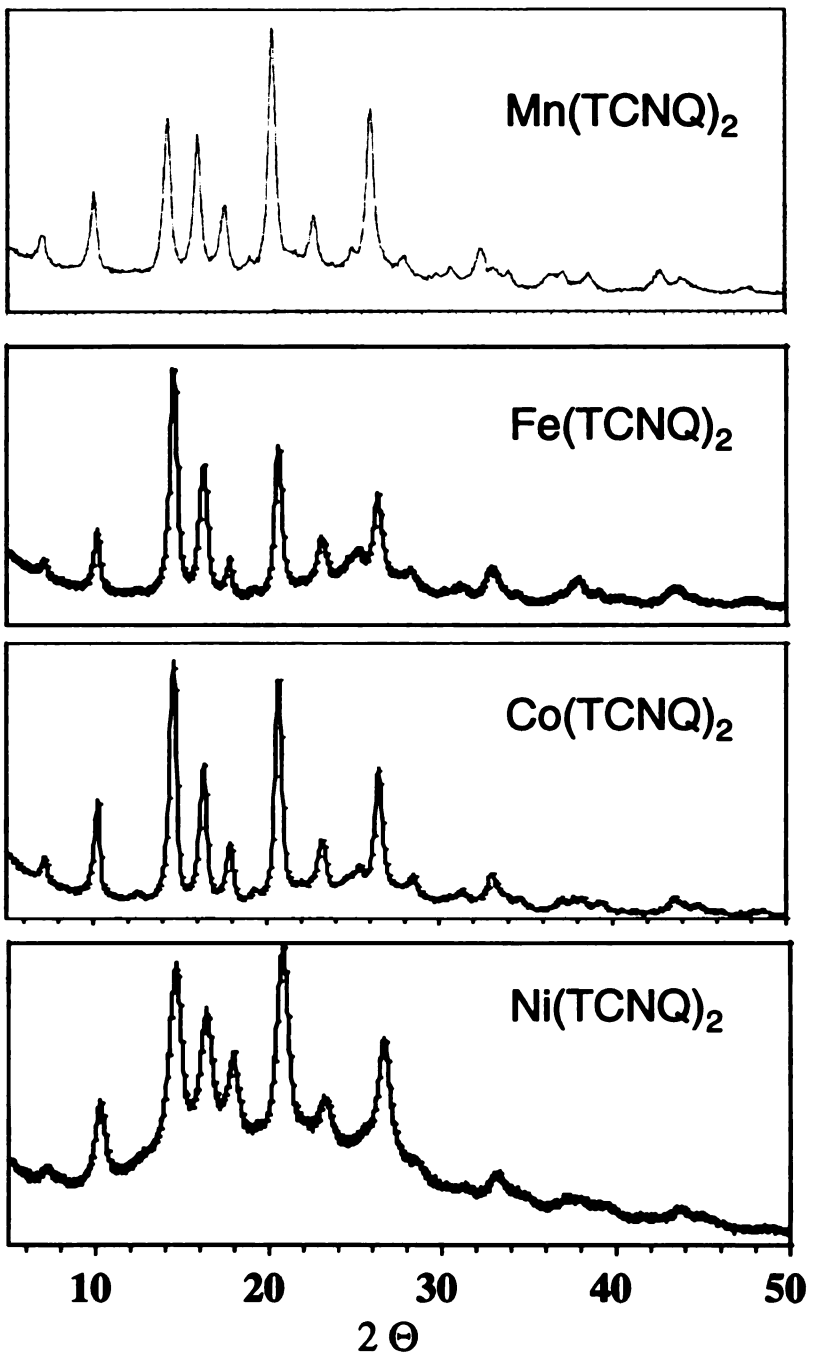

Figure 27. X-ray powder diffraction patterns for isostructural compounds 1 - 4.

D. Magnetic Properties

(a) Magnetic Data Analysis

The temperature-dependent d. c. magnetic susceptibilities (χ) for compounds **1 - 4** (M = Mn^{II} S = 5/2; Fe^{II} S = 2; Co^{II} S = 3/2; Ni^{II} S = 1) were measured from 5 to 300 K on a SQUID magnetometer. Plots of χ_{mol}^{corr} , μ_{eff}, and $1/\chi_{mol}^{corr}$ versus temperature are shown in Figures 28-31. All four compounds exhibit globally similar magnetic behavior therefore only the magnetic properties of $Mn(TCNQ)_2$ will be discussed. In the plots of χ_{mol}^{corr} and $1/\chi_{mol}^{corr}$ versus temperature (Figure 28 and 29), the compounds follow Curie-Weiss behavior at high temperatures. At a certain temperature, there is an increase in the response (the highest temperature in the series is for Mn at 44 K). Application of the field causes domains of spins within the material to align in a parallel manner, which is typically thought of in terms of ferromagnetic ordering. This phenomenon is recorded in Figure 28 as a sharp increase in magnetic susceptibility at low temperatures. It is evident in Figure 29 that a positive Weiss constant characteristic of ferromagnetic behavior is observed. A plot of μ_{eff} vs. temperature for $Mn(TCNQ)_2$ (Figure 30) reveals a room temperature μ_{eff} value of ~ 5.9 μ_B, which is the spin-only value for Mn(II). Analysis of the d.c. measurements point to the conclusion that these compounds are ferrromagnetic in nature. However, their synthetic instability and non-reproducibility represented in previous magnetic plots (Figures 21 and 22) indicate that they are not typical ferromagnets. Physical defects, such as a variation in the percentage of the diamagnetic σ-dimer within these compounds or just the physically small size, can both be

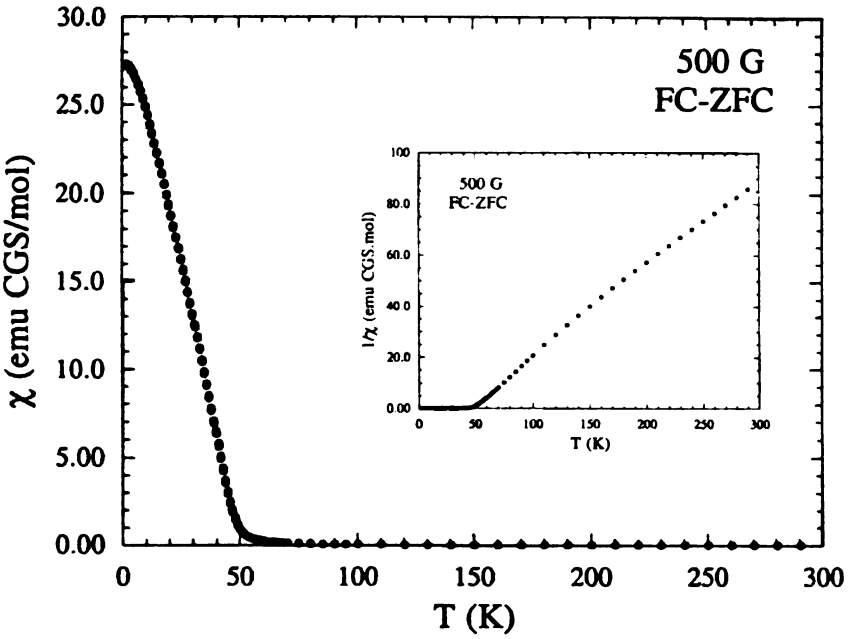

Figure 28. Plots of χ_{mol}^{corr} and $1/\chi_{mol}^{corr}$ versus temperature for $Mn(TCNQ)_2$.

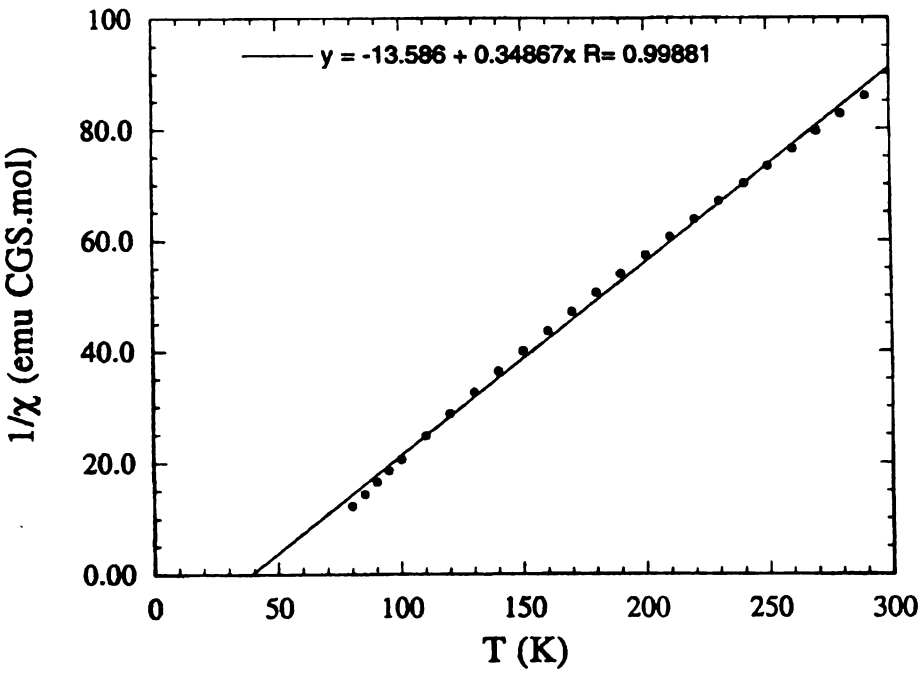

Figure 29. Fitting of $1/\chi_{mol}^{corr}$ versus temperature for $Mn(TCNQ)_2$ to ascertain the exact critical temperature, T_c.

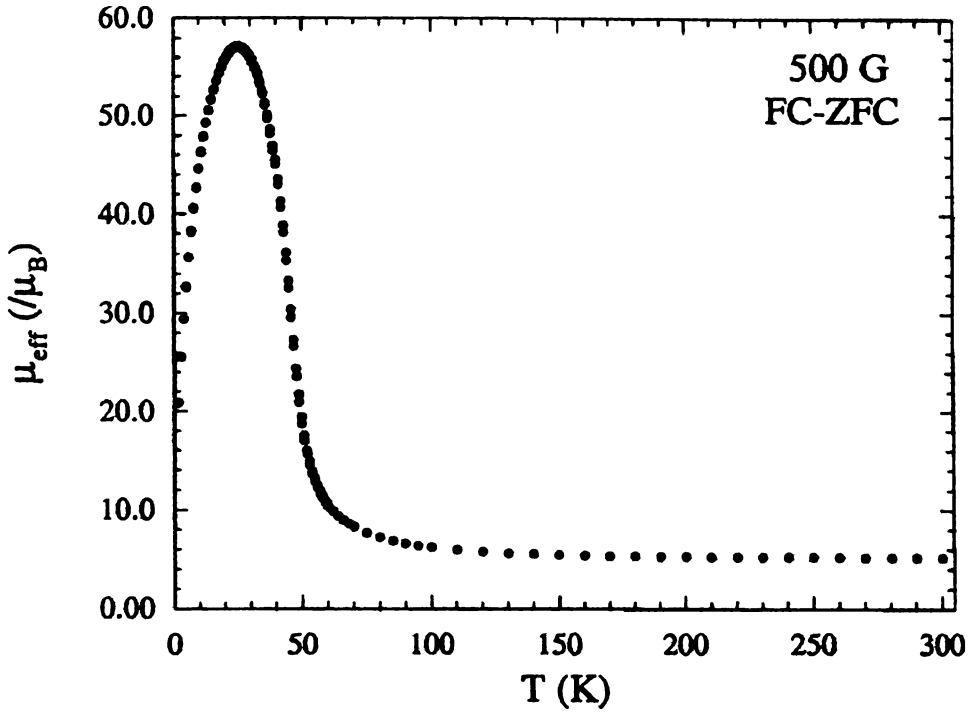

Figure 30. Plot of μ_{eff} versus temperature for $Mn(TCNQ)_2$.

contributors to spin-glass behavior. Further magnetic studies using the a.c. method allowed for these compounds to be classified as spin-glass materials based on observation of a frequency dependence for these compounds. Compounds that exhibit a ferromagnetic ordering do not show a frequency dependence, in contrast to spin glass materials. A.C. studies are the principal methods used to distinguish closely related magnetic behavior.

A plot of $\chi'_{mol}{}^{corr}$ versus temperature is shown in Figure 31. Different frequencies were applied over the temperature range and all data were plotted. For each frequency study, the maximum was located at slightly different temperatures. In general, as the frequency is decreased the maxima are located at lower temperatures. The frequency dependence is a key characteristic for spin glass materials. As the frequency of the field oscillates very rapidly, the spins within a ferromagnet remain correlated with the field,

whereas those of a spin glass become blocked. A spin glass has small domains of ordering rather than long-range ordering, and in these domains a blocking (or freezing) of the spins occurs that becomes more and more evident at higher frequencies. As previously indicated, defects in the compound or small particle sizes could be the main factor affecting the frequency measurements. Therefore, although d.c. measurements indicate an apparent ferromagnetic ordering, it is the a.c. measurements that classify the $M(TCNQ)_2$ family of compounds as spin glass materials.

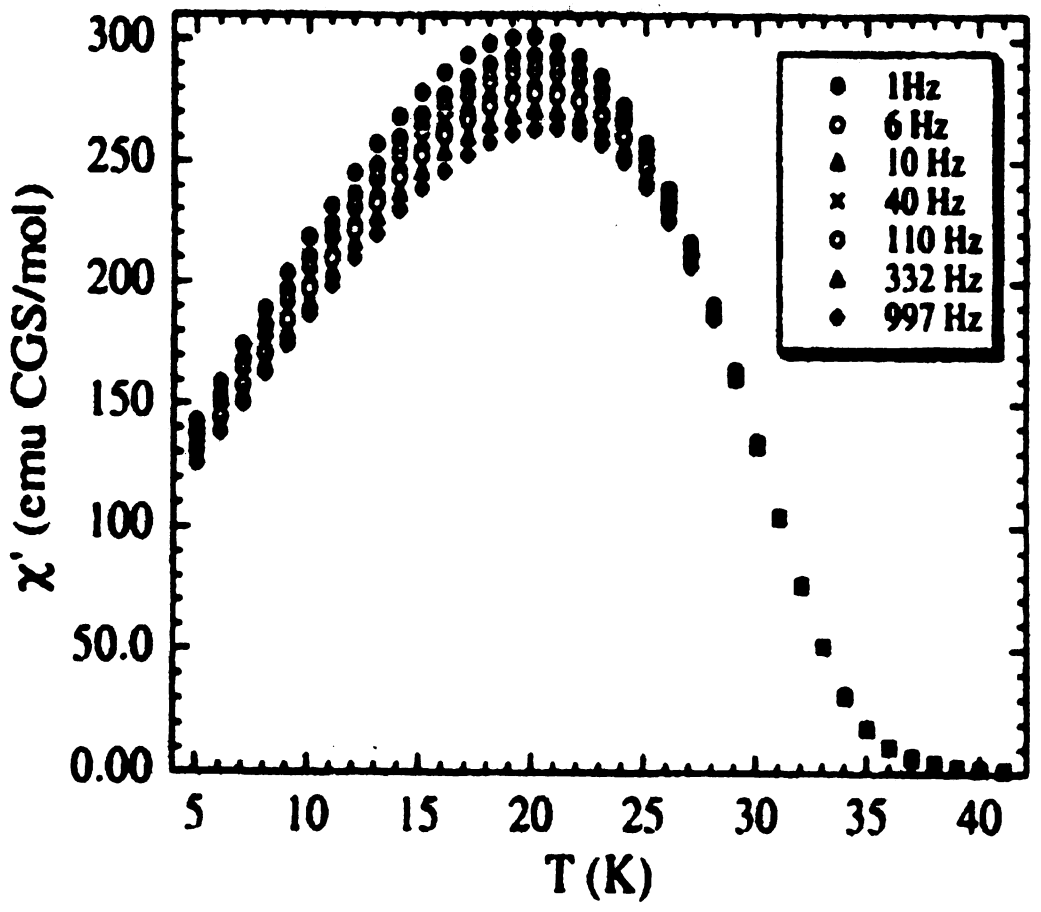

Figure 31. Plots of $\chi'_{mol}{}^{corr}$ versus temperature illustrating the frequency dependence of the $M(TCNQ)_2$ compounds.

Whether the $M(TCNQ)_2$ family of compounds are spin glass or ferromagnetic materials, they are magnets. This conclusion is well illustrated in Figure 32. A plot of magnetization versus field indicates that a hysteresis or "memory effect" is observed for $Mn(TCNQ)_2$. If a material exhibits magnetic hysteresis, then it has a memory and therefore is, by definition, a magnet. Our interests lie primarily with the discovery of novel magnetic materials, but, when extraordinary phenomenon such as the spin glass nature of these compounds is observed, scrupulous analysis of the magnetic behavior is warranted.

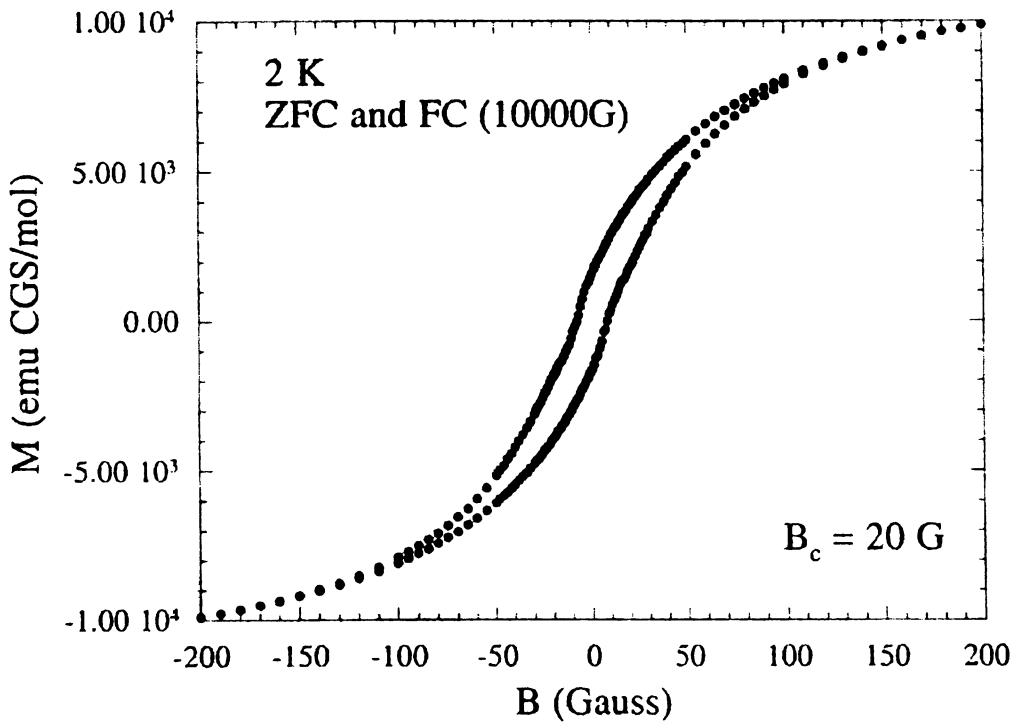

Figure 32. Plot of magnetization versus field illustrating the hysteresis observed for $Mn(TCNQ)_2$.

(b) Heat Capacity Measurements

Heat capacity measurements are useful for corroborating the existence of bulk magnetic transitions. If the material undergoes a change in magnetic state, it necessarily

must undergo a concomitant change in entropy, which is manifested as a peak in the heat capacity data at the transition temperature. Materials that undergo ferro-, ferri-, or antiferromagnetic ordering often exhibit temperature dependent heat capacity behavior. Spin glasses and totally amorphous materials undergo short-range magnetic interactions, thus the thermodynamic properties of the system are not drastically altered and there is no maximum in their heat capacity plots. In this vein, we are using heat capacity data for discerning whether these $M(TCNQ)_2$ compounds are bulk ferromagnets or actually spin glass materials.

The heat capacity measurements of compounds **1** - **4** are shown in Figure 33. It is obvious that there is an absence of a peak indicative of ferromagnetic ordering.

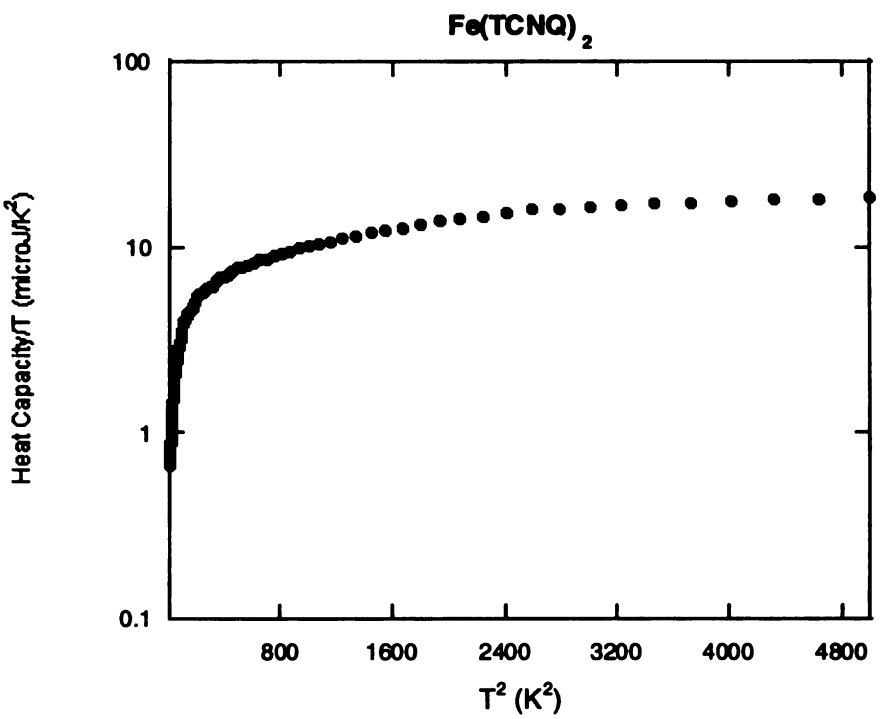

Figure 33. Plot of heat capacity measurements for $Fe(TCNQ)_2$.

Conclusions

Our use of paramagnetic transition metal ions as building blocks for the synthesis of novel TCNQ materials has resulted in the formation of three-dimensional crystalline materials with interesting magnetic properties. In this family of compounds, the high number of spins on the metal centers of Mn, Fe, Co and Ni along with the S = 1/2 spin on the TCNQ anion produces a strong ferromagnetic coupling according to dc measurements. Synthetic studies and magnetic studies in the a.c. mode point to the conclusion that these compounds are not ordinary ferromagnetic materials. When reaction conditions are varied only slightly, net magnetization and "critical temperature" values are very different. Attempts to reproduce the magnetic data for a particular compound proved to be futile, as χ_{mol}^{corr} versus temperature plots indicated that both net magnetization as well as critical temperature values were never exactly the same. It appears that small quantities of impurities are being produced which are causing some of the inconsistencies in the magnetic measurements. It has been shown by infrared spectroscopy that the σ-dimer unit, $[TCNQ\text{-}TCNQ]^{2-}$, begins to form in the solid with increased reaction times. The formation of this component is occurring even at the shortest reaction times, therefore it will always be a minor impurity of varying degree in these samples. The presence of σ-dimer $[TCNQ\text{-}TCNQ]^{2-}$ impurities may be contributing to the spin glass magnetic behavior; certainly the presence of another structural unit does not help in terms of leading to a pure material with long-range ferromagnetic ordering!

The FESEM images of these materials indicate that they consist of rough-edged spheres with a very large surface area. The fact that such a large volume of the material

is tied up in surface defect sites is most likely the largest contributing factor to the anomalous magnetic properties. The dangling bonds are structural defects that disrupt the two or three-dimensional metal/TCNQ framework. This structural discontinuity prohibits a ferromagnetic ordering and leads to local areas of competing interactions due to the breaking of symmetry. This situation is just the sort that Mydosh describes as leading to spin glass behavior.[9a] The absence of a maximum in the heat capacity measurements of these compounds, and the a.c. frequency dependence both support the conclusion that the $M(TCNQ)_2$ family of compounds are spin glasses.

Future syntheses and characterization of transition metal/TCNQ materials will likely produce interesting magnetic results as well. The incorporation of d^8, divalent Pt or Pd compounds, which typically form square planar compounds, will alter the geometrical requirements of the growing polymers, and may lead to a new class of materials in which a metal ion stack and an organic stack occurs in the same material. The diamagnetic nature of Pd^{2+} and Pt^{2+} would allow for the analysis of only the interactions of the TCNQ S=1/2 spins without complications due to metal ion spins. Furthermore, the use of other acceptors such as $TCNQF_4$, $TCNQ(OMe)_2$, or $TCNQBr_2$ would be an excellent means of probing the magnetic properties when small changes in the electronic properties of the ligand are implemented. Most importantly, structural analysis of new binary metal/TCNQ compounds is necessary, which requires much focus on new crystallization techniques to inhibit rapid precipitation of these materials.

References

1 (a) Acker, D. S.; Harder, R. J.; Hertler, W. R.; Mahler, W.; Melby, L. R.; Bensin, R. E.; Mochel, W. E. *J. Am. Chem. Soc.* **1960**, *82*, 6408. (b) Melby, L. R.; Harder, R. J.; Hertler, W. R.; Mahler, W.; Benson, R. E.; Mochel W. E. *J. Am. Chem. Soc.* **1962**, *84*, 3374. (c) Torrance, J. B. *Acc. Chem. Res.* **1979**, *12*, 79. (d) Endres, H. In *Extended Linear Chain Compounds*; Miller, J.S. Ed.; Plenum: New York. **1983**; Vol. 3, pp. 263-312. (e) Wudl, F. *Acc. Chem. Res.* **1984**, *17*, 227. (f) Jérome, D. *Science* **1991**, *252*, 1509. (g) Bryce, M. R. *Chem. Soc. Rev.* **1991**, *20*, 355. (h) Williams, J. M.; Schultz, A. J.; Geiser, U.; Carlson, K. D.; Kini, A. M.; Wang, H. H.; Kwok, W. - K.; Wangbo, M. - H.; Schirber, J. E. *Science*, **1991**, *252*, 1501. (i) Ward, M. D. *Electroanal Chem.* **1988**, *16*, 181. (j) Martin, N.; Segura, J. L.; Seoane, C. *J. Mater. Chem.* **1997**, *7*, 1661.

2 (a) Miller, J. S.; Calabrese, J. C.; Epstein, A. J.; Bigelow, R. W.; Zhang, J. H.; Reiff, W. M. *J. Chem. Soc., Chem. Commun.* **1986**, 1026. (b) Miller, J. S.; Zhang, J. H.; Reiff, W. M.; Dixon, D. A.; Preston, L. D.; Reis, A. H.; Gebert, E.; Extine, M.; Troup, J.; Epstein, A. J.; Ward, M. D. *J. Phys. Chem.* **1987**, *91*, 4344. (c) Broderick, W. E.; Thompson, J. A.; Day, E. P.; Hoffman, B. M. *Science*, **1990**, *249*, 401. (d) Kollmar, C. Couty, M.; Kahn, O. *J. Am. Chem. Soc.* **1991**, *113*, 7994. (e) Miller, J. S.; Epstein, A. J. *Angew. Chem., Int. Ed. Engl.* **1994**, *33*, 385. (f) Murphy, V. J.; O'Hare, D. *Inorg. Chem.* **1994**, *33*, 1833.

3 (a) Pénicaud, A.; Batail, P.; Perrin, C.; Coulon, C.; Parkin, S. S. P.; Torrence, J. B. *J. Cehm. Soc., Chem. Commun.* **1987**, 330. (b) Davidson, A.; Boubekeur, K.; Pénicaud, A.; Auban, P.; Lenoir, C.; Batail, P.; Hervé, G. *J. Chem. Soc., Chem. Commun.* **1989**, 1373. (c) Pénicaud, A.; Bourbekeur, K.; Batail, P.; Canadell, E.; Auban - Senzier, P.; Jérome, D. *J. Am. Chem. Soc.* **1993**, *115*, 4101. (d) Coulon, C.; Livage, C.; Gonzalavez, L.; Boubekeur, K.; Batail, P. *J. Phys. I Fr.* **1993**, *3*, 1. (e) Coronado, E.; Gómez - Garcia, C. J. *Comments Inorg. Chem.* **1995**, *17*, 255. (f) Gómez - Garcia, C. J; Giménez - Saiz, C. J.; Triki, S.; Coronado, E.; Manqueres, P. L.; Ouahab, L.; Ducasse, L.; Sourisseau, C.; Delhaes, P. *Inorg. Chem.* **1995**, *34*, 4139. (g) Coronado,

E.; Delhaus, P.; Galáan - Mascarós, J. R.; Giménez - Saiz, C. J. *Synth. Met.* **1997**, *85*, 1647.

4 (a) Bousseau, M.; Valade, L.; Legros, J. - P.; Cassoux, P.; Garbauskas, M.; Interrante, L. V. *J. Am. Chem. Soc.* **1986**, *108*, 1908. (b) Day, P.; Kurmoo, M.; Mallah, T.; Marsden, I. R.; Allan, M. R.; Friend, R. H.; Pratt, F. L.; Hayes, W.; Chasseau, D.; Bravic, G.; Ducasse, L. *J. Am. Chem. Soc.* **1992**, *114*, 10722. (c) Kurmoo, M.; Graham, A. W.; Day, P.; Coles, S. J.; Hursthouse, M. B.; Caulfield, J. L.; Singleton, J.; Pratt, F. L.; Hayes, W.; Ducasse, L.; Guionneau, P. *J. Am. Chem. Soc.* **1995**, *117*, 12209.; see also references therein.

5 (a) Lacroix, P.; Kahn, O.; Gliezes, A.; Valade, L.; Cassoux, P. *Nouv. J. Chim.* **1985**, 643. (b) Gross, R.; Kaim, W. *Angew. Chem., Int. Ed. Engl.* **1987**, *26*, 251. (c) Bartley, S. L.; Dunbar, K. R. *Angew. Chem., Int. Ed. Engl.* **1991**, *30*, 448. (d) Ballester, L.; Barral, M.; Gutiérrez, A.; Jiménez-Apararicio, R.; Martinez - Muyo, J.; Perpiñan, M.; Monge, M.; Ruiz - Valero, C. *J. Chem. Soc., Chem. Commun.* **1991**, 1396. (e) Humphrey, D. G.; Fallon, G. D.; Murray, K. S. *J. Chem. Soc., Chem. Commun.* **1988**, 1356 (f) Cornelissen, J. P.; van Diemen, J. H.; Groeneveld, L. R.; Haasnoot, J. G.; Spek, A. L.; Reedijk, J. *Inorg. Chem.* **1992**, *31*, 198. (g) Oshio, H.; Ino, E.; Mogi, I.; Ito, T. *Inorg. Chem.* **1993**, *33*, 5697. (h) Ballester, L.; Barral, M.; Gutiérrez, A.; Perpiñan, M.; Monge, M.; Ruiz-Valero, C.; Sánchez-Pélaez, A. *Inorg. Chem.* **1994**, *33*, 2142. (i) Dunbar, K. R.; Ouyang, X. *Mol. Cryst. Liq. Cryst. Sci. Technol.* **1995**, *273*, 21. (j) Oshio, H.; Ino, E.; Ito, T.; Maeda, Y. *Bull. Chem. Soc. Jpn.* **1995**, *68*, 889. (k) Dunbar, K. R. *Angew. Chem.* **1996**, *35*, 1659. (l) Decurtins, S.; Dunbar, K. R.; Gomez - Garcia, C. J.; Mallah, T.; Raptis, R. G.; Talham, D.; Veciana, J. In *Molecular Magnetism: From Molecular Assemblies to the Devices*; NATO ASI Series E321; Coronado, E.; Delhaès, P., Gatteschi, D., Miller J. S., Eds.; Kluwer: Dordrecht, 1996; 571. (m) Dunbar, K. R.; Ouyang, X. *Chem. Commun.* **1996**, 2427. (n) Zhao, H.; Heintz, R. A.; Rogers, R. D.; Dunbar, K. R. *J. Am. Chem. Soc.* **1996**, *118*, 12844. (o) Dunbar, K. R.; Ouyang, X. *Inorg. Chem.* **1996**, *35*, 7188. (p) Azcondo, M. T.; Ballester, C. J.; Gutiérrez,, A.; Perpiñan, M.; Amador, U.; Ruiz - Valero, C.; Bellitto, C. *J. Chem. Soc., Dalton Trans.* **1996**, 3015.

6 (a) Manriquez, J. M.; Yee, G. T.; McLean, S.; Epstein, A. J.; Miller, J. S. *Science* **1991**, *252*, 1415. (b) Miller, J. S.; Calabrese, J. C.; McLean, R. S.; Epstein, A. J. *Adv. Mater.* **1992**, *4*, 498. (c) Miller, J. S.; Vazquez, C.; Jones, N. L.; McLean, R. S.; Epstein, A. J. *J. Mater. Chem.* **1995**, *5*, 707. (d) Miller, J. S.; Calabrese, J. C.; Vazquez, C.; McLean, R. S.; Epstein, A. J. *Adv. Mater.* **1994**, *6*, 217. (e) Böhm, A.; Vazquez, C.; McLean, R. S.; Calabrese, J. C.; Kalm, S. E.; Manson, J. L.; Epstein, A.; Miller, J. S. *Inorg. Chem.* **1996**, *35*, 3083. (f) Brinckerhoff, W.B.; Morin, B.G.; Brandon, E. J.; Miller, J. S.; Epstein, A. *Appl. Phys.* **1996**, *79*, 6147.

7 (a) Aumüller, A.; Erk, P.; Klebe, G.; Hünig, S.; von Schütz, J.; Werner, H. *Angew. Chem., Int. Ed. Engl.* **1986**, *25*, 740. (b) Aumüller, A.; Erk, P.; Hünig, S. *Mol. Cryst. Liq. Cryst.* **1988**, *156*, 215. (c) Erk, P.; Gross, H. - J.; Hünig, U. L.; Meixner, H.; Werner, H. - P.; von Schütz, J. U.; Wolr, H. C. *Angew. Chem., Int. Ed. Engl.* **1989**, *28*, 1245. (d) Kato, R.; Kobayashi, H.; Kobayashi, A. *J. Am. Chem. Soc.* **1989**, *111*, 5224. (e) Aumüller, A.; Erk, P.; Hünig, S.; Hädicke, E.; Peters, K.; von Schnering, H.G. *Chem. Ber.* **1991**, *124*, 2001. (f) Sinzger, K.; Hünig, S.; Jopp, M.; Bauer, D.; Beitsch, W.; von Schütz, J. U.; Wolf, H. C.; Kremer, R. K.; Metzenthin, T.; Bau, R.; Khan, S. I.; Lindbaum, A.; Lengauer, C. L.; Tillmanns, E. *J. Am. Chem. Soc.* **1993**, *115*, 7696.

8 (a) Potember, R. S.; Poehler, T. O.; Cowan, D. O. *Appl. Phys. Lett.* **1979**, *34*, 405. (b) Potember, R. S.; Poehler, T. O.; Cowan, D. O.; Carter, F. L.; Brant, P. In *Molecular Electronic Devices II*; Carter, F. L., Ed.; Marcel Dekker: New York, 1982; p. 91 (c) Hoagland, J. J.; Wang, X.D.; Hipps, K. W. *Chem. Mater.* **1993**, *5*, 54. (d) Dunbar, K. R.; Cowen, J.; Heintz, R. A.; Grandinetti, G.; Ouyang, X.; Zhao, H. *Inorg. Chem.* **1999**, *38*, 144.

9 (a) Mydosh, J. A. *Spin Glasses: An Experimental Introduction*, Taylor &Francis, London, **1993**, pp. 64-73. (b) Chowdhury, D. *Spin Glasses and Other Frustrated Systems*, Princeton University Press, New Jersey, **1986**. (c) Moorjani, K. and Coey, J. M. D. *Magnetic Glasses*, Elsevier Ed., New York, **1984**.

10 Heintz, R.A.; Smith, J. A.; Szalay, P. S.; Weisgerber, A.; Dunbar, K.R . *Inorg. Synth.* in press.

11 (a) Holden, A. and Singer P. *Crystals and Crystal Growing*, Anchor Books-Doubleday, New York, 1960. (b) Laudise, R. A. *The Growth of Single Crystals*, Solid State Physixl Electronics Series, N. Holonyak Jr. Ed., Prentice-Hall, Inc., 1970. (c) Henisch, H. K. *Crystal Growth in Gels*, Pennsylvania State University Press, 1970. (d) Sulb, S. L. *J. Chem. Ed.* **1985**, *62*, 81. Hulliger, J. *Angew. Chem. Int. Ed. Engl.* **1994**, *33*, 143.

12 (a) Desiraju, G. R.; Curtin, D. Y.; Paul, I. C. *J. Am. Chem. Soc.* **1977**, *99*, 6148. (b) Arend, H.; Connelly, J. J. *J. Cry. Growth* **1982**, *56*, 642. (c) Robert, M. C.; Lefaucheux, F. *J. Cry. Growth* **1988**, *90*, 358. (d) Doxsee, K. M.; Chang, R. C.; Chen, E. *J. Am. Chem. Soc.* **1988**, *120*, 585. (e) Yaghi, O.; Li, G.; Li, H. *Chem. Mater.* **1997**, *9*, 1074.

13 Zhao, H.; Heintz, R. A.; Ouyang, X.; Dunbar, K. R. *Chem. Mater.* **1999**, *11*, 736.

14 Kaim, W.; Moscherosch, M. *Coord. Chem. Rev.* **1994**, *129*, 157.

15 (a) Lunille, B.; Pecile, C. *J. Chem. Phys.* **1970**, *52*, 2375. (b) Bozio, R.; Girlando, A.; Pecile, C. *J. Chem. Soc., Faraday Trans. 2* **1975**, *71*, 1237. (c) Van Duyne, R. P.; Suchanski, M. R.; Lakovits, J. M.; Siedle, A. R.; Parks, K. D.; Cotton, T. M. *J. Am. Chem. Soc.* **1979**, *101*, 2832. (d) Chappell, J. S.; Bloch, A. N.; Bryden, A.; Maxfield, M.; Poehler, T. O.; Cowan, D. O. *J. Am. Chem. Soc.* **1981**, *103*, 2442. (e) Farges, J. P.; Brau, A; Dupuis, P. *Solid State Commun.* **1985**, *54* (6), 531. (f) Inoue, M.; Inoue, M. B. *J. Chem. Soc., Faraday Trans. 2* **1985**, *81*, 539. (g) Inoue, M.; Inoue, M. B. *Inorg. Chem.* **1986**, *25*, 37. (h) Inoue, M.; Inoue, M. B.; Fernando, Q.; Nebesny, K. W. *J. Phys. Chem.* **1987**, *91*, 527.

16 Pukaki, W.; Pawlak, M.; Graja, A.; Lequan, M.; Lequan, R. M. *Inorg. Chem.* **1987**, *26*, 1328.

17 (a) Yashihiro, Y.; Furukawa, Y.; Kobayashi, A.; Tasumi, M.; Kato, R.; Kobayashi, H. *J. Chem. Phys.* **1994**, *100*, 2449. (b) Kobayashi, A.; Kato, R.; Kobayashi, H.; Mori, T.; Inokuchi, H. *Solid State Commun.* **1987**, *64*, 45. (c) Willett, R. D.; Long, G. Personal communication.

18 Werner, P. E. *J. Appl. Cryst.* **1985**, *18*, 367. TREOR program was adapted to PC and PROSZKI system at Jaqielloniam University 1989.

Chapter IV:

Identification of Two Paramagnetic Phases of $[Mn(TCNQ)_2(L)_2]$ (L = H_2O, MeOH) and their Conversion to the $Mn(TCNQ)_2$ Magnet

Introduction

The design of polymeric materials that contain a paramagnetic metal ion linked by an electron acceptor such as TCNQ[1] has resulted in a new area of hybrid inorganic/organic compounds[2] with interesting magnetic and conducting properties. The most well studied example is Cu with DCNQI acceptors,[3] but other recently reported examples of transition metals combined with TCNQ[4] and TCNE[5] exhibit interesting properties as well. For example, Cu(TCNQ) has been shown to undergo an electric-field induced bistable switching from a high to a low resistance state at a certain threshold potential.[4a] Reactions TCNE with the first row transition elements have produced ferromagnets with higher critical temperatures than any known synthetic magnets. In particular, the TCNE compound with the proposed formula, $V(TCNE)_x \cdot y(CH_2Cl_2)$,[5a] exhibits room temperature ferromagnetism, a goal many researchers have been trying to attain for the past forty years.

The synthesis of the aforementioned materials is not without it's difficulties and frustrations. Their high degree of insolubility in common solvents leads to extreme difficulty in crystallizing these compounds. This is unfortunate because knowledge of structure is crucial for interpreting the physical properties. Furthermore, as has been demonstrated for Cu(TCNQ) and Ag(TCNQ), polymorphism is an issue that further hinders understanding of these materials. The recognition of two phases of CuTCNQ and subsequent structural analysis helped to unravel the reproducibility problems with encountered in the switching experiments with this material. The confirmation of the existence of multiple polymorphs obviously requires careful analysis, but most

importantly, the study and possible application of these compounds requires separation of the phases into pure components.

The subject of this chapter is the isolation of the separate crystalline phases that have been identified in bulk samples of $Mn(TCNQ)_2(MeOH)_2$ (**1**) and $Mn(TCNQ)_2(H_2O)_2$ (**5**). The use slow diffusion techniques used to crystallize products of the methanol reaction led to the realization that two distinct structures were possible; these are designated (**1a**) and (**1b**) because they are both components of the bulk material (**1**). Crystallization of $Mn(TCNQ)_2(H_2O)_2$ (**5**) has resulted in only one phase to date, which is hereafter designated as (**5a**). According to X-ray structural analyses, the three types of TCNQ coordinated ligands found in these compounds are depicted schematically in Figure 34.[6]

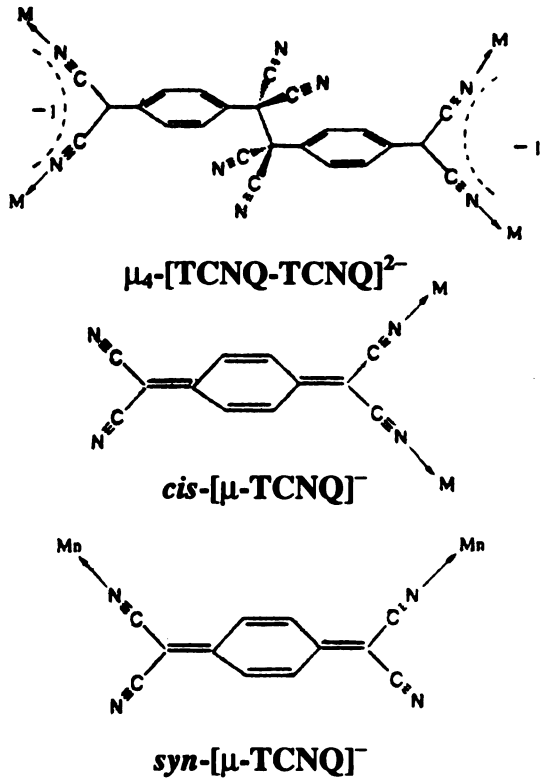

Figure 34. Different binding modes of TCNQ.

One of the two polymorphs of bulk $Mn(TCNQ)_2(MeOH)_2$ (**1**), namely, $[Mn(TCNQ)(TCNQ\text{-}TCNQ)_{0.5}(MeOH)_2]_\infty$ (**1a**), exhibits both the bidentate *cis*-[μ-TCNQ]$^-$ binding mode and the μ_4-[TCNQ-TCNQ]$^{2-}$ unit, which is the σ-dimer form of $(TCNQ^-)_2$. The other component, $[Mn(TCNQ\text{-}TCNQ)_2(MeOH)_4]_\infty$, (**1b**), contains only the μ_4-[TCNQ-TCNQ]$^{2-}$ binding mode. Diagrams in Figure 35 and 36 produced from the X-ray coordinates show these different binding modes within the structures). The other

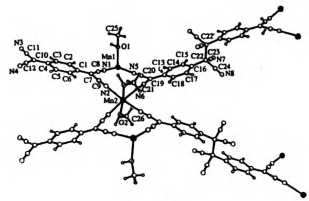

(a)

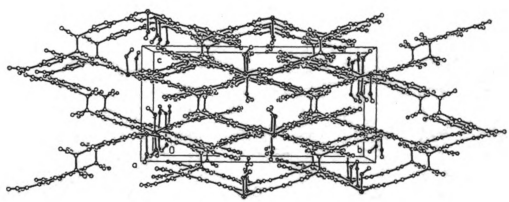

(b)

Figure 35. The (a) single unit and (b) packing diagram of $[Mn(TCNQ)(TCNQ\text{-}TCNQ)_{0.5}(MeOH)_2]_\infty$ (**1a**), illustrating the μ_4-[TCNQ-TCNQ]$^{2-}$ and bidentate *cis*-[μ- TCNQ]$^-$ binding modes.

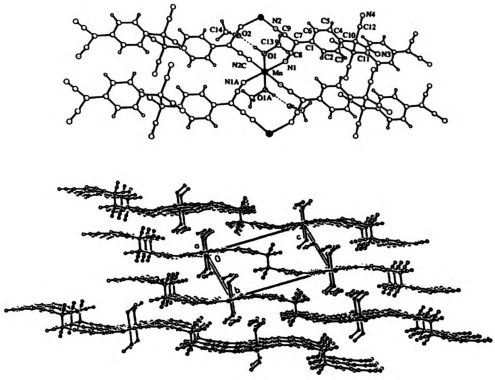

Figure 36. Two diagrams of the $[Mn(TCNQ\text{-}TCNQ)(MeOH)_4]_\infty$ (**1b**) structure, which contain only the μ_4-$[TCNQ\text{-}TCNQ]^{2-}$ binding mode.

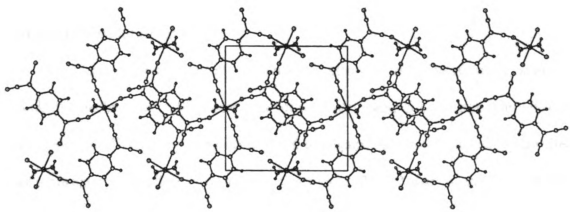

Figure 37. The structure of $[Mn(TCNQ)_2(H_2O)_2]_\infty$ (**5a**) which contains the *syn*-$[\mu\text{-}TCNQ]^-$ binding mode.

structurally characterized polymeric material, $[Mn(TCNQ)_2(H_2O)_2]_\infty$, (**5a**), contains only the *syn*-[μ-TCNQ]$^-$ ligand as shown in the diagram in Figure 37 which is also based on X-ray coordinates.

Unlike the bulk methanol product, only one polymorph (**5a**) has been structurally characterized for $Mn(TCNQ)_2(H_2O)_2$ (**5**), but the similarity of these compounds indicate that there may be another phase present. Also, the other metal/TCNQ materials with M = Fe, Co, and Ni are suspected of being able to form different solid-state structures. The topic of this chapter is the development of a general synthetic method for the bulk isolation and purification of pure materials of Mn^{2+} with $TCNQ^{-1}$ ligands. In particular, we are interested in phases that contain the σ-dimer μ_4-$[TCNQ\text{-}TCNQ]^{2-}$ binding mode, as there is evidence that these materials are on the structural evolution pathway to the desolvated magnets $M(TCNQ)_2$.

Experimental

A. General Considerations

All reactions were carried out under a nitrogen atmosphere using standard Schlenk-line techniques. Methanol was dried over magnesium methoxide whereas diethyl ether and THF were dried using Na/K amalgam; all three were freshly distilled under a nitrogen atmosphere prior to use. The reagent TCNQ was purchased from TCI Chemical Company and recrystallized from hot acetonitrile before use. LiI was purchased from Aldrich Chemical Company and used to prepare LiTCNQ and [*n*-Bu_4N][TCNQ] according to the synthesis outlined in chapter III. The divalent metal

salts, $[M(MeCN)_{4,6}][BF_4]_2$, where M = Mn, Fe, Co, and $[Ni(MeCN)_6][PF_6]_2$, were prepared as described in the literature.[8] The bulk polymeric products, $Mn(TCNQ)_2(MeOH)_2$ (**1**) and $Mn(TCNQ)_2(H_2O)_2$ (**5**), were prepared according to methods established in our laboratories.[6] Infrared spectra were recorded as Nujol mulls in the range 400-4000 cm^{-1} on a Nicolet IR/42 spectrometer. Powder X-ray diffraction data were collected on a Rigaku RU200B powder diffractometer with CuKα radiation in the range 5 - 60°.

B. Synthesis of Bulk Methanol Phases.

(a) Preparation of $Mn(TCNQ)_2(MeOH)_2$, (1)

Synthesis #1: A MeOH solution (20 mL) of [*n*-Bu_4N][TCNQ] (1.19 g, 2.55 mmol) was slowly added to a MeOH solution (10 mL) of $[Mn(MeCN)_4][BF_4]_2$ (0.500 g, 1.3 mmol). The resulting reaction solution was stirred for 20 min to give a dark purple precipitate, which was collected by filtration, washed with 20 mL of methanol followed by 20 mL of diethyl ether, and dried *in vacuo*. Yield: 0.320 g, 61%. Characteristic IR data (Nujol mull, KBr plates, cm^{-1}): ν(C≡N), 2205 s, 2180 s, 2141 s; ν(C=C), 1520 s; δ(C-H), 826 m, 802 sh.

Synthesis #2: A MeOH solution (20 mL) of [*n*-Bu_4N][TCNQ] (0.246 g, 0.550 mmol) was slowly added to a MeOH solution (10 mL) of $[Mn(MeCN)_4][BF_4]_2$ (0.108 g, 0.275 mmol). The resulting reaction solution was stirred for 20 min to give a dark purple precipitate, which was collected by filtration, washed with 20 mL of methanol followed by 20 mL of diethyl ether, and dried *in vacuo*. Yield: 0.060 g, 41%. Characteristic IR

data (Nujol mull, KBr plates, cm^{-1}): ν(C≡N), 2205 s, 2194 s, 2180 s, 2150 s; ν(C=C), 1509 s; δ(C-H), 826 m, 803 w.

Synthesis #3: A MeOH solution (25 mL) of [*n*-Bu_4N][TCNQ] (0.910 g, 2.04 mmol) was slowly added to a MeOH solution (5 mL) of $[Mn(MeCN)_4][BF_4]_2$ (0.400 g, 1.02 mmol). The resulting reaction solution was stirred for 25 min to give a dark purple precipitate, which was collected by filtration, washed with 10 mL of methanol followed by 20 mL of diethyl ether, and dried *in vacuo*. Yield: 0.134 g, 25%. Characteristic IR data (Nujol mull, KBr plates, cm^{-1}): ν(C≡N), 2206 s, 2188 s, 2150 s, 2133 s; ν(C=C), 1507 s; δ(C-H), 826 m, 802 s.

(b) Preparation of $Fe(TCNQ)_2(MeOH)_2$, (2)

Synthesis #1: A MeOH solution (60 mL) of [*n*-Bu_4N][TCNQ] (0.760 g, 1.70 mmol) was slowly added to a MeOH solution (20 mL) of $[Fe(MeCN)_6][BF_4]_2$ (0.405 g, 0.851 mmol). The resulting reaction solution was stirred for 20 min to give a dark purple precipitate that was collected by filtration, washed with 20 mL of methanol followed by 20 mL of diethyl ether, and dried *in vacuo*. Yield: 0.326 g, 62%. Characteristic IR data (Nujol mull, KBr plates, cm^{-1}): ν(C≡N), 2203 s, 2186 s, 2155 s, 2124 s; ν(C=C), 1505 s; δ(C-H), 826 s, 802 s.

Synthesis #2: A MeOH solution (40 mL) of [*n*-Bu_4N][TCNQ] (1.43 g, 3.19 mmol) was slowly added to a MeOH solution (10 mL) of $[Fe(MeCN)_6][BF_4]_2$ (0.760 g, 1.59 mmol). The resulting reaction solution was stirred for 20 min to give a dark purple precipitate that was collected by filtration over a period of 45 minutes, washed with 20 mL of methanol followed by 20 mL of diethyl ether, and dried *in vacuo*. Yield: 0.806 g, 96%.

Characteristic IR data (Nujol mull, KBr plates, cm^{-1}): ν(C≡N), 2203 s, 2187 s, 2155 s, 2130 s; ν(C=C), 1505 s; δ(C-H), 826 s, 802 s.

(c) Preparation of $Co(TCNQ)_2(MeOH)_2$, (3)

A MeOH solution (20 mL) of [*n*-Bu_4N][TCNQ] (0.187 g, 0.418 mmol) was slowly added to a MeOH solution (10 mL) of $[Co(MeCN)_6][BF_4]_2$ (0.100 g, 0.209 mmol). The resulting reaction solution was stirred for 20 min to give a dark purple precipitate that was collected by filtration, washed with 20 mL of methanol followed by 20 mL of diethyl ether, and dried *in vacuo*. Yield: 0.091 g, 73%. Characteristic IR data (Nujol mull, KBr plates, cm^{-1}): ν(C≡N), 2215 s, 2193 s, 2170 s, 2130 sh; ν(C=C), 1503 s; δ(C-H), 824 s, 802 sh.

(d) Preparation of $Ni(TCNQ)_2(MeOH)_2$, (4)

Synthesis #1: A MeOH solution (20 mL) of [*n*-Bu_4N][TCNQ] (0.754 g, 1.69 mmol) was slowly added to a MeOH solution (10 mL) of $[Ni(MeCN)_6][PF_6]_2$ (0.404 g, 0.844 mmol). The resulting reaction solution was stirred for 20 min to give a dark purple precipitate that was collected immediately by filtration, washed with 20 mL of methanol followed by 20 mL of diethyl ether, and dried *in vacuo*. Yield: 0.250 g, 47%. Characteristic IR data (Nujol mull, KBr plates, cm^{-1}): ν(C≡N), 2201 s, 2178 s, 2138 sh; ν(C=C), 1505 s; δ(C-H), 826 s, 802 sh.

Synthesis #2: A MeOH solution (30 mL) of [*n*-Bu_4N][TCNQ] (1.14 g, 2.55 mmol) was slowly added to a MeOH solution (10 mL) of $[Ni(MeCN)_6][PF_6]_2$ (0.76 g, 1.27 mmol). The resulting reaction solution was stirred for 20 min to give a dark purple precipitate

that was collected by filtration over a period of two hours, washed with 20 mL of methanol followed by 20 mL of diethyl ether, and dried *in vacuo*. Yield: 0.616 g, 91%. Characteristic IR data (Nujol mull, KBr plates, cm^{-1}): ν(C≡N), 2201 s, 2178 s, 2138 sh; ν(C=C), 1505 s; δ(C-H), 826 s, 802 s.

B. Separation of the Two Components in Bulk $Mn(TCNQ)_2(MeOH)_2$, (1).

(a) Low Temperature Reaction to yield $[Mn(TCNQ)(TCNQ\text{-}TCNQ)_{0.5}(MeOH)_2]_\infty$, (1a)

Separate MeOH solutions of [*n*-Bu_4N][TCNQ] (0.455 g, 1.018 mmol) (40 mL) and of $[Mn(MeCN)_4][BF_4]_2$ (0.200 g, 0.509 mmol) (10 mL) were chilled in an ice bath for 1 hour. The [*n*-Bu_4N][TCNQ] solution was added to the solution of $[Mn(MeCN)_4][BF_4]_2$ and allowed to stand at low temperature for 30 minutes. The dark purple precipitate was collected by filtration, washed with 20 mL of cold methanol followed by 20 mL of diethyl ether, and dried *in vacuo*. Yield: 0.117 g, 44%. Characteristic IR data (Nujol mull, KBr plates, cm^{-1}): ν(C≡N), 2214 s, 2193 s, 2167 s, 2152 s; ν(C=C), 1505 s; δ(C-H), 826 s, 803 sh.

(b) Higher Temperature Reactions to yield $[Mn(TCNQ\text{-}TCNQ)(MeOH)_4]_\infty$, (1b)

Synthesis #1: A quantity of THF (20 mL) was added to a Schlenk flask which contained $Mn(TCNQ)_2(MeOH)_2$ (0.150 g, 0.272 mmol). The reaction was stirred for 1.5 h at 60°C, then removed from heat and allowed to stand for 30 minutes. The resulting pale blue-green product was collected by filtration under nitrogen, washed with 20 mL of THF followed by 20 mL of diethyl ether and dried *in vacuo*. Yield: 0.120 g, 80%.

Characteristic IR data (Nujol mull, KBr plates, cm^{-1}): ν(C≡N), 2197 s, 2124 s; ν(C=C), 1507 s; δ(C-H), 802 s.

Synthesis #2: A quantity of MeOH (20 mL) was added under nitrogen to a Schlenk flask which contained $Mn(TCNQ)_2(MeOH)_2$ (0.150 g, 0.272 mmol). The reaction was stirred for 4 hours at 70°C then removed from the heat and allowed to stand for 30 minutes. The resulting pale blue product was collected by filtration under nitrogen, washed with 20 mL of MeOH followed by 20 mL of diethyl ether, and dried *in vacuo*. Yield: 0.123 g, 82%. Characteristic IR data (Nujol mull, KBr plates, cm^{-1}): ν(C≡N), 2197 s, 2124s; ν(C=C), 1507 s; δ(C-H), 802 s.

C. Isolation of a Second Phase of $Mn(TCNQ)_2(H_2O)_2$ (5) That Contains the σ-dimer Structural Unit (5b).

A quantity of THF (20 mL) was added to a bulk sample of $Mn(TCNQ)_2(H_2O)_2$ (0.150 g, 0.300 mmol) under nitrogen. The reaction was stirred for 2 days at 70°C then removed from the heat and allowed to stand for 30 minutes. The resulting pale blue-green product was collected by filtration under nitrogen, washed with 20 mL of THF followed by 20 mL of diethyl ether and dried *in vacuo*. Yield: 0.139 g, 93%. Characteristic IR data (Nujol mull, KBr plates, cm^{-1}): ν(C≡N), 2195 s, 2124 s; ν(C=C), 1509 s; δ(C-H), 828 w, 802 m.

D. Interconversion of $Mn(TCNQ)_2$ (6) and $Mn(TCNQ)_2(X)_2$ polymers where X = MeOH (1) or H_2O (5).

General procedure: For each reaction, a 0.150 g sample of the starting material was added to a 100 mL Schlenk flask after which time 20 mL of a particular solvent was added under nitrogen. The flask was heated to approximately 60 °C, and stirred for the designated time. The solvent was removed, the product was washed with 20 mL of diethyl ether and dried *in vacuo*.

E. Attempted Conversion of $Fe(TCNQ)_2(MeOH)_2$ (2) to $Fe(TCNQ)_2$ (7).

A quantity of $Fe(TCNQ)_2(MeOH)_2$ (0.150 g, 0.271 mmol) was added to a 100 mL Schlenk flask, and 20 mL of acetonitrile were added under nitrogen. The flask was heated to 52°C in an oil bath and stirred for 1.5 h, after which time the solution was allowed to cool for 30 minutes. After the solvent was removed by cannula, the product was washed with 20 mL of diethyl ether and dried *in vacuo*. Yield: 0.117 g, 78%. Characteristic IR data (Nujol mull, KBr plates, cm^{-1}): $\nu(C\equiv N)$, 2193 sh, 2120 s; $\nu(C=C)$, 1505 s; $\delta(C-H)$, 825 sh, 803 s.

F. Attempted Conversion of $Ni(TCNQ)_2(MeOH)_2$ (4) to $Ni(TCNQ)_2$ (8)

In this reaction, $Ni(TCNQ)_2(MeOH)_2$ (0.120 g, 0.216 mmol) was added to a 100 mL Schlenk flask and 20 mL of acetonitrile were added under nitrogen. The flask was heated to approximately 65°C and stirred for 1.5 h after which time the solution was allowed to cool for 30 minutes. The solvent was evaporated and the product was washed with 20 mL of diethyl ether and finally dried *in vacuo*. Yield: 0.120 g, 96%. Characteristic IR data (Nujol mull, KBr plates, cm^{-1}): $\nu(C\equiv N)$, 2208 s, 2198 sh, 2174 s, 2155 s, 2063s; $\nu(C=C)$, 1507 s; $\delta(C-H)$, 825 s, 800 m.

Results and Discussion

A. Synthesis

(a) Preparation of the Bulk Methanol Compounds, (1-4).

The bulk compounds $M(TCNQ)_2(MeOH)_2$, where M = Mn (**1**), Fe (**2**), Co (**3**), and Ni (**4**), were used as starting materials for various transformations in the present studies. The reported syntheses worked according to the earlier reports,[6] but it was noted that these reactions produce mixtures of products. We realized that we were obtaining different ratios of two crystal types that contain different forms of coordinated $TCNQ^{-1}$, namely the bidentate *cis*-$[\mu\text{-TCNQ}]^-$ and μ_4-$[TCNQ\text{-}TCNQ]^{2-}$ modes as outlined in the experimental section.

(b) Isolation of the two components (1a and 1b) of $Mn(TCNQ)_2(MeOH)_2$ (1).

Armed with the knowledge that there are two components in the bulk methanol phases, we tackled the next step, namely to determine synthetic methods for isolating them as pure solids. One obvious method, if possible, is to capitalize on any differences in thermal stability of the phases. The material $Mn(TCNQ)_2(MeOH)_2$ (**1**) was the prototype for these studies since two crystalline phases (**1a** and **1b**) had already been structurally characterized. During the course of investigating reactions that lead to $Mn(TCNQ)_2(MeOH)_2$, it was found that dilute conditions and short reaction times favor the kinetic phase, $[Mn(TCNQ)(TCNQ\text{-}TCNQ)_{0.5}(MeOH)_2]_\infty$ (**1a**) whereas higher concentrations and longer reaction times favor the thermodynamic phase, $[Mn(TCNQ\text{-}TCNQ)(MeOH)_4]_\infty$ (**1b**). The isolation of (**1a**) $[Mn(TCNQ)(TCNQ\text{-}TCNQ)_{0.5}(MeOH)_2]_\infty$

(**1a**) was performed at low temperatures to prevent rapid conversion to the second phase (**1b**) *in situ*. A reaction time of twenty minutes is considered optimal, as it produces the most crystalline product. After the designated reaction time, the filtration was performed quickly to prevent the solution from warming and thus possibly forming the thermodynamic phase. Isolation of the thermodynamic phase, $[Mn(TCNQ\text{-}TCNQ)(MeOH)_4]_\infty$ (**1b**) was achieved by heating a stirring suspension of the bulk product (**1**) for a long period of time. This reaction is best performed in MeOH to insure retention of axial MeOH ligands and to provide the additional methanol that is needed to fill the interstices in (**1b**). As determined by TGA analysis, the bulk product (**1**) only contains an average of two methanol ligands per metal, *i.e.* the formula is $Mn(TCNQ)_2(MeOH)_2$,[6] therefore an excess of solvent is necessary to provide the remaining methanol groups in (**1b**).

One final point that is worth noting when attempting to distinguish between the two phases is product color. Crystals of $[Mn(TCNQ)(TCNQ\text{-}TCNQ)_{0.5}(MeOH)_2]_\infty$ (**1a**) are dark purple which is similar to the color of the bulk methanol product (**1**), but crystals of $[Mn(TCNQ\text{-}TCNQ)(MeOH)_4]_\infty$ (**1b**) are a pale blue color. The same pale blue color (which is unusual for materials that contain reduced TCNQ) was observed for the bulk products obtained from the higher temperature reactions in THF and MeOH. In this way, color can be used to help determine whether the separation of the two phases has been achieved before one works up the reaction and analyzes the product spectroscopically. The explanation for the pale blue color of (**1b**) is that the TCNQ radicals are completely dimerized to form a new C-C bond, thus the intense π-π^* transition of the radical $TCNQ^-$ is no longer observed.

(c) Investigation of bulk $Mn(TCNQ)_2(H_2O)_2$ (5) which contains σ-dimers (5b).

The crystallization and characterization of one phase formed in the aqueous chemistry of Mn^{2+} with $TCNQ^-$ has been determined.[6] Crystals of $[Mn(TCNQ)_2(H_2O)_2]_\infty$ (**5**), are different from either of the two methanol products (**1a** and **1b**). The structure of $[Mn(TCNQ)_2(H_2O)_2]_\infty$ (**5a**) is composed of TCNQ anions acting as ligands but with no σ-dimer being present. This however, does not mean that alternative phases with σ-dimers cannot exist, and, in fact, we noted with consternation in our earlier work that the simulated powder pattern of $[Mn(TCNQ)_2(H_2O)_2]_\infty$ (**5a**) crystals do not perfectly match the experimental powder data on the bulk sample (**5**).[6] We therefore sought to isolate a new phase or phases of $Mn(TCNQ)_2(H_2O)_2$ (**5**). In a similar manner to the methanol chemistry, a suspension of the bulk product was heated in a solution of THF to quickly ascertain if a σ-dimer phase would form. As indicated by IR, a new phase containing σ-dimers formed upon heating.

(d) Conversions of bulk $Mn(TCNQ)_2(X)_2$ compounds, (X = MeOH or H_2O) to $Mn(TCNQ)_2$ (6).

The similarity of $Mn(TCNQ)_2$ and $Mn(TCNQ)_2(X)_2$ compounds, where X = MeOH or H_2O, prompted us to ask whether one can inter-convert these compounds by adding or removing solvent molecules. The results of these reactions are summarized in Table 6. The IR spectra of the materials were compared to the spectral features for the starting materials as well as to the pure crystalline phases established by single crystal X-ray methods. In the water-based material, removal of axial bound water was

Table 6. Conversion reactions of $Mn(TCNQ)_2$ and $Mn(TCNQ)_2(X)_2$ compounds, X = MeOH and H_2O.

Reaction/Expected product	**Reaction Conditions**	**Result/ IR Data**
1)$Mn(TCNQ)_2(MeOH)_2$ + MeCN → $Mn(TCNQ)_2$ 150 mg 20mL 7/16/98 Yield: 78% purple product 2) Product after exposure to X-rays	Heat at 57 °C and stir 1.5 h, under N_2	**$Mn(TCNQ)_2$** 1) IR- 2203 s, 2180 s, 2137 m, 1503 s, 826 w 2) IR- 2207 s, 2187 s, 2139 s, 1503 s, 826 m
$Mn(TCNQ)_2(MeOH)_2$ + MeCN → $Mn(TCNQ)_2$ 150 mg 20 mL 10/14/98 Yield: 80% purple product	No heat and stir, 5 days under N_2	**$Mn(TCNQ)_2$** IR- 2204 s, 2186 s, 2163 s, 2140 m, 1502 s, 824 m, 804 m
$Mn(TCNQ)_2(H_2O)_2$ + MeCN → $Mn(TCNQ)_2$ 150mg 20mL 7/17/98 Yield: 99% purple product	Heat at 57 °C Room temp and stir for 5 h under N_2	**$Mn(TCNQ)_2(H_2O)_2$** IR- 2195 m, 2180 m, 2157 m, 2054 w, 1507 m 828 m
$Mn(TCNQ)_2(H_2O)_2$ + MeCN → $Mn(TCNQ)_2$ 150 mg 20 mL 7/21/98 Yield: 91% purple product	Heat at 57 °C and stir for 7 h under N_2	**$Mn(TCNQ)_2(H_2O)_2$** IR- 2195 m, 2154 m, 2053 w, 1505 m, 826 m, 816 sh
$Mn(TCNQ)_2$ + H_2O → $Mn(TCNQ)_2(H_2O)_2$ 100 mg 20mL 7/31/98 Yield: 83% purple product	Heat at 57 °C and stir for 30h, under N_2	**$Mn(TCNQ)_2$** IR- 2205 s, 2187 s, 2131 sh, 826 w
$Mn(TCNQ)_2(H_2O)_2$ (150 mg) + MeOH (20mL) → $Mn(TCNQ)_2(MeOH)_2$ Yield: 99% purple product 7/21/98	Heat at 57 °C and stir for 1.5 h under N_2	**$Mn(TCNQ)_2(H_2O)_2$** IR- 2212 m, 2187 m, 2167 m, 2155 sh, 827 m, 802 w
$Mn(TCNQ)_2(H_2O)_2$ (100 mg) + MeOH (20mL) → $Mn(TCNQ)_2(MeOH)_2$ Yield: 80% purple product 7/31/98	Reflux and stir for 24h, under N_2	**$Mn(TCNQ)_2(H_2O)_2$** IR- 22111 m, 2187 m, 2166 m, 2152 sh, 826 m, 802 w

Compound	**IR data**
$Mn(TCNQ)_2(MeOH)_2$ (**1**)	ν(C≡N), 2214 s, 2191 s, 2176 s, 2159 s, 2139 sh; ν(C=C), 1520 s; δ(C-H), 827 m, 804 w
$[Mn(TCNQ)(TCNQ\text{-}TCNQ)_{0.5}(MeOH)_2]_\infty$ (**1a**)	ν(C≡N), 2216 s, 2187 s, 2168 m, 2156 sh; δ(C-H), 825 m
$[Mn(TCNQ\text{-}TCNQ)(MeOH)_4]_\infty$ (**1b**)	ν(C≡N), 2202 s, 2139 s; δ(C-H), 806 m
$Mn(TCNQ)_2(H_2O)_2$ (**5**)	ν(C≡N), 2211 s, 2194 s, 2168 m; ν(C=C),1508 s; δ(C-H), 825 m
$Mn(TCNQ)_2$ (**6**)	ν(C≡N), 2205 s, 2187 s, 2137 sh; ν(C=C), 1505 s; δ(C-H), 826 m

unsuccessful, despite the use of elevated temperatures and longer reflux times. This is disconcerting because the powder X-ray pattern of $[Mn(TCNQ)_2(H_2O)_2]_\infty$ (**5a**) is more similar to that of the magnetic phase, $Mn(TCNQ)_2$ (**6**), than any of the others, so we naturally thought the interconversion of these two be the easiest to perform. Even attempts to remove the water by heating in solid state were to no avail, as they occurred only with decomposition of the compound. On the other hand, the conversion of $[Mn(TCNQ)_2(MeOH)_2]_\infty$ to the solvent-free form, $Mn(TCNQ)_2$, was successful after being heated in acetonitrile for 1.5 hours. This is the first time that a solvent was used to facilitate this transformation. Earlier it had been observed in our laboratories that $[Mn(TCNQ\text{-}TCNQ)(MeOH)_4]_\infty$ crystals converted to $Mn(TCNQ)_2$ upon exposure to X-ray radiation or with heating in the solid-state.[6]

The successful conversion of bulk $Mn(TCNQ)_2(MeOH)_2$ (**1**) to $Mn(TCNQ)_2$ (**6**) was attempted with the isostructural materials, $Fe(TCNQ)_2(MeOH)_2$ (**2**) and $Ni(TCNQ)_2(MeOH)_2$ (**4**). In these cases, however, similar reaction times and temperatures produced only a mixture of the original phase and a σ-dimer phase instead of the magnetic phase. In case of Fe, the σ-dimer (**2b**) was the major product, while in the Ni case, both the original and σ-dimer phases (**4b**) are present in roughly equal concentrations as indicated by IR spectral features. Although they were not successful at producing the desolvated magnetic phases, these reactions provide further evidence that the σ-dimer form is important in the bulk methanol products of the other metals as well.

B. Infrared Spectroscopy

Infrared spectroscopy is the tool that was used to discern the formation, identity and conversion of the metal/TCNQ materials. Both the ν(C≡N) and ν(C=C) regions are useful in confirming the presence of the reduced form of TCNQ and its coordination to a metal, but the δ(C-H) region is the primary region used to distinguish $TCNQ^-$ vs. $[TCNQ\text{-}TCNQ]^{2-}$.[9] In the ν(C≡N) and ν(C=C) regions, compounds containing all types of TCNQ moieties exhibit similar energies which render specific assignments difficult. In the δ(C-H) region, however, reduced TCNQ exhibits a bend that appears at ~824 cm^{-1} while the TCNQ σ-dimer, $[TCNQ\text{-}TCNQ]^{2-}$, exhibits a characteristic bend at ~802 cm^{-1}. Therefore, compounds that contain either type or mixtures of both types of TCNQ units can be readily identified.

(a) Analyses of the bulk methanol compounds, (1 - 4).

The bulk methanol TCNQ starting materials, $M(TCNQ)_2(MeOH)_2$ where M = Mn (**1**), Fe (**2**), Co (**3**), and Ni (**4**), prepared for the present studies exhibit some striking differences in the IR spectra from the previously published results. It was, therefore a natural question to ask whether the bulk products of Fe, Co and Ni also contain two components of the types $[M(TCNQ)(TCNQ\text{-}TCNQ)_{0.5}(MeOH)_2]_\infty$ (**2 - 4a**) and $[M(TCNQ\text{-}TCNQ)(MeOH)_4]_\infty$ (**2 - 4b**) encountered in the Mn chemistry. If so, we reasoned that changes in the reaction conditions should also affect the relative distributions of these phases in the corresponding bulk products (**2 - 4**). Several reactions were attempted for Fe and Ni in which the concentrations and reaction times were increased in a manner similar to what was found to be successful with Mn. These

efforts resulted in equal mixtures of the two components or a slight favoring of the "all σ-dimer" phase (**2b** and **4b**) as indicated by IR spectroscopy. Clearly, these reactions lead to the same two products in the bulk materials as have been firmly established by single crystal X-ray for the Mn derivatives.

A comparison of the newly synthesized materials with the published data is summarized in Table 7. In the ν(C≡N) region, there are more signals in the spectra of the compounds prepared in the earlier studies, which is most likely due to the use of mild reaction conditions that favored two products. Most important in these comparisons is the overall trend evident from the recorded frequencies in the δ(C-H) region. When one increases the concentrations, there is an increase in percentage of σ-dimer present in the mixture. This is indicated by an intense (medium or strong) peak that appears at 802 cm^{-1} that is absent in the published data for samples prepared under conditions that are more dilute. The increased ratio of the σ-dimer feature with longer times, higher concentrations, and elevated temperatures evidence that it is a stable form of $TCNQ^{-1}$ under certain conditions.

Table 7. A comparison of $M(TCNQ)_2(MeOH)_2$ bulk products with varying reaction conditions.

Compound	Reaction Conditions: Time and concentration (mmol/mL)	IR region ν(C≡N)	ν(C=C)	δ(C-H)	Ref.
$Mn(TCNQ)_2$ -$(MeOH)_2$	20 min. 0.0125	2214 s, 2191 s, 2176 s, 2159 s, 2139 sh	—	827 m, 804 w	6
Synthesis #1	20 min. 0.0433	2205 s, 2180 s, 2141 s	1520 s	826 m, **802 sh**	this work
Synthesis #2	20 min. 0.0092	2205 s, 2194 s, 2180 s, 2150 s	1509 s	826 m, **803 m**	this work
Synthesis #3	25 min 0.0680	2206 s, 2188 s, 2150 s, 2133 s	1507 s	826 m, **802 *s***	this work
$Fe(TCNQ)_2$ -$(MeOH)_2$	20 min. 0.0125	2216 s, 2187 s, 2167 m, 2154 sh	—	827 m, 802 w	6
Synthesis #1	20 min. 0.0106	2203 s, 2186 s, 2155 s, 2124 s	1505 s	826 m, **802 m**	this work
Synthesis #2	20 min. + 45 min. filter 0.0318	2203 s, 2187 s, 2155 s, 2130 s	1505 s	826 m, **802 m**	this work
$Co(TCNQ)_2$ -$(MeOH)_2$	20 min. 0.0125	2213 s, 2189 s, 2169 m, 2156 sh	—	825 m, 804 w	6
Synthesis #1	20 min. 0.0070	2215 s, 2193 s, 2170 s, 2130 sh	1503 s	824 m, **802 sh**	this work
$Ni(TCNQ)_2$ -$(MeOH)_2$	20 min. 0.0125	2224 s, 2193 s, 2170 m, 2158 sh	—	825 m, 802 w	6
Synthesis #1	20 min. 0.0281	2201 s, 2178 s, 2138 sh	1505 s	826 m, **802 sh**	this work
Synthesis #2	20 min. 0.0318	2201 s, 2178 s, 2138 sh	1505 s	826 m, **802 m**	this work

(b) Confirmation of the isolation of phases (1a) and (1b) from bulk $Mn(TCNQ)_2(MeOH)_2$, (1).

The bulk separation of the two components of the $Mn(TCNQ)_2(MeOH)_2$ mixtures was performed by designing separation methods that focus on their relationship as kinetic and thermodynamic products. As Figure 38 indicates, the two phases of $Mn(TCNQ)_2(MeOH)_2$ (1) are a physical mixture of the bulk product. Therefore, infrared

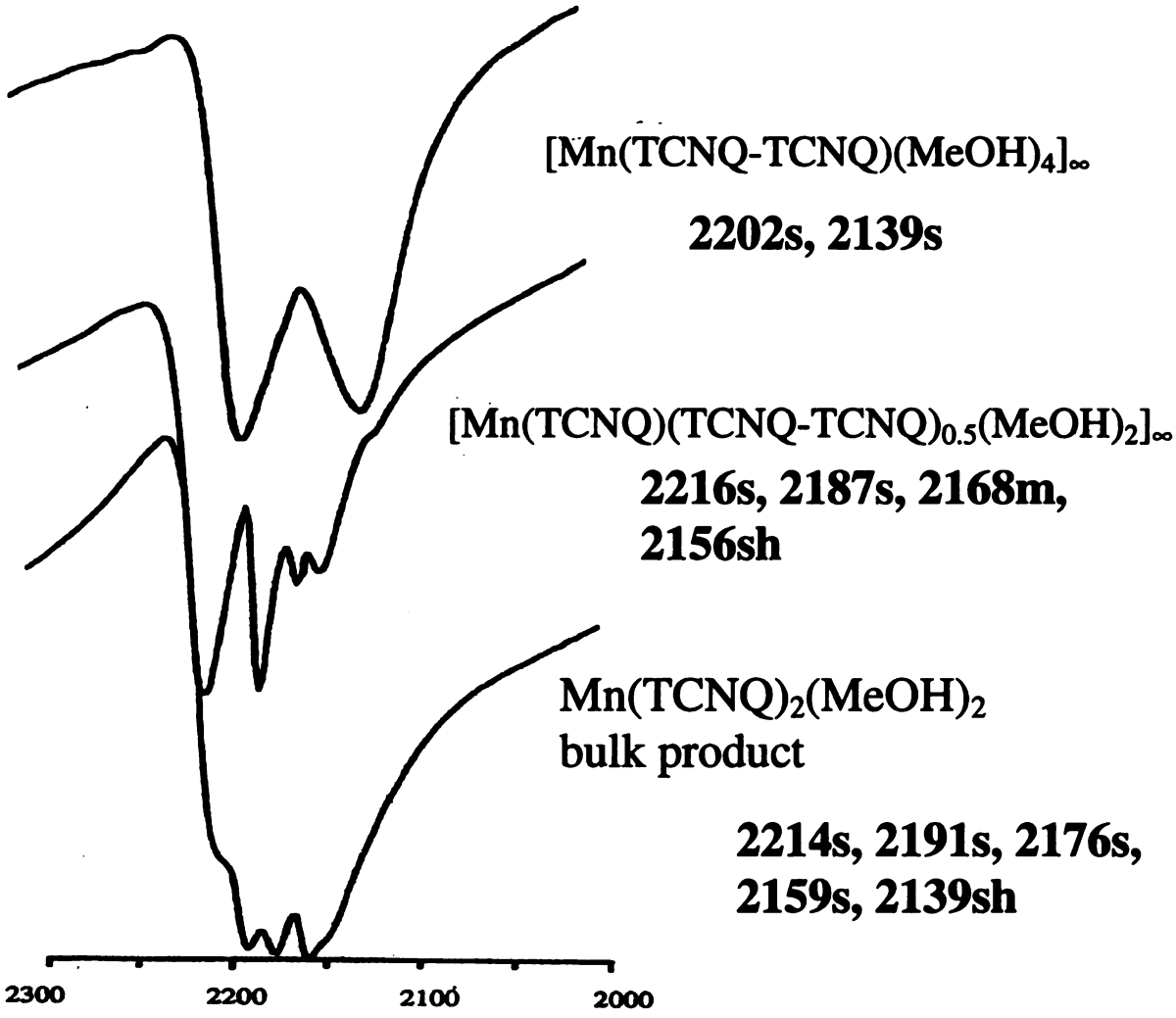

Figure 38. Infrared spectra in the ν(C≡N) region showing that both crystallographic forms are present in bulk $Mn(TCNQ)_2(MeOH)_2$ product.

spectral data of these three samples must be examined in order to check whether a particular sample contains one or both of these compounds. Spectra of the products from different experiments were carefully compared to original published data for the bulk product and two crystalline phases. *Both* isolated products exhibit frequencies in the ν(C≡N) region that can be related directly to those found in *bona fide* crystals of the respective components (Figures 39 and 40). Furthermore, in the δ(C-H) region, the isolated product that corresponds to $[Mn(TCNQ)(TCNQ\text{-}TCNQ)_{0.5}(MeOH)_2]_\infty$, (**1a**), exhibits frequencies at 826 cm^{-1} (s), *and* 803 cm^{-1} (w) while the product that corresponds to $[Mn(TCNQ\text{-}TCNQ)(MeOH)_4]_\infty$, (**1b**), exhibits a single intense feature at 802 cm^{-1}. These data firmly support the conclusion that isolation of the two components of $Mn(TCNQ)_2(MeOH)_2$ (**1**) was successful.

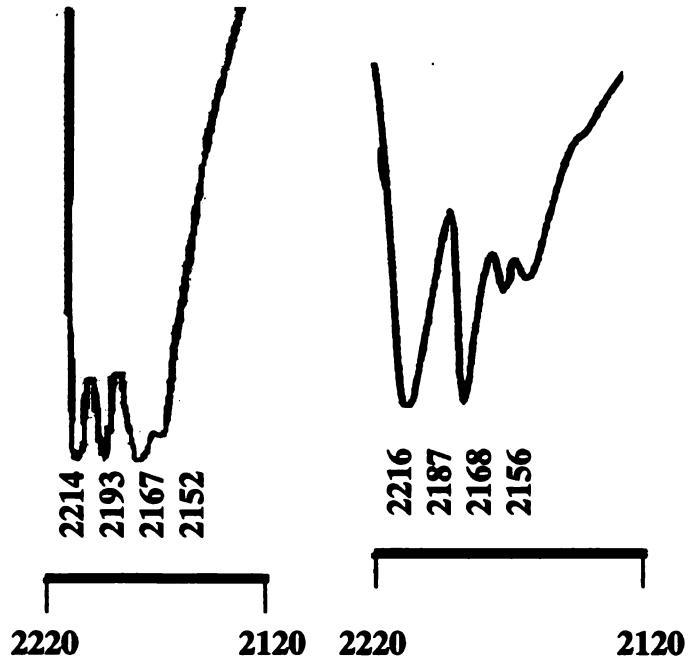

Figure 39. Comparison of the ν(C≡N) regions for an experimental sample obtained in the present studies (left) and for X-ray crystals (right) of $[Mn(TCNQ)(TCNQ\text{-}TCNQ)_{0.5}(MeOH)_2]_\infty$.

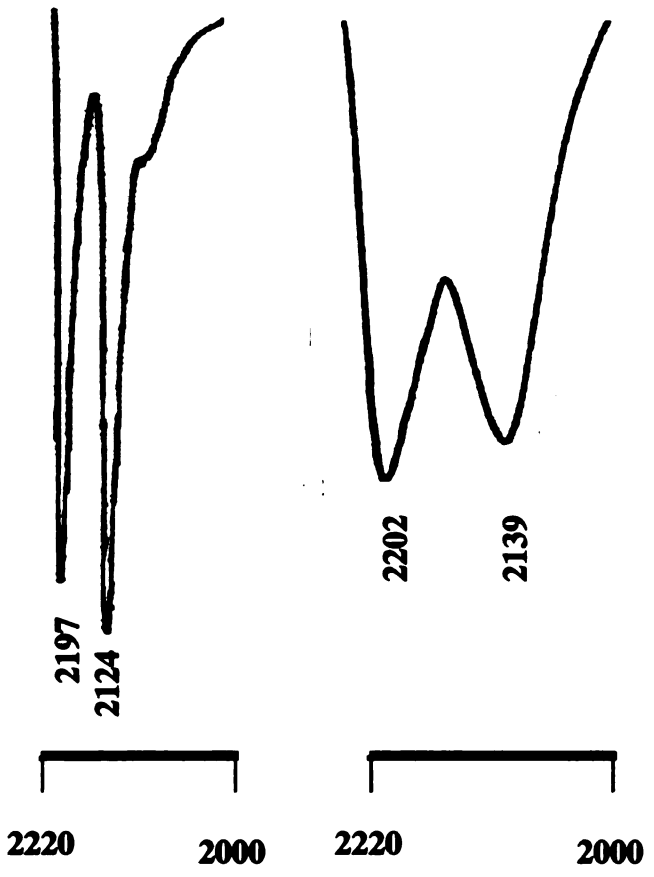

Figure 40. Comparison of the ν(C≡N) regions for powder (left) and crystals (right) obtained in the chemistry of $[Mn(TCNQ\text{-}TCNQ)(MeOH)_4]_\infty$.

(c) Identification of a second phase of $Mn(TCNQ)_2(H_2O)_2$, (5).

A second, previously unrecognized, phase of $Mn(TCNQ)_2(H_2O)_2$ (**5**) was identified using infrared spectroscopy as well. Conversion of the bulk product, which shows a mixture of the two forms of reduced TCNQ (**5a**), (δ(C-H) : 828 cm^{-1}(s), 803 cm^{-1} (w)), to one that only contains the σ-dimer form (**5b**), formulated as $[Mn(TCNQ\text{-}TCNQ)(H_2O)x]_\infty$, was attempted. We were encouraged to undertake this experiment by the presence of a low-energy feature in the δ (C-H) region where the σ-dimer occurs, *viz.*, near 800 cm^{-1}. Spectra in the ν(C≡N) and δ(C-H) regions for the starting material and the isolated product indicate that distinct differences exist (Figure 41). The σ-dimer

product contains only two broad features in the ν(C≡N) region, which is characteristic of the *all σ-dimer* methanol phase. Furthermore, the intense δ(C-H) bend at 802 cm^{-1} confirms its presence.

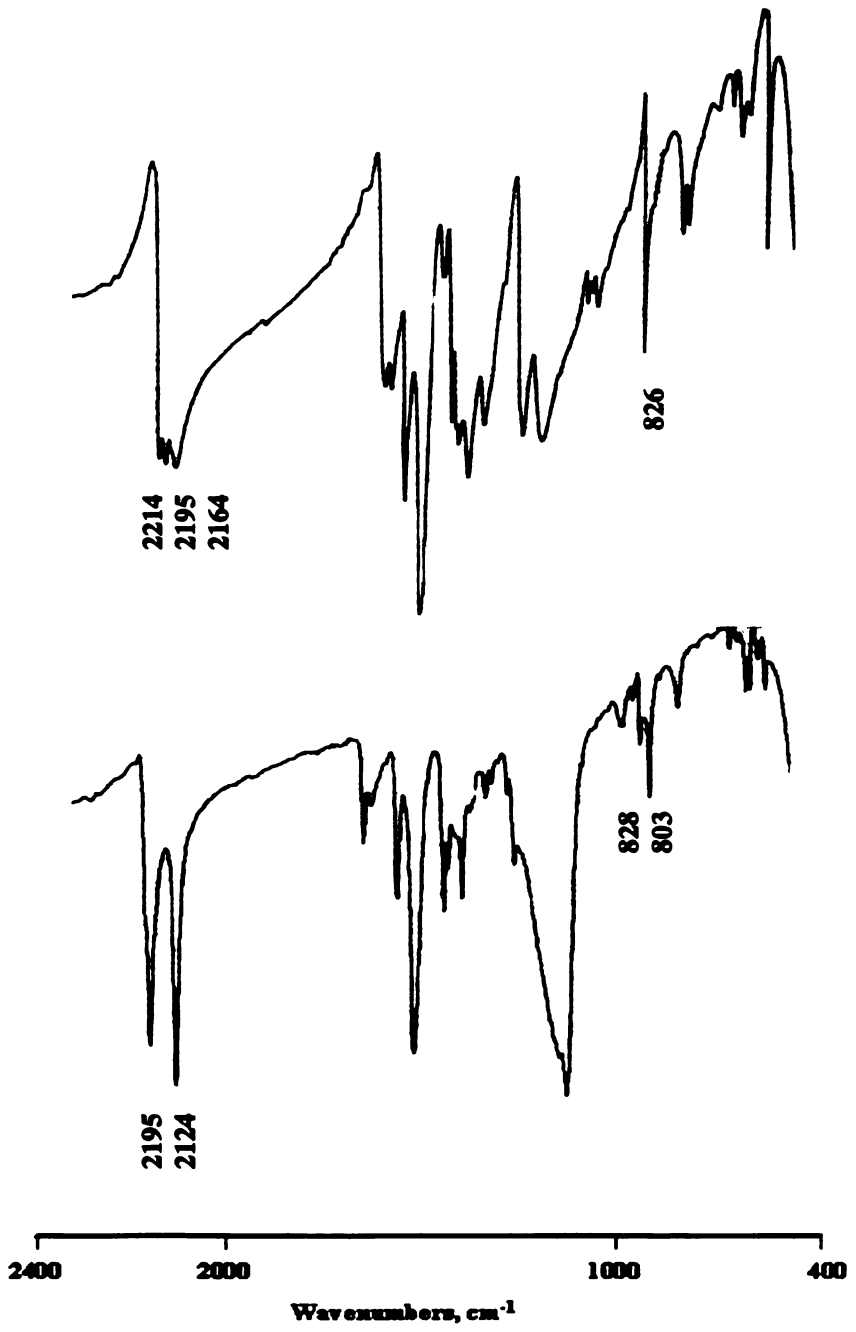

Figure 41. A comparison of the infrared spectra of the starting material (top), $Mn(TCNQ)_2(H_2O)_2$, and the converted phase (bottom). Both ν(C≡N) and δ(C-H) modes clearly indicate the differences in structure.

(c) Spectral evidence for the conversion of $Mn(TCNQ)_2(MeOH)_2$, (1) to $Mn(TCNQ)_2$, (6).

The infrared data for the *interconversions* of $Mn(TCNQ)_2$, $Mn(TCNQ)_2(MeOH)_2$, and $Mn(TCNQ)_2(H_2O)_2$ are listed in Table 6. As the data clearly show, the only successful conversion is that of $Mn(TCNQ)_2(MeOH)_2$ to $Mn(TCNQ)_2$ in acetonitrile. A spectral comparison is shown in Figure 42 for both the starting material, $Mn(TCNQ)_2(MeOH)_2$ (**1**), the heated material, and an authentic sample of $Mn(TCNQ)_2$ (**6**). Attempted conversions of the isostructural materials, $Fe(TCNQ)_2(MeOH)_2$ (**2**) and $Ni(TCNQ)_2(MeOH)_2$ (**4**), to $Mn(TCNQ)_2$ in acetonitrile resulted in the formation of mixtures of the original phase and σ-dimer phase or formation of only the σ-dimer phase as evidenced by the data in Figure 43, in which the ν(C≡N) and δ(C-H) modes are displayed for both compounds.

Finally, the instability of the C-C bond that connects the two TCNQ's in the σ-dimer ligand was confirmed by IR spectroscopy performed on samples after various treatments. Samples containing this form of coordinated $TCNQ^{-1}$ were exposed to an intense X-ray beam and then reanalyzed by infrared spectroscopy. Results consistently indicated that the σ-dimer phase was irreversibly destroyed into separate $TCNQ^-$ moieties in the solid state. As indicated in Figure 44, the spectra recorded after X-ray exposure indicate the presence of only reduced TCNQ, which displays a δ(C-H) mode at 825 cm^{-1}. This finding substantiates our earlier discovery of the thermal conversion of $Mn(TCNQ\text{-}TCNQ)(MeOH)_4$, (**1**), to the magnetic phase, $Mn(TCNQ)_2$, (**6**), in the solid-state.

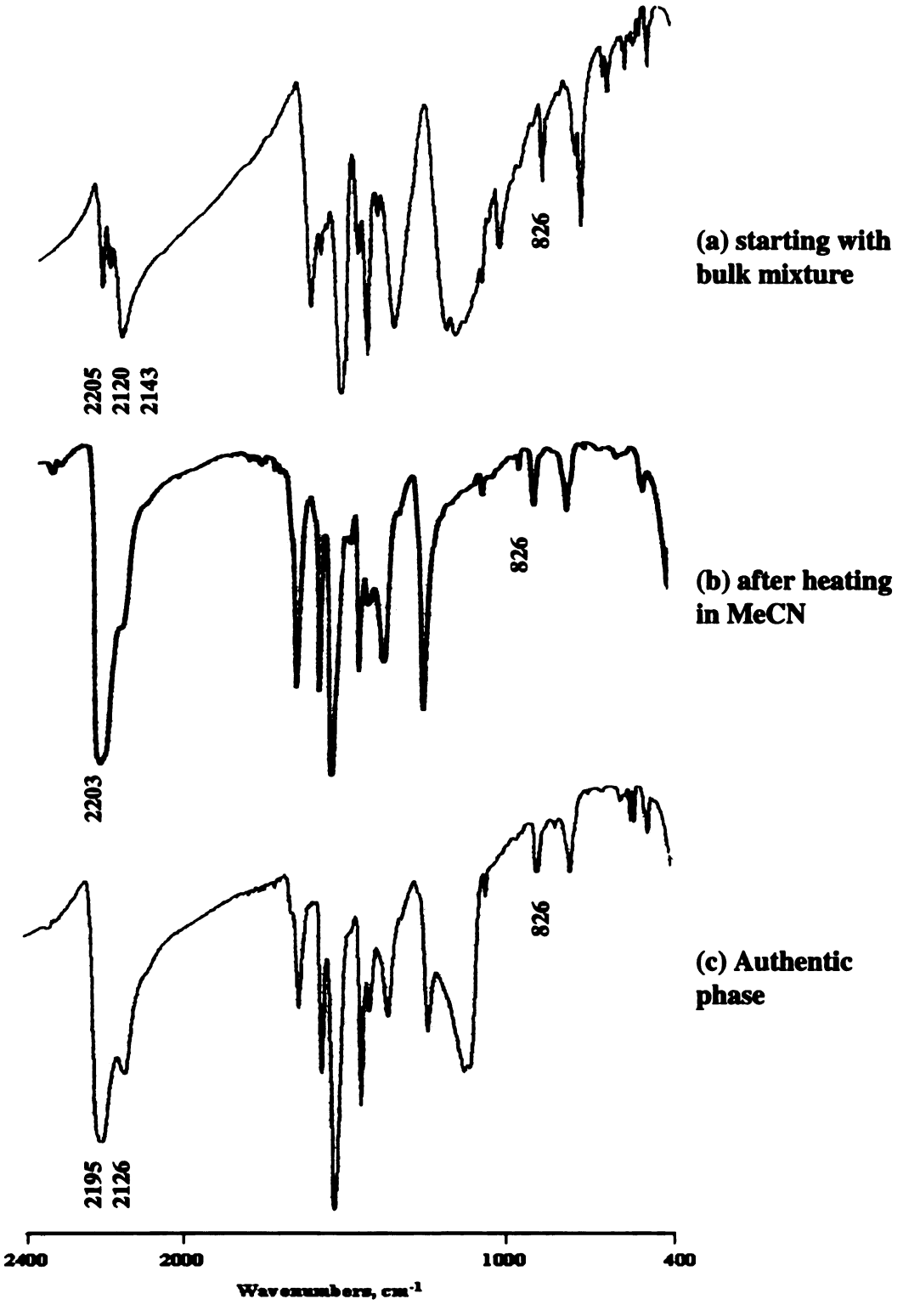

Figure 42. A comparison of the spectra of the starting material and final product in the conversion of (a) $Mn(TCNQ)_2(MeOH)_2$ (1) to (b) $Mn(TCNQ)_2$ and a comparison to a *bona fide* sample of $Mn(TCNQ)_2$.

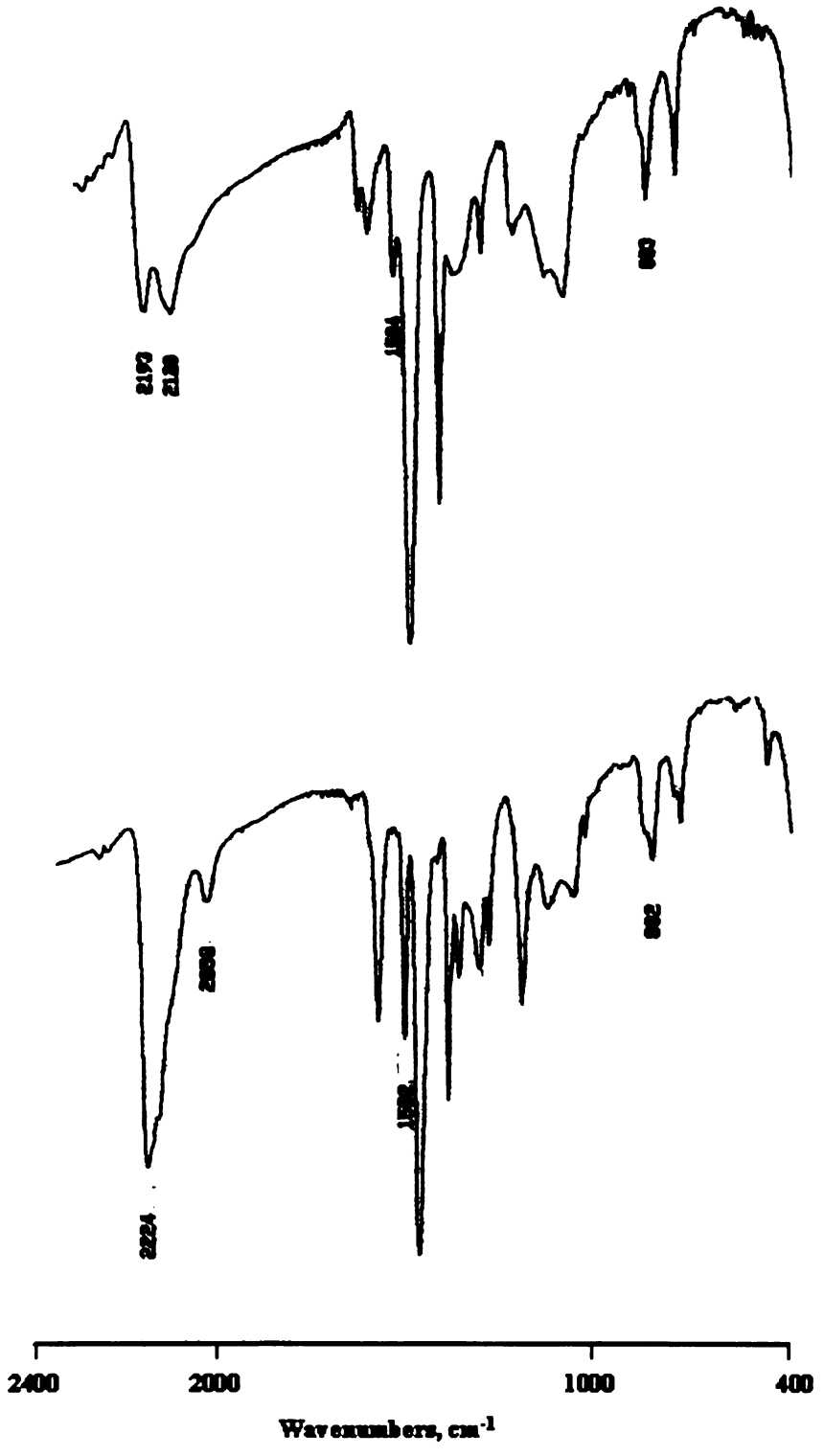

Figure 43. Illustration of the resulting σ-dimer products (**2b**, **4b**) obtained after heating suspensions of $M(TCNQ)_2(MeOH)_2$, M = Fe, (**2**), (top) and Ni, (**4**), (bottom).

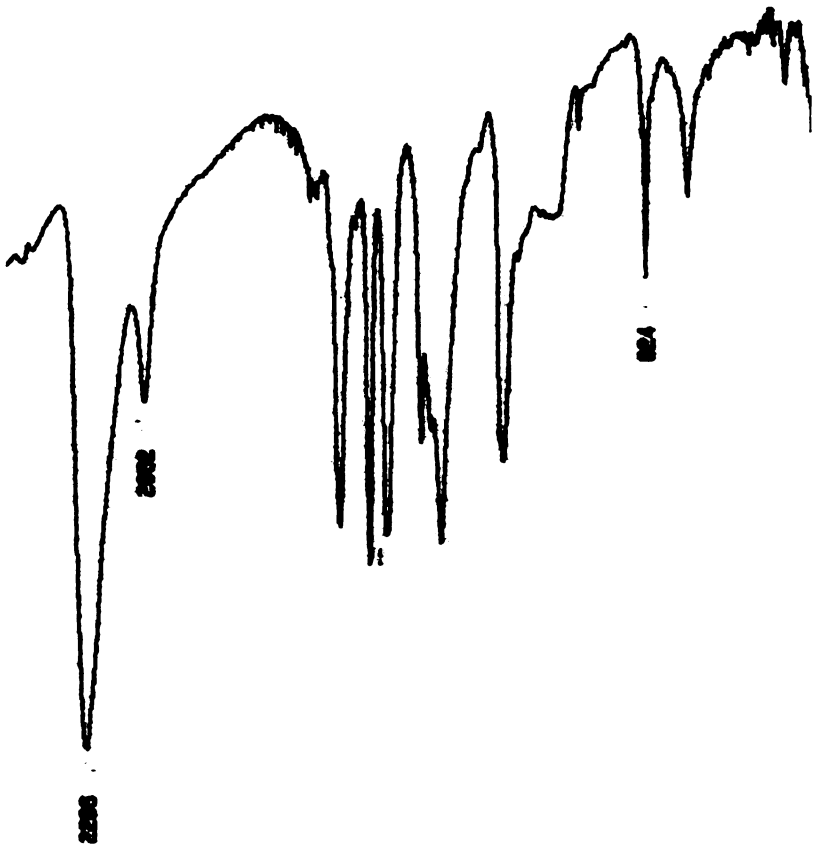

Figure 44. IR spectrum for the heated Ni product (**4b**), (Figure 42), recorded after exposure to X-rays. The δ(C-H) frequency at 824 cm^{-1} is present for $TCNQ^{-}$.

C. X-ray Powder Diffraction

(a) Confirmation of the successful isolation of (1a) and (1b) from $Mn(TCNQ)_2(MeOH)_2$ (1).

Compounds that contain the σ-dimer component are difficult to analyze using X-ray powder diffraction because the material changes during the course of the reaction; consequently, the resulting powder pattern is not representative of the compound being analyzed. At low temperatures, however, sample decomposition can be avoided during the powder diffraction experiment, and an accurate powder diffraction pattern can be obtained. Since decomposition of the σ–dimer compounds occurs upon exposure to the

X-ray beam, this low temperature technique was used to confirm the isolation of the heated sample corresponding to the formula, $[Mn(TCNQ\text{-}TCNQ)_2(MeOH)_4]_\infty$ (**1b**). The resulting powder pattern was compared to the one obtained for crystals of $[Mn(TCNQ\text{-}TCNQ)(MeOH)_4]_\infty$ in Figure 45. From this comparison, one can clearly see that heating a bulk methanol sample causes a conversion that is similar to the crystal phase but obviously mixed with something else.

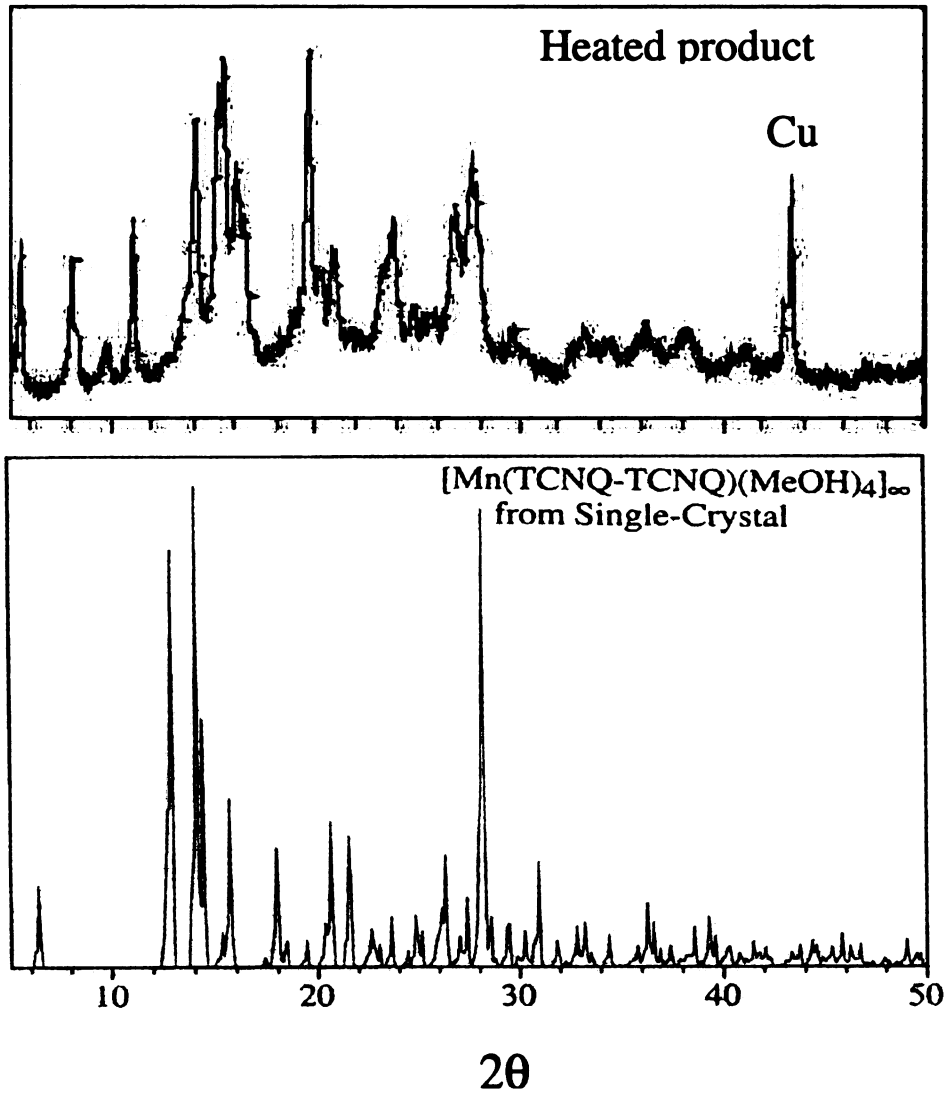

Figure 44. X-ray powder diffraction patterns for the heated material (**1b**) (top) and crystals of $[Mn(TCNQ\text{-}TCNQ)(MeOH)_4]_\infty$ (bottom).

A comparison of powder diffraction patterns for the heated $Mn(TCNQ)_2(H_2O)_2$ (**5**) phase and the original bulk sample is illustrated in Figure 46. The relative intensities and positions of the peaks indicate that a new phase has formed, (**5b**). Therefore, identification of a second phase using infrared and X-ray powder diffraction techniques was possible.

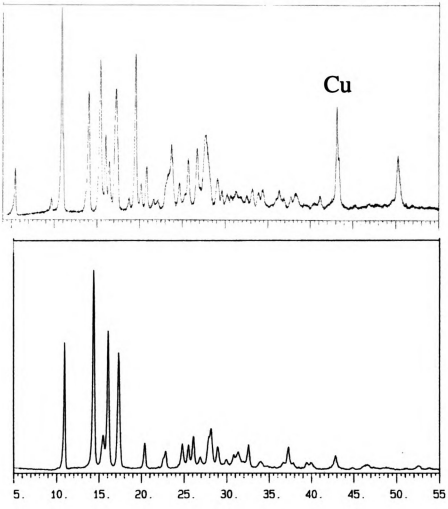

Figure 46. A comparison of the X-ray powder diffraction patterns for the heated phase (**5b**) (top) and the original bulk phase, $Mn(TCNQ)_2(H_2O)_2$ (**5**) (bottom).

Finally, powder diffraction X-ray data further confirmed the conversion of (**1**) to the magnetic phase, (**6**). At the solid state/solution interface, the samples were analyzed before and after conversion and clearly show that a conversion to $Mn(TCNQ)_2$ is taking place. Figure 47 illustrates the three powder patterns: bulk $Mn(TCNQ)_2(MeOH)_2$ (**1**), the heated material, and an authentic powder pattern of $Mn(TCNQ)_2$ (**6**). From these data, it is clear that the heated sample has converted to a phase that is similar to $Mn(TCNQ)_2$. These powder patterns as well as infrared data confirm that the conversion of (**1**) to (**6**) is possible, and also that the conversion of the σ-dimer phase to the magnetic phase by exposure to an X-ray beam has occurred.

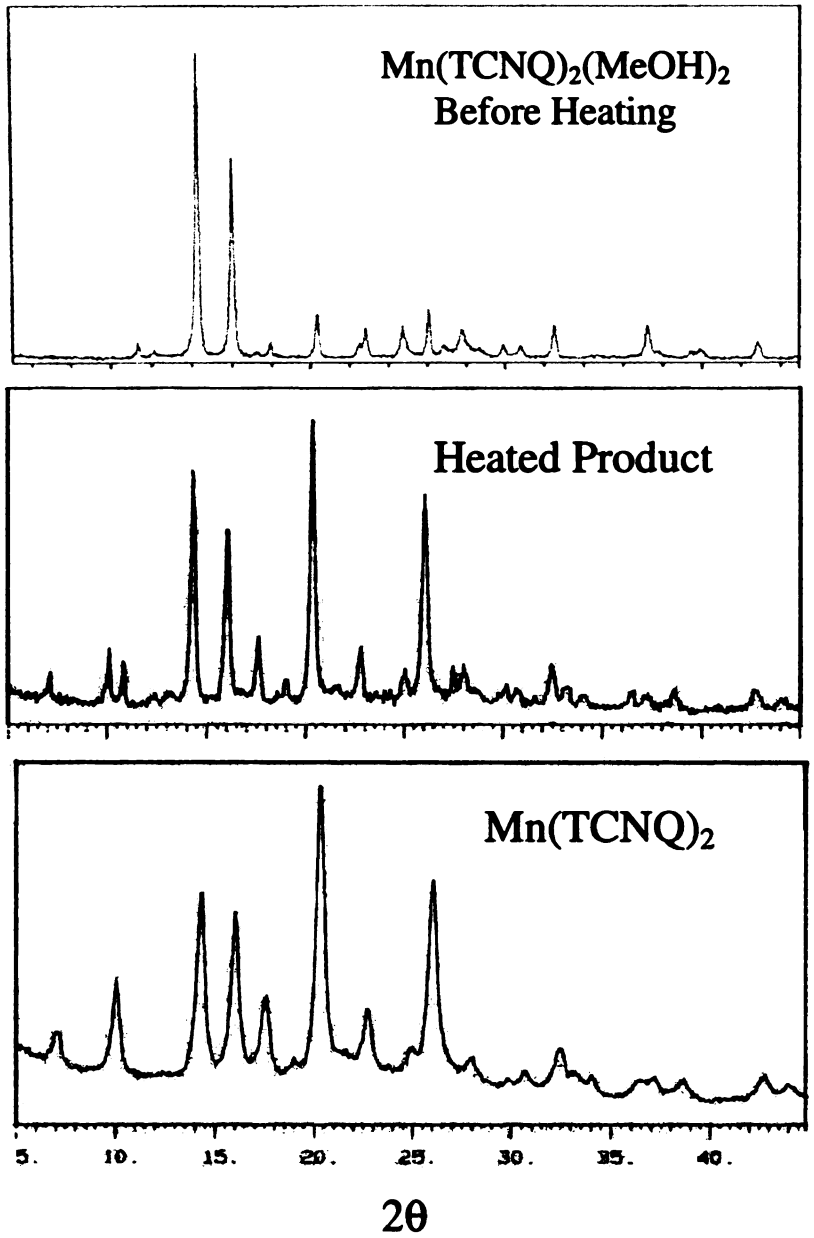

Figure 47. X-ray powder patterns measured before (top) and after (middle) the conversion reaction of $Mn(TCNQ)_2(MeOH)_2$ to $Mn(TCNQ)_2$. As a reference, a powder pattern of *bona fide* $Mn(TCNQ)_2$ is displayed at the bottom.

Conclusions

A number of the known metal-TCNQ polymer complexes have been recognized to exist as multiple phases, but it is likely to be a problem for most of these materials. Unfortunately, many of these will remain undiscovered as it is not a simple task to identify and characterize multiple components of insoluble materials. We were fortunate that two phases (**1a** and **1b**) could be crystallized from slow diffusion of the reactants of the bulk $Mn(TCNQ)_2(MeOH)_2$ compound (**1**). Characterization by infrared spectroscopy and X-ray powder diffraction of these crystals provided a basis for the analysis of related compounds. After detailed studies of the formation of the two components of bulk samples of $Mn(TCNQ)_2(MeOH)_2$ (**1**), it was obvious to us that $[Mn(TCNQ)(TCNQ\text{-}TCNQ)_{0.5}(MeOH)_2]_\infty$ (**1a**) is the kinetic product and $[Mn(TCNQ\text{-}TCNQ)_2(MeOH)_4]_\infty$ (**1b**) is the thermodynamic product.[7] The former is produced at short reaction times, and, according to infrared spectroscopy, it is the major component in the bulk methanol product (**1**).[6] The latter, however, has been shown experimentally to form over time, often with increased application of heat.

An interesting phenomenon was observed during analysis of $[Mn(TCNQ\text{-}TCNQ)_2(MeOH)_4]_\infty$ (**1b**) crystals by X-ray powder diffraction. Exposure to the X-ray source caused decomposition through the severing of the weakly bonded C-C σ bond in the μ_4-$[TCNQ\text{-}TCNQ]^{2-}$ ligand. Furthermore, there is a concomitant removal of axially coordinated methanol groups in these crystals. Even more surprising is the fact that the two $TCNQ^-$ radicals do not recombine in the solid state, but instead form a phase similar to the magnetic material prepared directly from $[Mn(MeCN)_4(BF_4)_2]$ and [*n*-Bu_4N][TCNQ]. We have now verified by X-ray powder diffraction and infrared

spectroscopy that crystals of $[Mn(TCNQ\text{-}TCNQ)_2(MeOH)_4]_\infty$ (**1b**) convert to the magnetic phase, $Mn(TCNQ)_2$ with exposure to heat or to an intense X-ray source.[6] Since it is the thermodynamic phase, $[Mn(TCNQ\text{-}TCNQ)_2(MeOH)_4]_\infty$ (**1b**), that is readily converted to the magnetic phase, obtaining pure samples of it from the bulk material $Mn(TCNQ)_2(MeOH)_2$ (**1**) became an extremely important goal. The use of slow diffusion techniques to grow single crystals of (**1b**) takes several months, therefore isolation via bulk methods was targeted instead. The successful separation of the two crystalline phases (**1a** and **1b**) was performed by taking advantage of the differences in their thermal stabilities and/or solubilities. The kinetic product (**1a**) was isolated at low temperatures and short reaction times, whereas the thermodynamic phase, (**1b**), appears to be favored with heating and longer reaction times.

A detailed examination of the synthetic conditions leading to $Mn(TCNQ)_2(H_2O)_2$ (**5**), a second phase, led to the discovery of composed of σ-dimers (**5b**) which was verified by infrared data and X-ray powder diffraction. The first phase, (**5a**), crystallized several years ago in our laboratories contains the *syn*-[μ-TCNQ]$^-$ coordination mode. Confirmation of the presence of two phases in the isostructural methanol products, (**2-4**), was also successful in that the presence of σ-dimer was detected, but conversion to the respective unsolvated, magnetic phases did not occur. It may be that the conditions were not forceful enough to effect the changes and loss of solvent, but this remains to be verified by further studies.

As the rapid expansion of binary metal/organocyanide acceptor compounds continues with the use of TCNQ derivatives and other more exotic acceptors, the identification of multiple polymorphs in compounds will doubtless be an important

priority. It is crucial that researchers obtain pure samples of each phase, or at the very least, ascertain how each component contributes to the general properties of the bulk product. If this is not done, then much wasted effort in trying to understand magnetic and other physical data will ensue.

References

1 (a) Acker, D. S.; Harder, R. J.; Hertler, W. R.; Mahler, W.; Melby, L. R.; Bensin, R. E.; Mochel, W. E. *J. Am. Chem. Soc.* **1960**, *82*, 6408. (b) Melby, L. R.; Harder, R. J.; Hertler, W. R.; Mahler, W.; Benson, R. E.; Mochel, W. E. *J. Am. Chem. Soc.* **1962**, *84*, 3374. (c) Torrance, J. B. *Acc. Chem. Res.* **1979**, *12*, 79. (d) Endres, H. In *Extended Linear Chain Compounds*; Miller, J.S. Ed.; Plenum: New York. **1983**; Vol. 3, pp. 263-312. (e) Wudl, F. *Acc. Chem. Res.* **1984**, *17*, 227. (f) Jérome, D. *Science* **1991**, *252*, 1509. (g) Bryce, M. R. *Chem. Soc. Rev.* **1991**, *20*, 355. (h) Williams, J. M.; Schultz, A. J.; Geiser, U.; Carlson, K. D.; Kini, A. M.; Wang, H. H.; Kwok, W.-K.; Wangbo, M. - H.; Schirber, J. E. *Science*, **1991**, *252*, 1501. (i) Ward, M. D. *Electroanal. Chem.* **1988**, *16*, 181. (j) Martin, N.; Segura, J. L.; Seoane, C. *J. Mater. Chem.* **1997**, *7*, 1661.

2 (a) Pénicaud, A.; Batail, P.; Perrin, C.; Coulon, C.; Parkin, S. S. P.; Torrence, J. B. *J. Cehm. Soc., Chem. Commun.* **1987**, 330. (b) Davidson, A.; Boubekeur, K.; Pénicaud, A.; Auban, P.; Lenoir, C.; Batail, P.; Hervé, G. *J. Chem. Soc., Chem. Commun.* **1989**, 1373. (c) Pénicaud, A.; Bourbekeur, K.; Batail, P.; Canadell, E.; Auban-Senzier, P.; Jérome, D. *J. Am. Chem. Soc.* **1993**, *115*, 4101. (d) Coulon, C.; Livage, C.; Gonzalavez, L.; Boubekeur-K.; Batail, P. *J. Phys. I Fr.* **1993**, *3*, 1. (e) Coronado, E.; Gómez-Garcia, C. J. *Comments Inorg. Chem.* **1995**, *17*, 255. (f) Gómez-Garcia, C. J; Giménez-Saiz, C. J.; Triki, S.; Coronado, E.; Manqueres, P. L.; Ouahab, L.; Ducasse, L.; Sourisseau, C.; Delhaes, P. *Inorg. Chem.* **1995**, *34*, 4139. (g) Coronado, E.; Delhaus, P.; Galáan-Mascarós, J. R.; Giménez - Saiz, C. J. *Synth. Met.* **1997**, *85*, 1647.

3 (a) Aumüller, A.; Erk, P.; Klebe, G.; Hünig, S.; von Schütz, J.; Werner, H. *Angew. Chem., Int. Ed. Engl.* **1986**, *25*, 740. (b) Aumüller, A.; Erk, P.; Hünig, S. *Mol. Cryst. Liq. Cryst.* **1988**, *156*, 215. (c) Erk, P.; Gross, H. - J.; Hünig, U. L.; Meixner, H.; Werner, H. - P.; von Schütz, J. U.; Wolr, H. C. *Angew. Chem., Int. Ed. Engl.* **1989**, *28*, 1245. (d) Kato, R.; Kobayashi, H.; Kobayashi, A. *J. Am. Chem. Soc.* **1989**, *111*, 5224. (e) Aumüller, A.; Erk, P.; Hünig, S.; Hädicke, E.; Peters, K.; von Schnering, H.G. *Chem. Ber.* **1991**, *124*, 2001. (f) Sinzger, K.; Hünig, S.; Jopp, M.; Bauer, D.;

Beitsch, W.; von Schütz, J. U.; Wolf, H. C.; Kremer, R. K.; Metzenthin, T.; Bau, R.; Khan, S. I.; Lindbaum, A.; Lengauer, C. L.; Tillmanns, E. *J. Am. Chem. Soc.* **1993**, *115*, 7696.

4 (a) Potember, R. S.; Poehler, T. O.; Cowan, D. O.; *Appl. Phys. Lett.* **1979**, *34*, 405. (b) Potember, R. S.; Poehler, T. O.; Cowan, D. O.; Carter, F. L.; Brant, P. In *Molecular Electronic Devices II*; Carter, F.L., Ed.; Marcel Dekker: New York, 1982; p. 91 (c) Hoagland, J. J.; Wang, X. D.; Hipps, K. W. *Chem. Mater.* **1993**, *5*, 54. (d) Dunbar, K. R.; Cowen, J.; Heintz, R. A.; Grandinetti, G.; Ouyang, X.; Zhao, H. *Inorg. Chem.* **1999**, *38*, 144.

5 (a) Manriquez, J. M.; Yee, G. T.; McLean, S.; Epstein, A. J.; Miller, J. S. *Science* **1991**, *252*, 1415. (b) Miller, J. S.; Calabrese, J. C.; McLean, R. S.; Epstein, A. J. *Adv. Mater.* **1992**, *4*, 498. (c) Miller, J. S.; Vazquez, C.; Jones, N. L.; McLean, R. S.; Epstein, A. J. *J. Mater. Chem.* **1995**, *5*, 707. (d) Miller, J. S.; Calabrese, J. C.; Vazquez, C.; McLean, R. S.; Epstein, A. J.; *Adv. Mater.* **1994**, *6*, 217. (e) Böhm, A.; Vazquez, C.; McLean, R. S.; Calabrese, J. C.; Kalm, S. E.; Manson, J. L.; Epstein, A. J.; Miller, J. S. *Inorg. Chem.* **1996**, *35*, 3083. (f) Brinckerhoff, W. B.; Morin, B.G.; Brandon, E. J.; Miller, J. S.; Epstein, A. J. *Appl. Phys.* **1996**, *79*, 6147.

6 Zhao, H.; Heintz, R. A.; Ouyang, X.; Dunbar, K. R. *Chem. Mater.* **1999**, *11*, 736.

7 Dunitz, J. D.; Bernstein, J. *Acc. Chem. Res.* **1995**, *28*, 193.

8 Heintz, R. A.; Smith, J. A.; Szalay, P. S.; Weisgerber, A.; Dunbar, K. R. *Inorg. Synth.* in press.

9 (a) Pukacki, W.; Pawlak, M.; Graja, A.; Lequan, M.; Lequan, R. M. *Inorg. Chem.* **1987**, *26*, 1328. (b) Cornelissen, J. P.; van Diemen, J. H.; Groeneveld, L. R.; Haasnoot, J. G.; Spek, A. L.; Reedijk, J. *Inorg. Chem.* **1992**, *31*, 198.